WEAR OF A MICA-CONTAINING GLASS-CERAMIC

A THESIS SUBMITTED TO
THE GRADUATE SCHOOL OF NATURAL AND APPLIED SCIENCES
OF
THE MIDDLE EAST TECHNICAL UNIVERSITY

BY

TAYLAN KÜÇÜK

IN PARTIAL FULFILLMENT OF THE REQUIREMENTS FOR THE DEGREE OF

MASTER OF SCIENCE

IN

THE DEPARTMENT OF METALLURGICAL AND MATERIALS ENGINEERING

AUGUST 2003

Approval of The Graduate School of Natural and Applied Sciences

Prof. Dr. Canan ÖZGEN
Director

I certify that this thesis satisfies all the requirements as a thesis for the degree of Master of Science.

Prof. Dr. Bilgehan ÖGEL
Head of Department

This is to certify that we have read this thesis and that in our opinion it is fully adequate, in scope and quality, as a thesis for the degree of Master of Science.

Prof. Dr. Abdullah ÖZTÜRK
Supervisor

Examining Committee Members

Prof. Dr. Muharrem TİMUÇİN

Prof. Dr. Macit ÖZENBAŞ

Prof. Dr. İhsan EFEOĞLU

Prof. Dr. Abdullah ÖZTÜRK

Assoc. Prof. Dr. Ali KALKANLI

ABSTRACT

WEAR OF A MICA-CONTAINING GLASS-CERAMIC

Küçük, Taylan
M.Sc., Department of Metallurgical and Materials Engineering
Supervisor: Prof. Dr. Abdullah Öztürk

August 2003, 102 pages

Tribological properties of a mica glass-ceramic designed for use in dental applications were assessed experimentally in accord with the ASTM pin on disk technique. The glass ceramic was produced through controlled crystallization of the glass in the system SiO_2, Al_2O_3, CaO, MgO, K_2O, and F. Crystallization was accomplished by subjecting the parent glass to a regulated heat treatment that resulted in the nucleation and growth of crystal phases formed in the glass.

The tests were conducted by sliding a zirconia ball against the glass and glass ceramic disk. The friction coefficient and wear rate were determined as functions of the applied load, sliding speed and sliding time in ambient laboratory conditions and in acidic and basic solutions. The friction coefficient was monitored during the tests. The wear volumes determined from surface profile traces obtained on the wear tracks after completion of the tests were used for calculation of the wear rates. The wear rates increased with increasing applied load and sliding speed but decreased with increasing sliding distance. Results were correlated with the tribological properties of the parent glass, and tribological properties of selected glasses, glass-ceramics and ceramics reported in the literature.

Keywords: mica, glass, mica glass-ceramic, tribology, friction, wear.

ÖZ

MİKA İÇEREN BİR CAM SERAMİĞİN AŞINMASI

Küçük, Taylan
Yüksek Lisans, Metalurji ve Malzeme Mühendisliği Bölümü
Tez Danışmanı: Prof. Dr. Abdullah Öztürk

Ağustos 2003, 102 sayfa

Diş uygulamaları için tasarlanmış olan bir mika cam-seramiğin tribolojik özellikleri ASTM pin on disk tekniğine göre deneysel olarak değerlendirildi. Cam seramik, SiO_2, Al_2O_3, CaO, MgO, K_2O, ve F sisteminden oluşturulmuş bir camın kontrollü kristalleştirilmesi sonucunda üretildi. Kristalleştirme, camın kontrollü ısıl işlemi sonucunda çekirdeklendirilmesi ve cam içinde oluşan kristal fazların büyümesiyle sağlandı.

Testler zirkonyadan oluşturulmuş bir kürenin disk şeklindeki cam ve cam seramik numuneler üzerinde kaydırılması ile gerçekleştirildi. Sürtünme katsayısı ve aşınma hızı, uygulanan yükün, kayma hızının ve kayma zamanının fonksiyonu olarak normal laboratuvar atmosferinde, asidik ve bazik solüsyonlarda belirlendi. Sürtünme katsayısı deneyler esnasında ekranda görüntülendi. Testlerin tamamlanmasından sonra elde edilen yüzey profil izlerinden faydalanarak belirlenen aşınma hacimleri, aşınma oranlarının hesaplanmasında kullanıldı. Aşınma hızları uygulanan yükün ve kayma hızının artması ile artmakta, fakat kayma mesafesinin artması ile azalmaktadır.

Sonuçlar mika cam seramiğini oluşturan camın ve literatürde raporlanan değişik camların, cam seramiklerin ve seramiklerin tribolojik özellikleriyle ilişkilendirildi.

Anahtar Kelimeler: Mika, cam, mika cam-seramik, triboloji, sürtünme, aşınma.

To my dear parents;

Akgül and Mustafa KÜÇÜK

ACKNOWLEDGEMENTS

First, it is a pleasure to thank my supervisor Prof. Dr. Abdullah ÖZTÜRK, for his helpful guidance, criticism, encouragement thrughout the every stage of this study.

I wish to express my appreciation to my examining committee members Prof. Dr. Muharrem TİMUÇİN, Prof. Dr. Macit ÖZENBAŞ, Prof. Dr. İhsan EFEOĞLU, and Assoc. Prof. Dr. Ali KALKANLI for their regards and valuable recommendations.

I wish to express my gratitute to my mother, my father and my brother for their complimentary love and unshakable faith in me during my life.

The financial support provided by The Scientific and Technical Research Council of Turkey (TÜBİTAK), which made this study possible, is greatly appreciated.

Thanks are also extended to my company, EMTAMİTAŞ Energy and Metal Construction Inc. and especially to our quality manager Dr. İlhami PEKTAŞ for his understanding during the preparation stage of this thesis.

Finally, I would like to express my special and frank thanks to Binhan Koyuncuoğlu for her understanding and endless support in me.

TABLE OF CONTENTS

CHAPTER

LIST OF TABLES

TABLE

LIST OF FIGURES

FIGURE

CHAPTER 1

INTRODUCTION

Mica glass-ceramics are polycrystalline solids, obtained through the controlled crystallization of glasses in the SiO_2 –MgO–K_2O–F system, and contain fluoro-phologopite (synthetic fluormica) crystals as the main crystalline phase [1]. Crystallization is achieved by subjecting the suitable glass to a heat treatment, which results in the nucleation and growth of crystal phases in the glass [1-3]. Minor additives such as CaO, P_2O_5 and TiO_2 may also be incorporated to modify or enhance the properties [3-5].

Mica glass-ceramics have drawn exalted attention principally due to their machinability in addition to their superior and unique chemical, thermal, and dielectric properties [3-6]. Dimensional changes are small, and complex shapes can be obtained using standard glass-forming techniques, such as rolling, blowing, pressing, and casting prior to crystallization [4]. Absence of porosity and uniform reproducible fine grain structure that can be tailored by changes in composition and heat treatment make them useful for special applications [1-6]. Because of their desirable engineering properties mica glass-ceramics find uses in the production of optical devices, insulators, missile radoms, mechanical components, cooking ware, surface coating materials in the buildings, magnetic disc recording, components in space travel, pipes and heat resistant windows [3-8]. Glass ceramics have been commercially used as synthetic tooth filling materials and in some dental prostheses [9,10]. Some compositions have been melted and cast into the form of tooth and have been marketed under different commercial names such as Dicor [11], Macor [12,13], and Bioverit [14]. Dicor is a kind of commercial product of mica glass-ceramics and it is presently recommended for the construction of crown and veneer restorations in aesthetic dentistry [15,16].

Metals, alloys, organic polymers, ceramics and their composites can not compose whole tooth due to design criteria, aesthetic considerations, and due to mechanical and chemical considerations. They are used either as root or crown of a tooth but not a complete part as a whole. It is possible to produce a whole tooth from a mica glass-ceramic [17]. Therefore they have generated interest in the biomedical field, especially in the replacement of natural bone and dental restoration.

Machinability is a useful and unique property of mica glass-ceramics. The material can be machined to close tolerances with conventional tool bits. That is; it is cut, drilled, ground, turned, sawed, etc. Exceptional machinability results from the interlocking plate-like structure and easily cleavable mica crystals dispersed in a glassy matrix so that fine particles can be removed from the surface by pulverization [4]. The microstructure plays a great role in determining the machinability of glass ceramics [1]. Particle size, amount and distribution of precipitated mica crystals have a great influence on the machinability [12]. The best machinability was secured where the product was highly crystalline and the crystals themselves were large and exhibited high aspect ratios [1,12].

In spite of the good peculiarities of the mica glass-ceramics, they are hard to prepare due to their high melting and forming temperatures, large crystallization tendency, phase separation on cooling, and compositional change due to the fluorine volatilization on melting [18]. Although literature is rich on evaluation of the mechanical properties of these materials [1,7,12,19-21], data on the tribological properties are rare. Tribological properties are important for optimizing material selection and development especially if the material is utilized in the critical biomedical applications such as tooth restoration and implantation. Researches on the tribological properties of mica glass-ceramics are needed to develop a sound database before these materials can be used with confidence. Therefore, studies conducted on the tribological properties of these materials have both technological and scientific significance. Determination of tribological behavior of mica glass-ceramics under different experimental conditions is among the main research topics since they possess unique mechanical performance in combination with the osteoconductive characteristics [22]. However, most of the published research has been devoted to the design and development of test techniques for the simulation of wear in the oral environment [23-26]. Simulated wear studies in the artificial mouth involving human enamel occluding on a commercial castable glass ceramic, Dicor, have resulted in a low wear coefficient for Dicor. The specific wear rate of enamel tested against Dicor was half as much as the specific wear rate of enamel sliding against the porcelain [27]. Recently, Nagarajan and Jahanmir [28] have investigated the relationship between microstructure and wear of mica containing glass ceramics by pin on disc tribometer under distilled water lubrication. Their investigation has revealed that at a given test condition, i.e. load and number of passes, the specific wear rate increased with the increase in the mica crystal diameter. Jahanmir and Dong [11] have studied wear mechanisms of a dental glass ceramic under two types of lubrication conditions and have concluded that wear primarily occurs by a microfracture process along the mica-glass interface, and; could be controlled by altering the microstructure.

Hu et al.[29] have investigated frictional behavior of the mica surfaces by using atomic force microscope and silicon nitride tips as a function of load, tip geometry, mica lattice orientation and humidity. They concluded that the frictional force was proportional to loads between 10 nN to 80 nN. A non-linear behavior of the friction versus load was observed at low loads and at high (>70%) relative humidity and, in water friction is reduced.

The purpose of this study was to produce a mica glass-ceramic for dental applications and to determine its tribological behavior under various experimental conditions. The friction coefficient and specific wear rate was determined as functions of the applied load, sliding speed, sliding distance and sliding time. The results of this study were correlated with the results of the studies conducted on similar glass and glass-ceramic compositions reported in the literature.

CHAPTER 2

THEORY

2.1 GENERAL

Materials for bone implantations may be classified as being either “bioinert” or “bioactive”. In the case of the former, the implant plays a passive role in the biological environment. The local biological reaction is often characterized by fibrous tissue encapsulation of the material. In bioactive or osteoconductive materials, new tissue bone is formed in direct or intimate contact with the implant surface [30,31]. Hydroxyapatite (HAp) is an example of an osteoconductive bioceramic [32]. However, an inherent shortcoming of HAp is its brittle nature and poor mechanical strength, which limits the application of such materials to implant coatings or situations of low mechanical load [33]. Thus, there is a need for new biomaterials that combine the osteoconductive characteristics of bioactive ceramics with sufficient strength and toughness for load-bearing applications [22].

In recent years, the demand for long lasting dental restorations has grown since people retain their teeth until later life. The health and environmental problems have increased. A need to produce new, durable and aesthetically acceptable materials for dental applications is growing. Lately, attention has been focused on the use of machinable mica based glass-ceramics [34]. The glass-ceramic route has the potential for development of high strength, osteoconductive bioceramics for mineralized tissue repair and augmentation as well as the dental restorations [14,35,36].

The first glass ceramic materials prepared by the controlled crystallization of special glasses were developed nearly forty years ago [37]. Since then a wide variety of applications of these versatile materials have developed as a result of their many outstanding properties and distinct advantages of the glass ceramic method in certain circumstances over conventional ceramic processing routes.

Glass-ceramics have a wide variety of established uses dependent on their uniform, reproducible, fine grain microstructure, absence of porosity and wide-ranging properties, which can be tailored by changes in composition and heat treatment conditions. Moreover, components with a variety of complex shapes can be manufactured using standard glass-forming techniques such as blowing, casting, pressing, rolling, etc. Subsequently the glass component is converted into a fine-grained polycrystalline solid by a heat treatment including nucleation and crystal growth [3,13].

A mica containing glass ceramic developed for dental restoration, Dicor, (Dentsply, Milford, DE, USA) is specifically designed for use with dental CAD/CAM systems. The properties of Dicor such as chemical durability, density, thermal conductivity, translucency, hardness, machining rates and specific wear rates are closely match to those of human enamel. Dicor is a glass ceramic of the SiO_2–MgO-K_2O–F system. It is formed as a glass by melt-casting the starting materials. Then, in order to obtain optimum strength and other desirable properties in the cast products, it is cerammed (heat treated) by subjecting to a special embedding procedure [2]. The size of the mica platelets has a significant effect on strength and on the removal rate during machining with dental diamond burr [38]. The size and orientation of the mica crystals can be controlled through heat treatment. The microstructural characteristic of this kind of materials, which consists of highly interlocked mica crystals embedded in a glass matrix, facilitate microfracture along the weak mica-glass interfaces and mica basal planes, avoiding macroscopic failure during machining. Very high machinable precision can be achieved (±10μm) using regular high-speed tools [6].

Generally, mechanical properties of glass-ceramics are influenced by the particle size, amount and strength of the precipitated crystal since they do not possess any porosity. The bonding strength in mica crystals apparently is determined by the bonding strength of the interlayer ions [18]. Tzeng et. al. [12] have reported that strength of mica glass ceramics can be enhanced by obtaining well-oriented microstructure and adding reinforcement elements like alumina and zirconia.

2.2 STRUCTURE OF MICA

The micas are layer silicates with the foliform habit and excellent cleavage at the (001) plane. The structural formula of mica is generally expressed as $X_{0.5-1}Y_{2-3}Z_4O_{10}$ (OH, F)$_2$, where X, Y, and Z are cations in 12-, 6-, and 4-fold coordination, respectively. Figure 2.1 shows the structure of a common fluorophlogopite, $K/NaMg_3AlSi_3O_{10}F_2$, mica. It involves two units [38]; one consisting of closely packed oxygen and hydroxyl or fluorine in which cations of radii 0.05 to 0.08 nm are present in octahedral coordination. The other unit is built of silicon-oxygen tetrahedra linked together in a hexagonal network so as to form a sheet in which a layer of octahedrally coordinated cations is sandwiched between identical layers of tetrahedral sheets pointing toward each other. The three-layer composite sheet has a net negative charge arising from substitutions. The excess charge is balanced by uptake of large cations between the composite sheets in 12-fold coordination. The inter-layer cations are weekly bonded, giving rise to a perfect set of basal cleavage. Their structure is characterized by the loose connection via K^+ or Na^+ ions layer packets. These layer packets in turn consist of two tightly connected $(Si_2O_5)^{-5}$ layers. Characteristically, each fourth tetrahedron in such a layer of six rings of tetrahedra is an AlO_4 tetrahedron. The firm connection of a layer packet is achieved by Mg^{+3} and F^+ ions in the form of brucite layer. In special cases, where these have a strong tendency to hydrate, water swelling and consequent lattice expansion result [13,38].

The Mg^{+2} ions are bonded directly to O^{-2} ion, which represent corners of tetrahedra. The valance of the Mg^{+2} ion is satisfied by the F^- ion located in the center of six-ring tetrahedra. In this way, the tetrahedron layers appear interlocked.

Also all Mg^{+2} ions connecting the tetrahedron layers are in six-coordination. Such three layer packets are loosely connected K^+ and Na^+ ions. These alkali ions have a function of charge balancing for the unsatisfied oxygen valances of protruding SiO_4 and AlO_4 tetrahedra. Therefore by addition of fluorine to the glass-ceramic composition, the machinability of mica glass-ceramic is established by construction of fluorophlogopite phase [38].

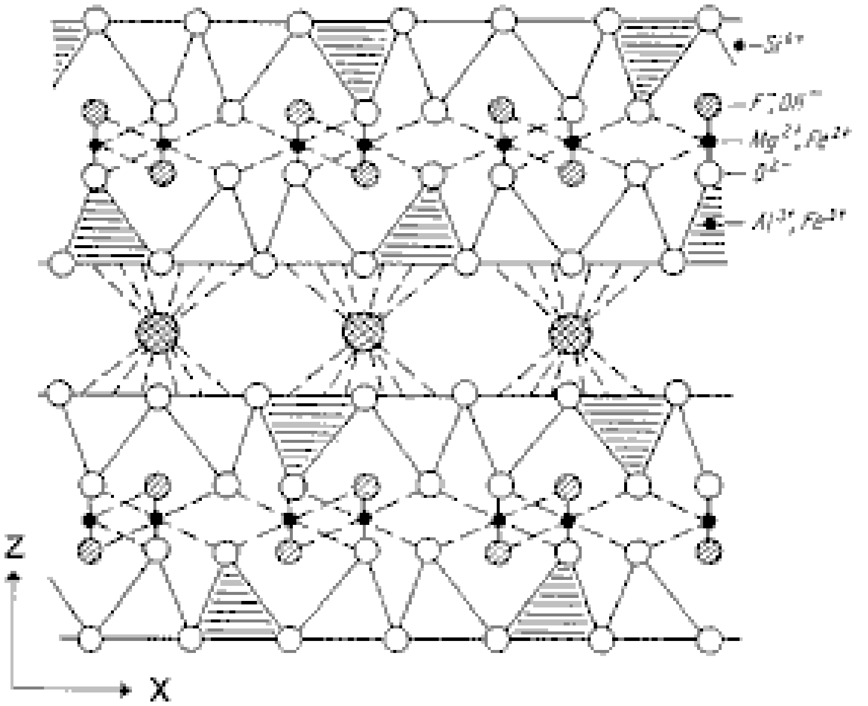

Figure 2.1 Crystal structure of the (010) plane of fluorophlogopite [39].

2.3 CRYSTALLIZATION OF GLASS

Although glass formation means the avoidance of crystallization from the cooling of a melt, production of a glass-ceramic requires the achievement of controlled crystallization. Avoiding uncontrolled crystallization during cooling and shaping of the material is important due to the reason of desirable fine grained microstructure [40].

Crystallization is accomplished by subjecting the suitable glass to a regulated heat treatment, which results in the nucleation and growth of crystal phases in the glass. The nucleation and crystallization of glass are important for properties [3]. As controlled crystallization requires the optimum of the crystallization and nucleation rates, it can affect the size of the grains. If the former rate is too low, growth will take place from too few centers and a coarse grained microstructure is likely to result. If the crystal growth rate is too high, coarsening of the microstructure can result [3].

The significant difference between controlled and uncontrolled crystallization is that [21]: Unintentional crystallization phenomena during the production of technical and optical glasses (i.e., crystallization as a defect) are usually characterized by the presence of entire spectrum of crystals of various sizes. In a relatively homogeneous glass, often sporadically and accidentally temporal and local conditions occur, at which the critical nuclei dimension is surpassed and a nucleus becomes capable of growth. If these conditions might occur later at another location the nucleus that grew first might already have grown to considerable size. The characteristics of controlled crystallization differ fundamentally from such nucleation and growth phenomena occurring sporadically at different times and locations. Criteria of controlled crystallization are (1) high nucleation frequency (2) very uniform crystal size, and (3) very small crystallite dimensions [21].

Nucleating agents; such as TiO_2, P_2O_5, ZrO_2, are incorporated into the parent glass compositions to generate high-density nucleating sites within the bulk of the material. So that phase separation, which is caused by the formation of stable molecular structural groups and their enrichment in certain regions, can occur. Every crystallization process in glass requires controlled phase separation [3].

Titanium dioxide, TiO_2, is commonly used as nucleating agent. Amount of addition generally does not exceed 5 weight percent of the batch [18]. Liquid phase separation occurs first in glass-ceramics with TiO_2 added as a nucleating agent, then crystalline compounds or solid solutions containing TiO_2 and some

components of the glass $MgO.TiO_2$ or TiO_2 itself precipitate as a high density of the fine crystals [41]. Consequently these crystals act as a surface-active agent and increase the nucleation rate. The efficiency of TiO_2 as a nucleating agent is severely impaired if heat treatment is carried out in a non-oxidizing atmosphere and in certain glass-ceramics, crystal growth rates can also be affected [40]. The addition of small amount of TiO_2 decreases the glass transition temperature significantly, and further decrease of T_g is observed as TiO_2 content increases [42]. This is attributed to a reduced number of bridging bonds in the silica based network leading to a decrease of the viscosity and, consequently, of the glass transition temperature.

Also the addition of TiO_2 improves both of the nucleation and growth rates of appetite by decreasing the viscosity and decreasing the surface energy between crystal and glass [41]. Additions of TiO_2 enhance the formation of phlogopite, too. For double step heat treatment, the TiO_2 content should not exceed 2 weight percent, beyond that the phlogopite formation is reduced and some TiO_2 crystals begins to form. It has been reported that 1000 °C is the optimum temperature for phlogopite crystallization; above this temperature, glass begins to soften and some crystals begins to redissolve [5]. Addition of Al_2O_3 in combination with TiO_2 and SiO_2 promotes fine-scale volume crystal nucleation [4].

The improvement on controlled crystallization and the development of glass-ceramics make them important for the dental and bone implantation. Apatite-containing glass-ceramics are potentially important for surgical implantation due to close crystallographic and chemical similarity to bone tissue. The crystalline phases occurring in these glass-ceramics include essentially apatite, the major crystalline phase, which provides the biocompatibility of the glass ceramics, and secondary crystalline phase(s) crystallized at higher temperature providing the interesting mechanical properties such as machinability and strength [41].

2.4 TRIBOLOGICAL PROPERTIES

Wear is damage to a solid surface as a result of relative motion between it and surface of another substance [43]. The damage usually results in the progressive loss of material. Wear testing has been used to rank wear resistance of materials for the purpose of optimizing material selection and development for a given application. Standardization, repeatability, convenience, short testing time, and simple measuring and ranking techniques are desirable in these tests. Wear is closely related to friction, and lubrication; the study of these three subjects is known as tribology [44].

The word tribology was introduced only just over thirty years ago and is defined as the science and technology of interacting surfaces in relative motion and of related subjects and practices; it deals every aspect of friction, lubrication, and wear. The word is derived from the Greek “tribos” meaning rubbing, although the subject embraces a great deal more than just the study of rubbing surfaces [45,46].

Collection of all the mechanical, chemical, and environmental parameters that can affect wear and wear behavior is referred to as the tribo-system. Typical factors that can affect wear behavior are the properties of the materials, the nature of the relative motion, the nature of the loading, the shape of the surface(s), the surface roughness, the ambient temperature, and the composition of the environment in which the wear occurs [43]. Coefficients of friction and wear are parameters describing the state of contact bodies in a tribo-system, and they are not material constants of the bodies in contact.

Restorative materials may wear as a result of tooth brushing, tooth contact, or mastication of abrasive food [23]. Glass-ceramics are a class of materials used for the restoration purposes in the dentistry. Although wear of this material has received much attention, most of the published research has been devoted to the design and development of tribometers to simulate wear in the oral environment [23,24]. A noteworthy achievement is the development of artificial oral environment [47], which simulates several important factors using a biaxial force

and motion control system. Simulated wear studies in the artificial mouth involving human enamel occluding on dental porcelain resulted in a high wear coefficient for the porcelain [48]. However, the specific wear rate of a commercial castable glass-ceramic, Dicor, sliding against enamel was much lower than that of the porcelain. More importantly, the specific wear rate of enamel tested against Dicor was half as much as the specific wear rate of enamel sliding against the porcelain [27,49]. Based on the higher strength of Dicor as compared to the platinum-bonded aluminious porcelains, a superior clinical performance for crown and bridgework restorations made from glass ceramics was predicted [50].

Specific wear rate changes drastically in the range of 10^{-15} to 10^{-1} mm^3/Nm, depending on operating conditions and material selection [51-54]. Therefore, it is inherent that designing of the operating conditions and selection for the materials are the keys to controlling wear. As one way to meet these requirements, wear maps have been proposed for prediction of wear modes and specific wear rates. A wear map is considered one of the best descriptions of tribological condition and is useful in selecting materials in a wide range of operating conditions.

In order to design and investigate the tribological behavior of the mica glass-ceramic it is essential to an understanding of specific wear rate, varieties of wear modes, and wear mechanism [55,56]. Wear is the result of material removal by physical separation due to microfracture, by chemical dissolution, or by melting at the contact interface. In addition, there are several types of wear; adhesive, abrasive, fatigue, and corrosive. The dominant wear mode may change from one to another for reasons that include changes in surface material properties and dynamic surface responses caused by frictional heating, chemical film formation, and wear. However, in general, wear does not occur through a single wear mechanism [57].

Three representative types of wear volume curves are shown in Figure 2.2. Type 1 shows a constant specific wear rate throughout the whole process. Type II shows the transition from an initially high specific wear rate to steady wear at low rate. This type of wear is quite often observed in metals [58]. Type III shows catastrophic wear is the period at which crack initiation takes place and depends on the initial surface finish, material properties, and frictional conditions.

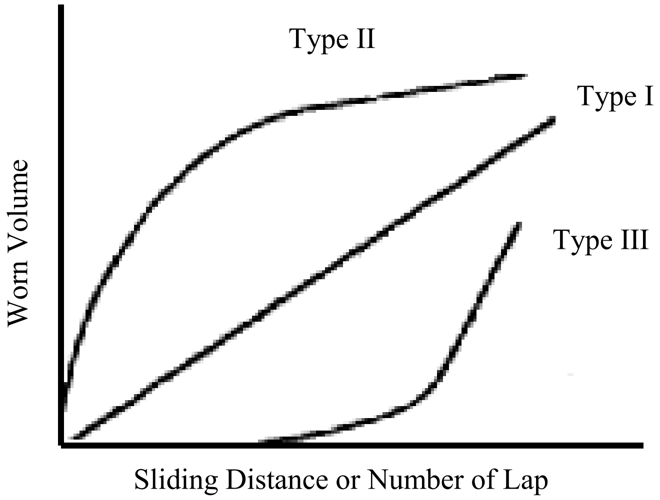

Figure 2.2 The representative types of wear volume curves [46].

The following four wear modes are generally recognized as fundamental and major wear modes [59]: Adhesive wear, Abrasive wear, Fatigue wear, Corrosive wear. Schematic representation of the wear modes is illustrated in Figure 2.3. Adhesive and abrasive wear are wear modes generated under plastic contact. In the case of plastic contact between similar materials, the contact interface has adhesive bonding strength. When fracture is supposed to be essentially brought about as the result of strong adhesion at the contact interface, the resultant wear is called adhesive wear, without particularizing about the fracture mode.

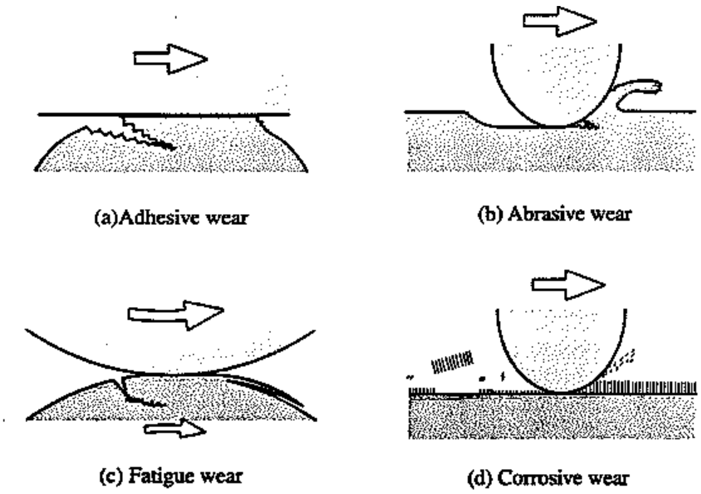

Figure 2.3 Wear modes [46].

In the case of plastic contact between hard and sharp material and relatively soft material, the harder material penetrates to the softer one. When the fracture is supposed to be brought about in the manner of micro-cutting by the intended material, the resultant wear is called abrasive wear, recognizing the interlocking contact configuration necessary for cutting, without particularizing about adhesive forces and fracture mode.

In the case of contact in the running-in state, fatigue fracture is generated after repeated friction cycles. When surface failure is generated by fatigue, the resultant wear is called fatigue wear. In contact in corrosive media, the tribochemical reaction at the contact interface is accelerated. When the tribochemical reaction in the corrosive media is supposed to be brought about by material removal, the resultant wear is called as corrosive wear.

Fatigue and corrosive wear can take place in both plastic and elastic contacts. The material removal in adhesive, abrasive, or fatigue wear is governed by deformation and fracture in the contact region, where fracture modes are fatigue, brittle or ductile fracture. Such deformation and fracture are generated by mechanically induced strains and stresses. Therefore, this type of wear is generally described as mechanical wear. The material removal in corrosive wear is governed by the growth of chemical reaction film or its chisolution on wear surface, where chemical reactions are highly activated and accelerated by frictional deformation, frictional heating, microfracture, and successive removal of reaction products. This type of wear is generally described as chemical wear or tribochemical wear.

In some cases, material removal is governed by surface melting caused by frictional heating or by surface cracking caused by thermal stress. These types of wear are described as thermal wear, where frictional heating and partial high temperature govern the process. Erosion and abrasive wear situations can also be subdivided into more specific categories. Examples of these are cavitation erosion, solid particle erosion, gouging abrasion, and slurry erosion [43].

2.5 STANDARDIZATION OF THE TESTING METHOD

A particular type of wear problem usually motivates wear testing, it can be basic-research-oriented or application related. Frequently, the developer of a new material or surface treatment wants to know how the new material compares with other existing materials. If there is a specific application in mind, the selection of a particular wear test method is easier because the type of motion, contact conditions, and environment are dictated by the application. If no application is in mind, conducting a series of different standard wear tests can be appropriate. Motivations to do a wear testing are [60]:

1. To conduct basic scientific research on the characteristics and mechanism of a particular type of wear,

2. To evaluate the relative wear resistance of set of materials or the anti-wear properties of a lubricant,
3. To evaluate the relative wear resistance of a set of materials, including lubricants, for a specific application,
4. To evaluate the characteristics of a particular type of test procedure,
5. To aid in the development of a new wear-resistant materials or treatment,
6. To ensure uniform quality of a particular product.

The standardisation of wear testing conditions is not consistent with all the above motivations to do wear testing. In basic research, for example, it is often desirable to vary testing conditions over a large range, and enforcing a standard set of testing conditions would be inappropriate. In screening materials for a specific application, there may or may not be standard tests available for that application, and extrapolation of data for use in a new design or set of operating conditions that differs significantly from the one on which the existing standard based is generally ill-advised. The best correlation of testing with performance in a particular application may be obtained with a custom-design simulator, which may bear little resemblance to configurations in standard wear testing methods.

The diversity of wear test methods being applied to materials has created problems in comparing results and in establishing a coherent wear technology based for these materials. Standardization of wear testing is a means to alleviate many of these problems, and ASTM is a historic leader in this field. ASTM is attempting to develop standard wear tests specifically suited for ceramic materials, either by modifying existing methods developed for other materials, or by developing new methods. In May 1987, ASTM Committee G-2 on wear and erosion conducted a symposium on “Selection and Use of Wear Tests for Ceramics”, and a publication with the same name resulted [60].

Standards in the field of tribology can extend beyond the specifications for conducting tests. They can involve standards for specimen preparation, specimen material characterization, and even standards for the completion and presentation of friction and wear data. In addition to standard test methods, there are standard test methods, and standard practices [44,61,62]. Each has a role in tribology. For example; for abrasive wear, ASTM test for measuring abrasion using the dry sand/rubber apparatus G65, for erosive wear; ASTM practice for conducting erosion tests by solid particle impingement using gas jets G76, for rolling contact fatigue and sliding wear; ASTM practice for ranking resistance of materials to sliding wear using block on ring wear test G77 or ASTM test for wear testing with a pin on disc apparatus G99 could be used. Even if a material displays poor wear behaviour in one wear mode, it could still be shown to have superior wear in another, and the value of a new material would not be overlooked by restricting wear testing to only one kind.

The principal advantages of using ASTM standard wear test methods are [62]:

1) The test methods have been rigorously evaluated and the procedures carefully documented.
2) The repeatability and reproducibility of results tends to be better documented and understood than for a specialized or one-of-a-kind types of wear testing machines;
3) In many cases, a great deal of previous data exists and it is convenient to compare new results with the existing data, and
4) Documentation and reporting requirements have been established so that all the major variables and results of the work can be presented in a complete and organized manner.

2.6 PIN ON DISC TRIBOLOGICAL TESTING METHOD

Schematic representation of the pin on disc testing machine used in this study is shown in Figure 2.4. The machine can be used for testing the friction and wear characteristics of dry or lubricated sliding contact of a wide variety of materials including metals, polymers, composites, ceramics, lubricants, cutting fluids, abrasive slurries, coatings, and heat-treated samples [63]. Rotating a counter-face test disc against a stationary test specimen pin performs the test. Wear, friction force, and interface temperature can be monitored using winlube, the supplied windows-based data acquisition software. The normal load, rotational speed, and wear track diameter can be adjusted in accordance with test standard.

Figure 2.4 Pin on disc tribometer used in this study.

The sliding wear caused by a loaded spherical pin contacting a rotating disc is typical of that which occurs in pin-on-disc tests used to study friction and wear phenomena. In a pin on disc test, the pin is held stationary under a specified load, while the disc rotates beneath it at a constant velocity. If a sliding wear mechanism is being examined, the pin generally has a spherical head and the disc is fabricated from the material whose wear behavior is investigated which is usually much softer than the pin material. The results obtained from a pin on disc test are usually expressed in the form of a specific wear rate, defined as the volume of material removed per sliding distance for a given load [63].

Usually the 'pin' consists of a bearing steel ball, which is clamped in place with a chuck. Tests are also carried out using harder materials e.g. silicone nitride, aluminum oxide, zirconium oxide. The standard pin-on-disk tribometer uses a simple load arm with a tangential force sensor mounted close to the contact point so as to reduce errors due to arm compliance. The load is applied on the end of the cantilever arm (connected to the pin). Sliding speed can be varied. Friction coefficient and specific wear rate are determined. Geometry of wear track, radius, and forces on disc is schematically represented in Figure 2.5.

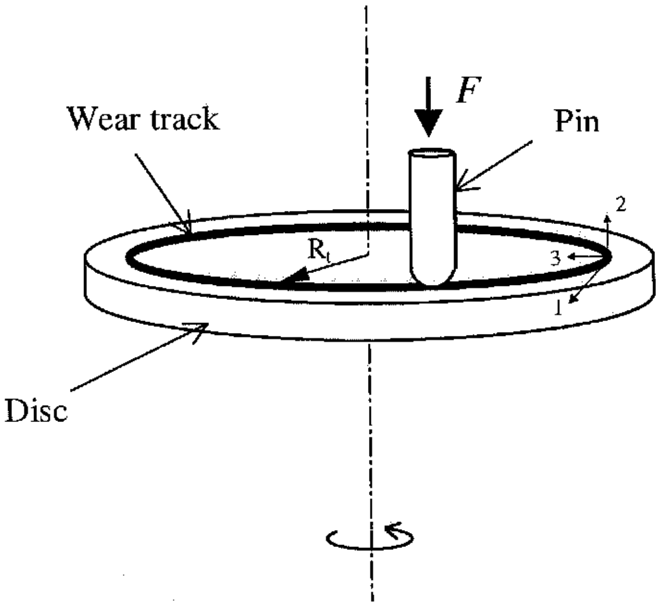

Figure 2.5 Geometry of wear track, radius, forces on disc [63].

CHAPTER 3

EXPERIMENTAL PROCEDURE

3.1 SAMPLE PREPARATION

3.1.1 Starting Materials

The characteristics of the starting materials have great influence on the formation and the structure of the final glass-ceramic, as well as their performance and reproducibility. The starting materials must not be toxic. It is also known that toxic materials decrease the biocompatibility of implant materials [64]. Hence, extra pure grade chemicals obtained from MERCK were used as starting materials. The sources of silica, magnesia and titania were SiO_2, MgO and TiO_2 powders, respectively. Fluorine was obtained from MgF_2. CaO and K_2O were supplied from their carbonates; $CaCO_3$ and K_2CO_3, respectively. $Al(OH)_3$ was used to obtain Al_2O_3. The starting materials were assumed to decompose into their stable oxides during melting. The decomposition reactions of the raw materials are assumed to take place as follows:

$2\ Al(OH)_3 \rightarrow Al_2O_3 + 3\ H_2O$

$Mg(OH)_2 \rightarrow MgO + H_2O$

$CaCO_3 \rightarrow CaO + CO_2$

$K_2CO_3 \rightarrow K_2O + CO_2$

$MgF_2 + {}^1/_2\ O_2 \rightarrow MgO + F_2$

3.1.2 Preparation of the Glass

On the basis of the formation of mica glass-ceramic, a batch composition given by Der [64] was taken under consideration. It has been shown that this composition yields to the formation of a desired microstructure for dental applications. Besides chemicals TiO_2 was added into the batch as a nucleating agent in the amount of 1 weight percent (wt%) of the total batch materials. The ingredients and the batch composition of the glasses produced in this study are given in Table 3.1.

Table 3.1 Ingredients and batch composition of the glasses used in this study.

Batch Materials	Batch Composition (wt %)
SiO_2	50.73
K_2CO_3	23.21
$Al(OH)_3$	0.80
$Mg(OH)_2$	10.42
MgF_2	8.98
$CaCO_3$	5.86
TiO_2	1.00

The starting materials were carefully weighed (± 0.0005 g) to their proper amount in an electronic balance and mixed in order to form the batches. The mixtures were ground and blended in an agatate mortar with pestle for 1/2 hour. Alcohol was used as blending medium since it hinders the loss of batch materials by drying. Also, it does not affect the final composition of the glass due to its volatility. Batches prepared were placed into an oven for drying. Drying took place at about 80 °C approximately 24 hours.

After drying, the batches were put in a platinum crucible. The crucible and its content were placed into an electrically heated muffle furnace for melting. The batch was melted at 1495 ± 5 °C. Melting took place at normal laboratory conditions without controlling the atmosphere. The melt was kept at the maximum temperature for about 20 minutes to provide chemical homogeneity. When the melting was complete; the melt was poured into a stainless steel mold to obtain disc shaped glass. Disc shaped glasses were clear and indicated no evidence of crystallinity or unmolten batch particles. The dimensions of the glass discs were approximately 30 mm in diameter and 15 mm in height. Three glass discs were cast and formed to make the necessary tribology tests. Discs were annealed at 600 °C to eliminate internal stresses formed during solidification. Schematic representation of the annealing process was illustrated in Figure 3.1. The heating and cooling rates applied during annealing were 3 °C/min.

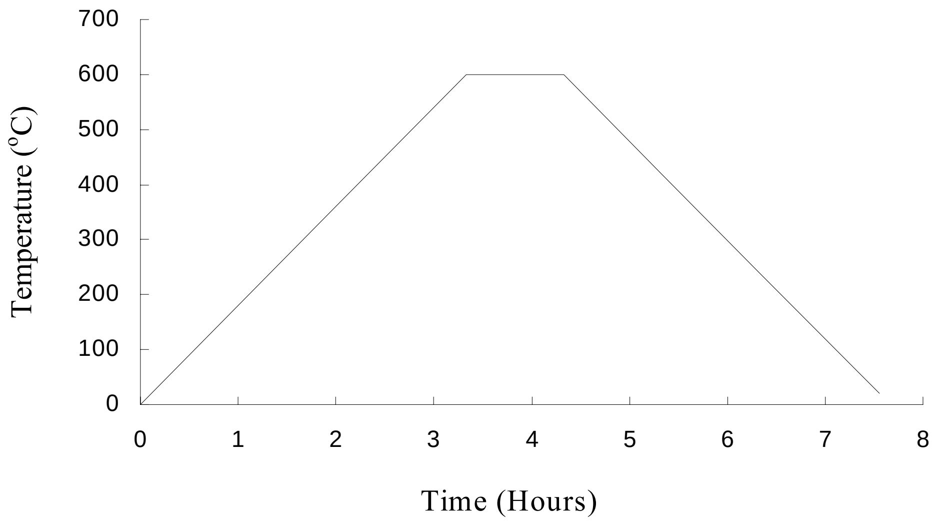

Figure 3.1 Annealing process applied to glasses.

After annealing, the glass sample was ground to eliminate surface roughness and tiny surface cracks. During this stage, four grinding papers with grades of 320, 400, 600 and 800 were used subsequently, and surface polishing followed the grinding process. The polishing was performed with the application of 0.3 μm alumina powder solution on a cloth.

3.1.3 Preparation of the Glass-Ceramic

Disc shaped glasses were subjected to a controlled heat treatment to convert them into mica glass-ceramics. The conversion was achieved by double step heat treatment. That is, the specimens were heated up to a temperature at which nuclei formed. (Hereafter it will be called as nucleation temperature.) Then, they were kept at this temperature for some time. After that, they were heated further to a temperature at which the nuclei growth took place. (Hereafter it will be called as growth temperature.) Finally, the specimens were cooled to ambient temperatures after keeping for some time at the growth temperature. The nucleation temperature and crystal growth temperature were taken as 620 °C and 940 °C, respectively. The time period at which the samples were held at nucleation temperature and the time period at which the samples were held at crystal growth temperature (hereafter they will be called as nucleation time and crystal growth time, respectively) were kept constant for 8 hours. The heating rate for the nucleation and crystal growth processes was kept constant at 5 °C/min. The samples were cooled from growth temperature to room temperature in one step at a rate of 5 °C/min. Heat treatment schedule applied to the glasses to convert them to the glass ceramics is shown schematically in Figure 3.2.

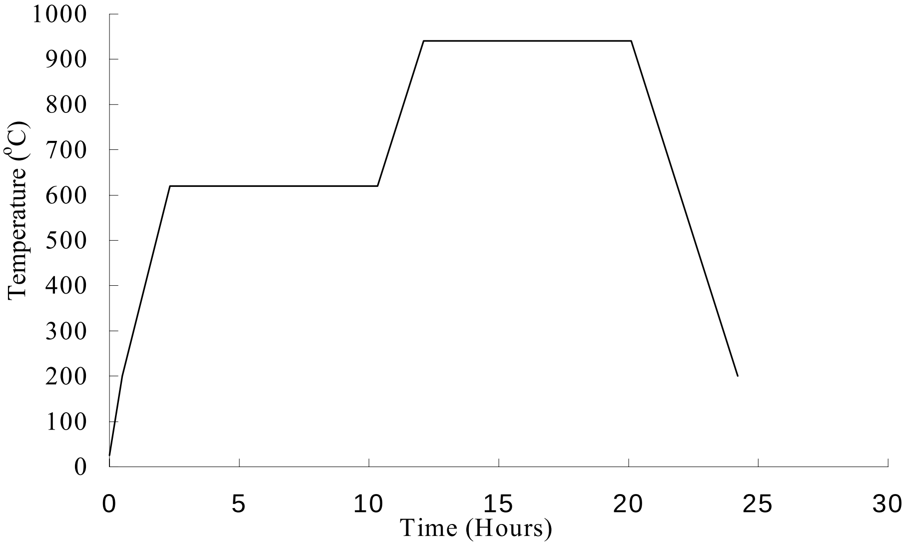

Figure 3.2 Heat treatment applied to the glasses to obtain glass ceramics.

After the heat treatment the discs appeared in milky (white) color exhibiting darker and whiter spots in the form of waves. The physical appearance of the discs implied that the phase separation occurred during heat treatment process. The nominal dimensions of the discs were approximately 31 mm in diameter and 14 mm in height. Glass-ceramic samples were surface polished to assure the surface parallelism. The polishing was performed with the application of 0.3 μm alumina powder solution on a cloth. After surface polishing the specimens were ready for the tribological tests.

3.2 TESTING

3.2.1 Tribological Testing

A pin on disc type of tribometer supplied from CSEM Instruments was employed to conduct tribological tests under the conditions listed in Table 2. The tests were done in accord with ASTM G99-95A, entitled as “Standard Test Method for Wear Testing with a Pin on Disc Apparatus”. Lubrication was not applied to avoid the complications of tribo-chemical effects.

Table 3.2 Tribology test conditions.

Ball Material	High purity zirconia
Disc Material	Glass and mica glass-ceramic
Load	2, 4, 8 N
Sliding speed	0.0025 m/s, 0.025 m/s
Data interval	100, 500, 1000, 3000, 5000, 10,000 laps (314 m maximum)
Application radius	0.005 m
Temperature	Room temperature
Environment	Ambient laboratory atmosphere, Acidic (pH=5) and Basic (pH=9) solution.
Lubrication	None

Zirconia was chosen as the counterface because of its relatively high hardness and low specific wear rate against the glass-ceramics. High purity (99.5 %) commercial zirconia balls were used as the counterface. The elastic modulus and Vickers hardness of the zirconia balls were 158-241 GPa and 7-8 GPa, respectively [65].

Average bending strength and elastic modulus of the disc shaped milky colored mica glass-ceramic sample and the parent glass sample were 121±11.5 (MPa) and 60.4±3.3 (GPa) ; 111±19.5 (MPa) and 50.7±2.1 (GPa), respectively[66]. Average Vickers mirohardness values of the mica glass-ceramic sample and the parent glass sample were 4.63±0.06(GPa) and 5.49±0.05 (GPa), respectively[66].

A sliding speed of 0.0025 m/s was chosen since this value represents a typical condition in the oral environment during mastication [27]. To compare the effects of the increasing sliding speed to the tribological behavior of the specimens, the tests were also conducted under the sliding speed of 0.025 m/s. Wear track diameter was fixed to 0.005 m. to provide the same conditions for all experiments.

For the sliding speed of 0.0025 m/s test duration ranging from 1 to 5000 laps was applied. For the sliding speed of 0.025 m/s test duration ranging from 1 to 10000 laps (maximum sliding distance of 629 m.) was applied, so that the long term wear behavior of the samples could be predicted accurately.

Loads of 2N, 4N and 8N were applied to the parent glass and mica glass-ceramic so that the effect of the load on the friction coefficient and on the worn amount could be determined.

At the last stage of the experiments, since the tooth is always in contact with different environments during mastication, environmental effect to the tribological properties of the mica glass-ceramic were tested at a constant load of 4N, with the sliding speed of 0.0025 m/s in two different solutions having the pH values of 5 and of 9. The tests were conducted with the contact surface submerged in acidic and basic environment. This was achieved by fixing the disc in a cup and filling the cup with about 20 ml. of solution.

The tests at ambient atmospheric condition were performed by placing the sample into the rotating holder against a stationary test specimen pin performs the test. Friction coefficients were monitored using winlube, the supplied windows-based data acquisition software. The normal applied load, rotational speed, and numbers of lap were adjusted before the tests conducted. Friction coefficient values were detected by means of the deflection of the elastic arm.

3.2.2 Surface Profile Measurement

For the easiness and trustability of the experiments, two points in the surface were selected as the reference points. Before starting and after completion of the certain number of laps to the tribological tests, a portable surface roughness tester supplied from Taylor Hobson, Precision Surtronic 3+. Surface profile was detected from the selected cross-sectional areas by tracing the wear track and the data obtained from two measurements were averaged.

3.3 WORN VOLUME AND SPECIFIC WEAR RATE CALCULATIONS

The track cross section area measured was converted into the worn volume by simply multiplying it by the circumference of the wear track according to the following formula:

$$V_W = A \times \pi \times d \quad \text{.........Eq.1}$$

Where V_W, is worn volume in mm^3, A is the worn area in mm^2, π is the constant (22/7), and d is the mean wear track diameter, which is fixed to a value of 0.01m during the experiment.

There was no significant pin wear in the samples during the tribological tests. Therefore pin wear has not been taken into consideration when wear volume is calculated. The specific wear rate of samples were calculated by the following formula[67].

$$W_s = \frac{V_W}{F \times S} \quad \text{.......................................Eq.2}$$

Where W_s is the specific wear rate of the sample in $mm^3/N.m$, V_W is the worn volume, F is the friction force applied in Newton(N), S is the total sliding distance in meters (m).

3.4 EXPERIMENTAL FLOWCHART

Schematic representation of the experimental procedure for determining the tribological propeties behavior of the mica glass-ceramic studied is shown in Figure 3.3.

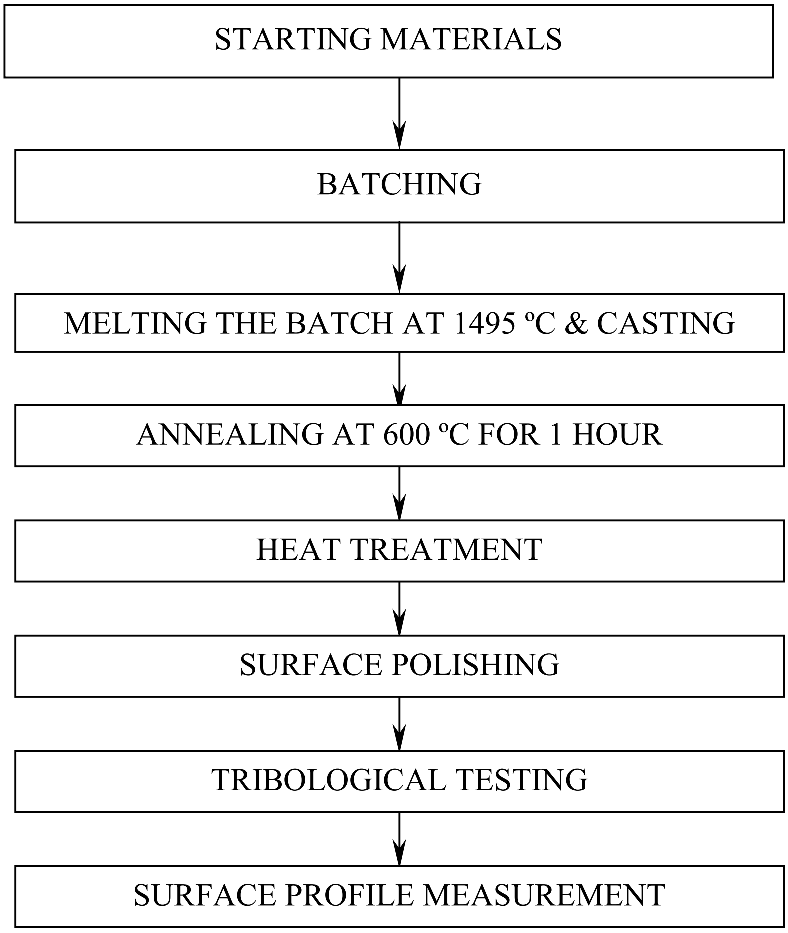

Figure 3.3 Schematic representation of the experimental procedure for detemining the tribological properties of the mica glass-ceramic studied.

CHAPTER 4

RESULTS AND DISCUSSION

4.1 GENERAL

The data obtained during experimental studies of the thesis work are presented in this section.

The disc shaped glass samples were formed by using the experimental procedure as described in Section 3.1.2. Then a double step heat treatment schedule as described in Section 3.1.3 was applied to one of the glasses, to convert it into the mica glass-ceramic. Nucleation and crystall growth temperatures were taken as 620 °C and 940°C, respectively. The sample was held at these temperatures for 8 hours. The heating, and the cooling rates were 5 °C/min .

After completion of the heat treatment the samples were surface polished. Finally tribological tests, as described in Sections 3.3.1-3.3.3, were conducted to obtain data on the tribological properties of the samples. The data were gathered through quantitative measurements and calculations.

4.2 FRICTION COEFFICIENTS

Friction coefficients were determined as functions of number of laps, sliding distance, sliding time, applied load, sliding speed, and environment.

4.2.1 Friction Coefficient of the Parent Glass

Although the data on the friction coefficient of the parent glass and mica glass-ceramic were gathered, only the results of mica glass-ceramic have been discussed since the tribological properties of mica glass-ceramic are of interest of this study. However the results gathered on the parent glass were tabulated in Appendix A.

4.2.2 Friction Coefficient of the Mica Glass-Ceramic

Mean friction coefficient of the mica glass-ceramic studied were measured under different experimental conditions and were given in Tables 4.1 and 4.2. Some of the data points were not determined due to the discontinuity of the electricity during the tests. The standard deviations of the determinations were presented in Tables 4.3 and 4.4. As seen from the tables, in general, friction coefficient of the glass-ceramic increased with increasing number of laps, sliding speed, applied load; and pH of the environment.

As the data indicates, friction coefficient of the mica glass-ceramic studied varied between 0.184 and 0.913 depending upon the test parameters. The friction coefficients could be seperated into distinct high or low levels, where the friction coefficients less than 0.1 corresponded to low level and 0.4 to 0.9 corresponded to the high level [68]. Therefore, the data obtained in this study can be interpreted as low, medium, and high level of friction coefficients.

When a comparison is made between the data obtained on the mica glass-ceramic, (see Tables 4.1 and 4.2), and those obtained on the parent glass, (see tables A1 and A2), in general, the mica glass-ceramic had lower friction coefficient than the parent glass. For some experimental conditons the mica glass-ceramic had higher friction coefficient than the parent glass. The difference between the friction coefficients of these two materials was not large.

Table 4.1 Mean friction coefficient of the mica glass-ceramic measured at loads of 2N, 4N, and 8N and at sliding speeds of 0.0025m/s and 0.025 m/s for different number of laps.

Number of Laps	Mean Friction Coefficient (μ)					
	2N		4N		8N	
	0.0025 m/s	0.025m/s	0.0025 m/s	0.025m/s	0.0025 m/s	0.025m/s
0-100	0.294	0.339	0.188	0.325	0.505	0.184
100-500	0.323	0.346	0.191	0.715	0.193	0.436
500-1000	0.344	0.343	0.198	0.901	0.197	0.535
1000-3000	0.336	-	0.182	0.903	0.194	0.640
3000-5000	0.331	0.355	0.220	0.899	0.188	0.913
5000-10000	-	0.543	-	0.908	-	0.831

Table 4.2 Mean friction coefficient of the mica glass-ceramic measured at a load of 4N and at a sliding speed of 0.0025m/s in acidic and basic solutions for different number of laps.

Number of Laps	Friction Coefficient (μ)	
	pH=5	pH=9
0-100	0.248	0.646
100-500	0.245	0.695
500-1000	0.256	0.718
1000-3000	0.284	0.723
3000-5000	0.265	0.793

Table 4.3 Standard deviations of the mean friction coefficient of the mica glass ceramic measured at loads of 2N, 4N, and 8N and at sliding speeds of 0.0025m/s and 0.025 m/s for different number of laps.

Number of Laps	Mean Friction Coefficient (μ)					
	2N		4N		8N	
	0.0025 m/s	0.025m/s	0.0025 m/s	0.025m/s	0.0025 m/s	0.025m/s
0-100	0.029	0.021	0.016	0.180	0.290	0.074
100-500	0.015	0.034	0.017	0.248	0.086	0.252
500-1000	0.016	0.018	0.016	0.070	0.034	0.119
1000-3000	0.013	-	0.016	0.026	0.029	0.065
3000-5000	0.016	0.028	0.040	0.032	0.038	0.044
5000-10000	-	0.185	-	0.024	-	0.194

Table 4.4 Standard deviations of the mean friction coefficient of the mica glass-ceramic measured at a load of 4N and at a sliding speed of 0.0025m/s in acidic and basic solutions for different number of laps.

Number of Laps	Friction Coefficient (μ)	
	pH=5	pH=9
0-100	0.025	0.111
100-500	0.033	0.122
500-1000	0.046	0.086
1000-3000	0.044	0.117
3000-5000	0.044	0.108

Friction coefficients obtained after completion of the 1st, 100th, 500th, 1000th, 3000th, 5000th, and the 10000th laps were tabulated in Tables 4.5 and 4.6. As seen from the tables friction coefficients varied from a lowest value of 0.1775 to a highest value of 0.9425. The determination points, in general, reflected the maximum values obtained during the test for a given set of experimental conditions. A comparison of Tables 4.1 and 4.2 with Tables 4.5 and 4.6 reveals that the mean and the maximum friction coefficients were different from each other although the difference is small. The difference is attributed to the surface properties of the samples. At the beginning of the test surface of the sample was smooth and even but, surface irregularities were formed due to friction and wear during the experiment. Mean friction coefficients were taken into consideration rather than the coefficients obtained after completion of certain number of laps throughout this study.

Table 4.5 Friction coefficient of the mica glass-ceramic measured at loads of 2N, 4N, and 8N and at sliding speeds of 0.0025m/s and 0.025 m/s at the end of different number of laps.

Number of Laps	Friction Coefficient (μ)					
	2N		4N		8N	
	0.0025 m/s	0.025m/s	0.0025 m/s	0.025m/s	0.0025 m/s	0.025m/s
1	0.2808	0.3013	0.1775	0.2030	0.1846	0.0650
100	0.3075	0.3405	0.2000	0.5028	0.7068	0.2451
500	0.3371	0.3424	0.1820	0.9126	0.1965	0.9375
1000	0.3294	0.3419	0.2178	0.9142	0.1888	0.8722
3000	0.3270	0.3875	0.1993	0.9037	01892	0.7587
5000	0.3121	0.4058	0.3250	0.9153	0.2266	0.9237
10000	-	0.8897	-	0.9011	-	0.9425

Table 4.6 Friction coefficient of the mica glass-ceramic measured at a load of 4N and at a sliding speed of 0.025 m/s in acidic and basic solutions at the end of different number of laps.

Number of Laps	Friction Coefficient (μ)	
	pH=5	pH=9
1	0.2798	0.3876
100	0.2557	0.4235
500	0.2887	0.6577
1000	0.2586	0.8931
3000	0.3103	0.7594
5000	0.3518	0.8204

A representative figure showing the variation of the friction coefficient of the mica glass-ceramic studied as functions of number of laps, sliding distance, and sliding time for the short term (within the first 100 laps), and for the long term (between the 1000th and the 3000th laps) were illustrated in Figures 4.1.(a) and 4.1.(b). The test was conducted under ambient atmospheric conditions at a sliding speed of 0.0025 m/s and at a load of 2N. As seen from Figure 4.1.(a) friction coefficient changed from 0.2808 to 0.3075, when the number of laps increased from the 1st to the 100th lap. Friction coefficients obtained from initial number of laps, had relatively low values when compared to those obtained from later number of laps. It is clearly seen in Figure 4.1.(b) that the friction coefficient increased with increasing number of laps, sliding distance, and sliding time due to the long term wear process. The mean friction coefficient obtained within this range was 0.331. The increase in the coefficient, with increasing number of laps was an expected result since the roughness of the contact area increases as the surface worn out by the zirconia pin.

In general, an increase followed by a decrease in the friction coefficient was observed within the first 5 laps for all of the tests. Thereafter friction coefficients were more or less the same. Similar behavior was observed also by Kopalinsky and Black [69]. They have explained this decrease or increase in the friction coefficient at the early stage of sliding with the surface properties. Another reason for the increase or decrease at the initial laps may be attributed to the stabilization of the machine to the friction between the pin and the surface of the material.

Therefore the values obtained at the initial number of laps may not be reliable and representative. The overall increase in the friction coefficients of the mica glass-ceramic from the 1st lap till the end of the 100th lap was 9.51%. However if the first 5 laps are ignored, then the increase from 0.2875 to 0.3075 becomes 6.96%. The results reveal that there is not a significant change in the friction coefficient.

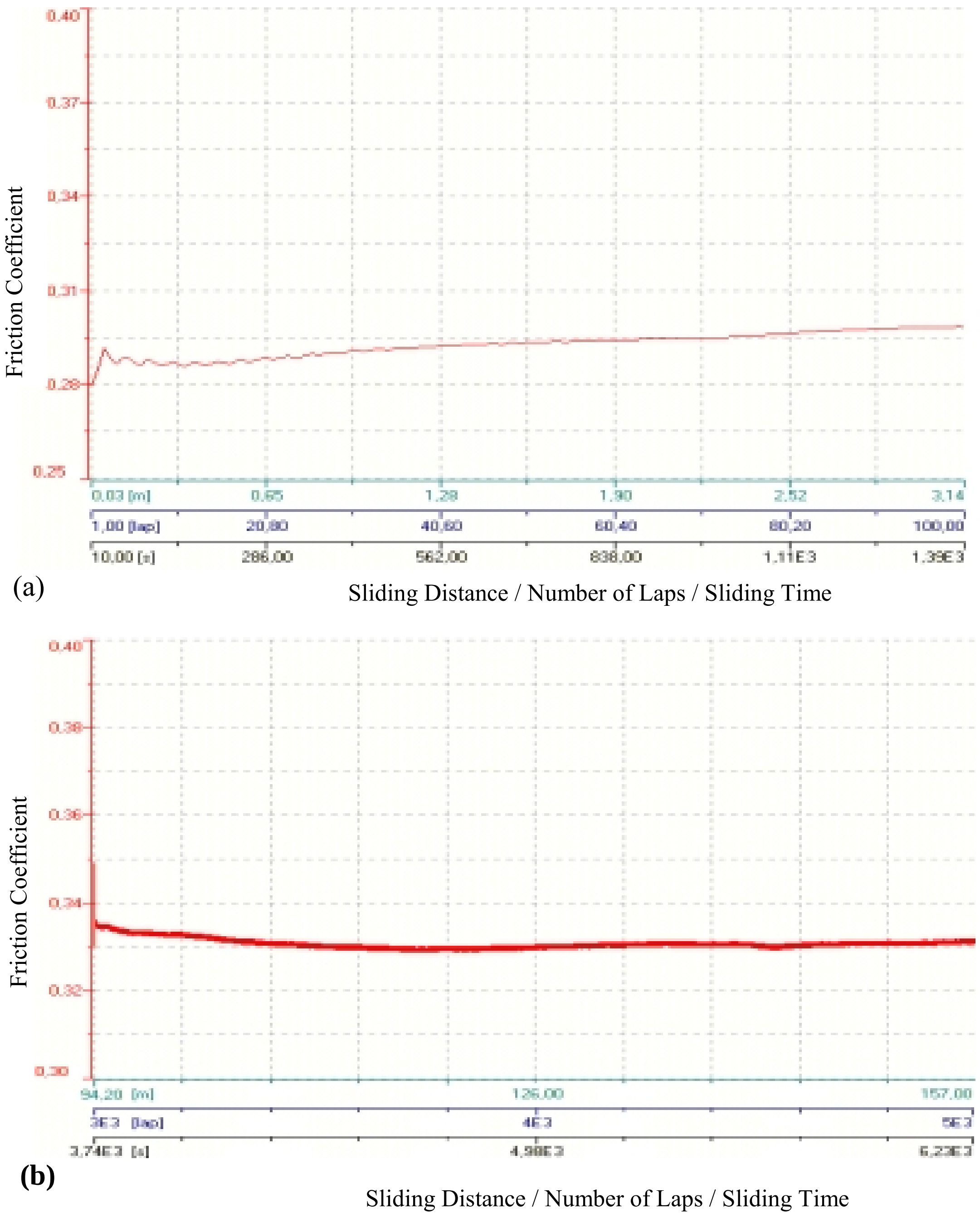

Figure 4.1 Variation of friction coefficient of the mica glass-ceramic studied as functions of number of laps, sliding distance, and sliding time. The applied load was 2N the sliding speed was 0.0025 m/s and the environment was ambient. Data was obtained between;

(a) 1-100 laps.

(b) 3000-5000 laps.

In order to determine the effect of sliding speed on the friction coefficient of the mica glass ceramic, the tests were conducted at the same experimental conditions but at a faster sliding speed of 0.025 m/s. Representative figures showing the variation of the friction coefficient of the mica glass-ceramic studied as functions of number of laps, sliding distance, and sliding time for the short term (within the first 100 laps), and for the long term (between the 3000th and the 5000th laps), and between the 5000th and the 10000th laps were illustrated in Figures 4.2.(a)-4.2.(c).

As seen from Figure 4.2.(a), friction coefficient gradually increased from 0.3013 to 0.3405, between the 1st lap and the 100th lap, corresponding to a 13.01% increase. However friction coefficient in long term increased abruptly with strong fluctuations. The increase in friction coefficients was from 0.3875 to 0.4058 in Figure 4.2.(b), and increase in Figure 4.2.(c) was from 0.4058 to 0.8897 between the 3000th and the 5000th, and between the 5000th and the 10000th laps, respectively. The results indicate that as expected the sliding distance had an effect on the friction coefficient. However, there occurred an unexpected behavior in long-term wear after the 7500th lap as seen in Figure 4.2.(c). This behavior is attributed to the change of dominant wear mechanism from abrasive to adhesive. However the change in the wear modes could not be completely clarified by just looking into the graphical representations; instead a microstructural study together with the graphical representations would give a more realistic approach.

A comparison made on Figures 4.1 and 4.2, revealed that even though there was a noticeable increase in friction coefficient with increasing sliding speed from 0.0025 m/s to 0.025 m/s, the increase was not much at the applied load of 2N at ambient atmosphere till the 5000th lap. However at a sliding speed of 0.025 m/s, fluctuations in friction coefficient caused by the increasing sliding speed were detected with increasing number of laps.

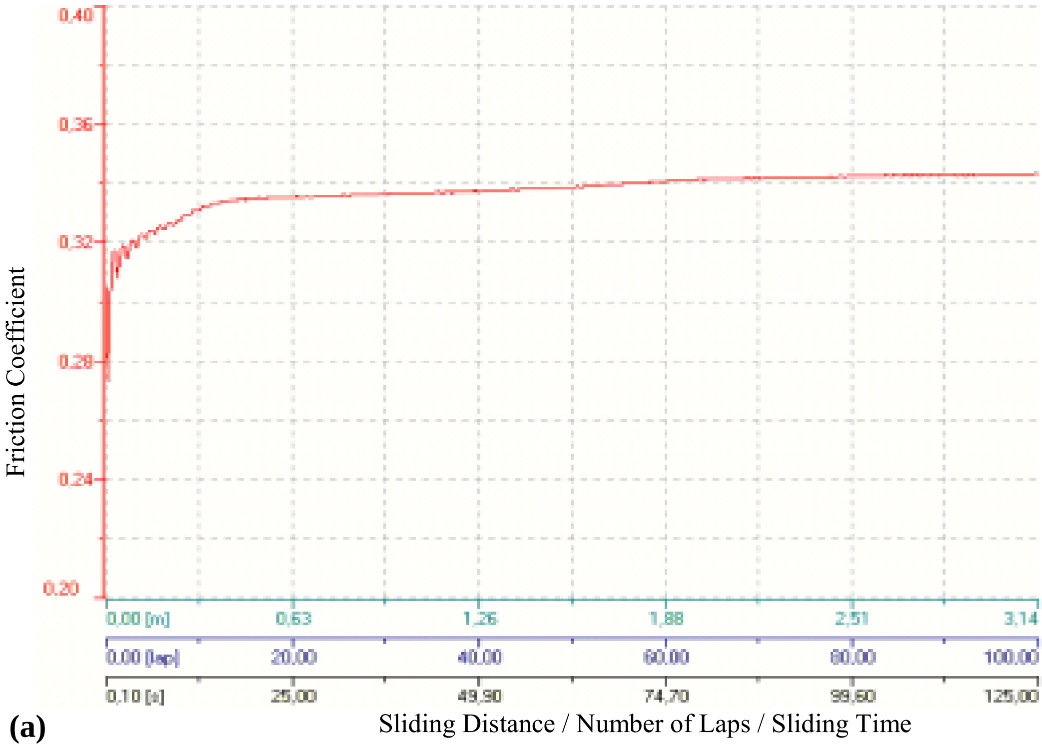
0,40
0,36
0,32
0,28
0,24
0,20
Friction Coefficient
0,00 [m]
0,63
1,26
1,88
2,51
3,14
0,00 [lap]
20,00
40,00
60,00
80,00
100,00
0,10 [s]
25,00
49,90
74,70
99,60
125,00
(a)
Sliding Distance / Number of Laps / Sliding Time

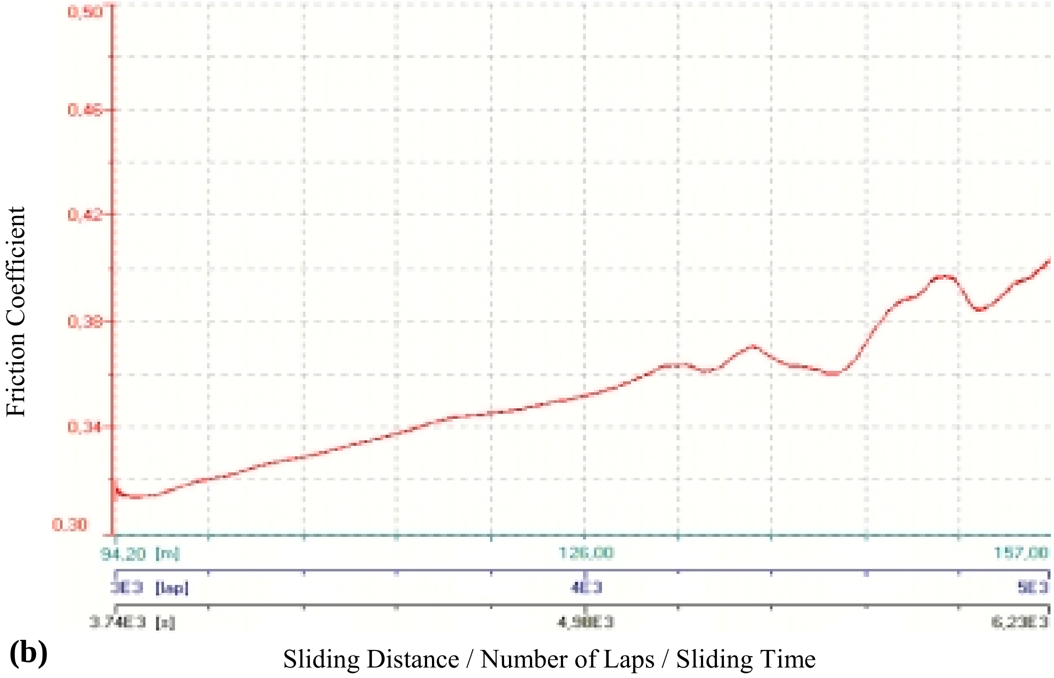
0,50
0,46
0,42
0,38
0,34
0,30
Friction Coefficient
94,20 [m]
126,00
157,00
3E3 [lap]
4E3
5E3
3,74E3 [s]
4,98E3
6,23E3
(b)
Sliding Distance / Number of Laps / Sliding Time

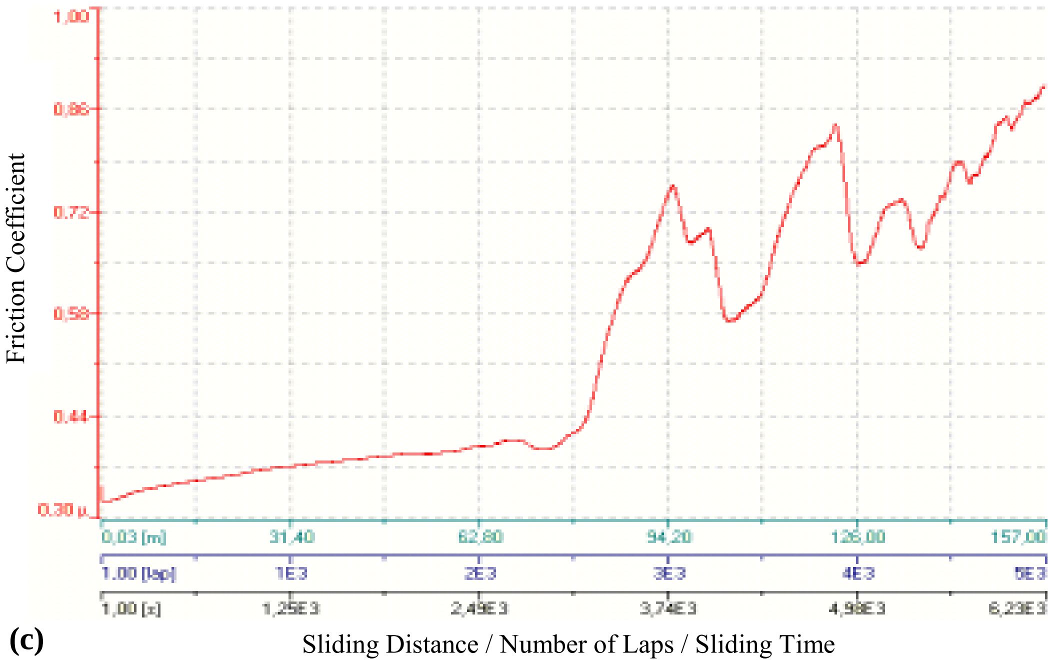

Figure 4.2 Variation of friction coefficient of the mica glass-ceramic studied as functions of number of laps, sliding distance, and sliding time. The applied load was 2N the sliding speed was 0.025 m/s and the environment was ambient. Data was obtained between;
(a) 1-100 laps.
(b) 3000-5000 laps.
(c) 5000-10000 laps.

In order to determine the effect of applied load on the friction coefficient of the mica glass ceramic, the tests were conducted at the same experimental conditions but at the loads of 4N and 8N. The results obtained with a load of 4N were presented in Figures 4.3.(a), and 4.3.(b) for the sliding speed of 0.0025 m/s and in Figures 4.4.(a) - 4.4.(c) for the sliding speed of 0.025 m/s.

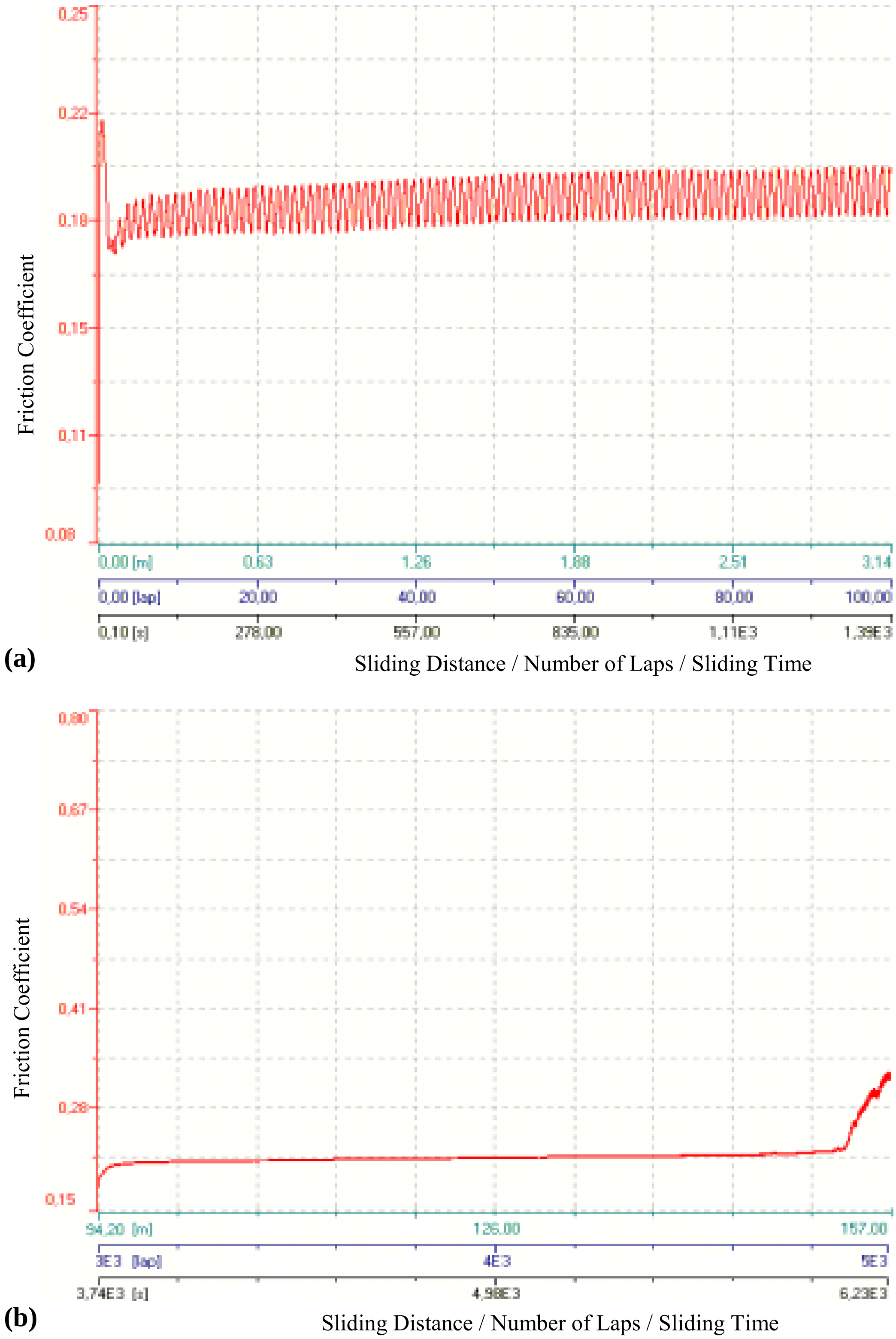

Figure 4.3 Variation of friction coefficient of the mica glass-ceramic studied as functions of number of laps, sliding distance, and sliding time. The applied load was 4N the sliding speed was 0.0025 m/s and the environment was ambient**.** Data was obtained between;

(a) 1-100 laps.

(b) 3000-5000 laps.

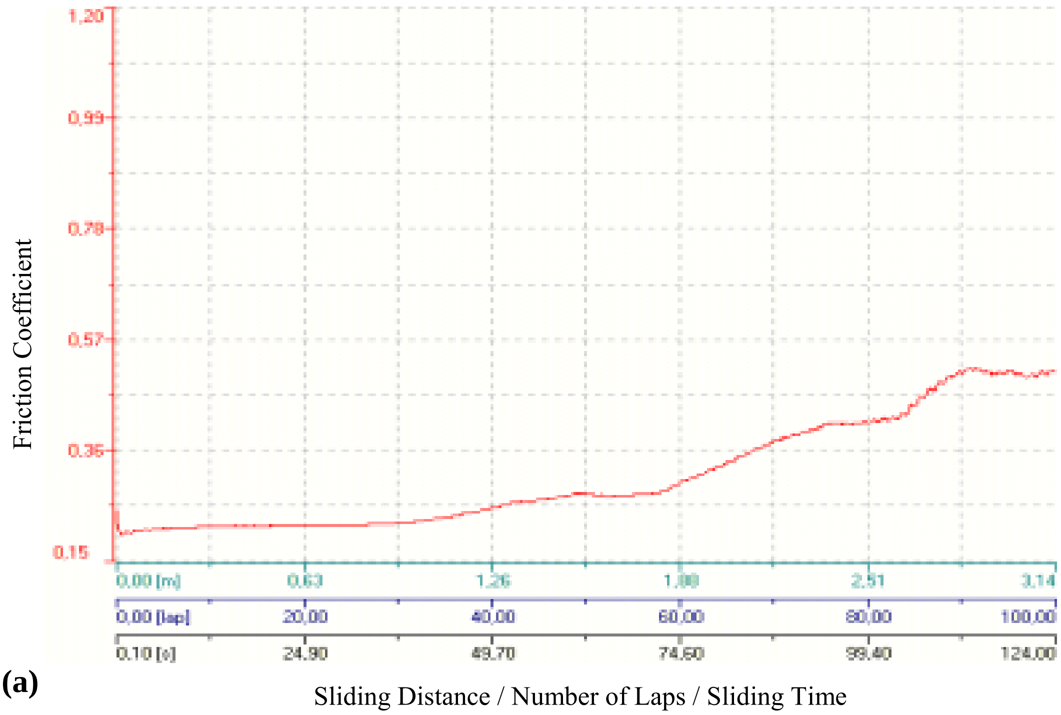
Friction Coefficient
1,20
0,99
0,78
0,57
0,36
0,15
0,00 [m]
0,63
1,26
1,88
2,51
3,14
0,00 [lap]
20,00
40,00
60,00
80,00
100,00
0,10 [s]
24,90
49,70
74,60
99,40
124,00
Sliding Distance / Number of Laps / Sliding Time

(a)

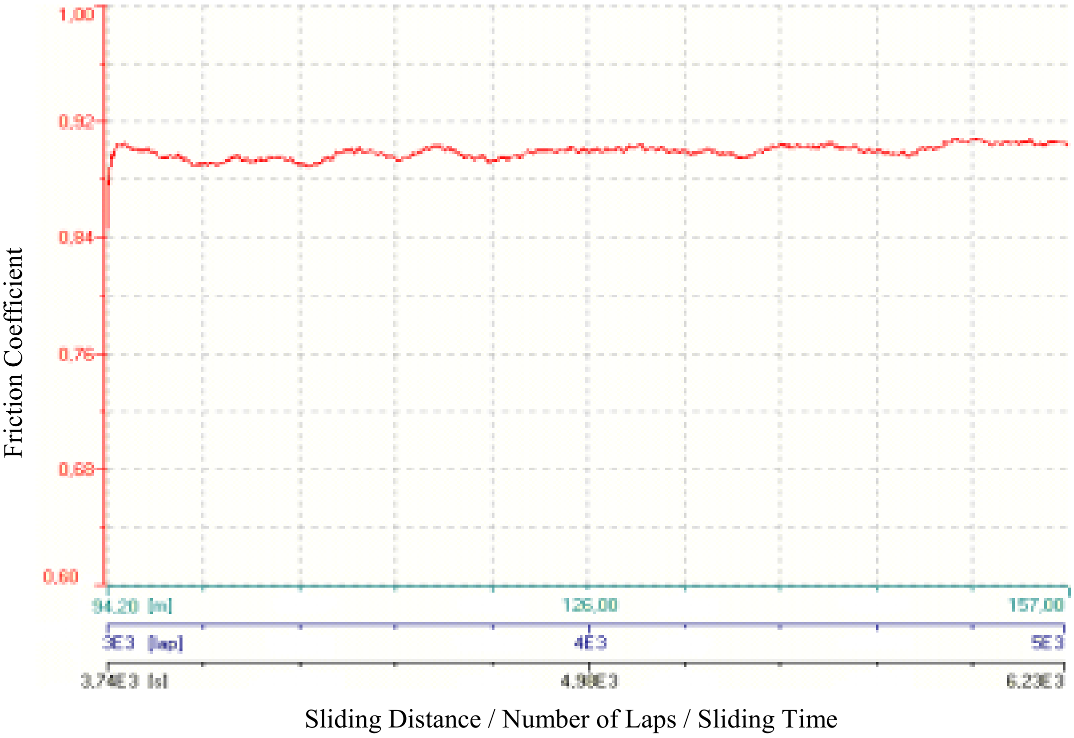
Friction Coefficient
1,00
0,92
0,84
0,76
0,68
0,60
94,20 [m]
126,00
157,00
3E3 [lap]
4E3
5E3
3,74E3 [s]
4,98E3
6,23E3
Sliding Distance / Number of Laps / Sliding Time

(b)

(c)

Figure 4.4 Variation of friction coefficient of the mica glass-ceramic studied as functions of number of laps, sliding distance, and sliding time. The applied load was 4N the sliding speed was 0.025 m/s and the environment was ambient. Data was obtained between;
(a) 1-100 laps.
(b) 3000-5000 laps.
(c) 5000-10000 laps.

The variation of friction coefficient within the first 100 laps, and between the 3000th and the 5000th laps were given in Figure 4.3.(a), and in Figure 4.3.(b), respectively. Although 100% filtering applied to get rid of the fluctuations in very short intervals such as in ¼ seconds there were fluctuations in small intervals. These fluctuations mainly resulted from the local friction coefficient, which is a function of the local shear strength at the contact interface and the local contact geometry[70]. In addition, various statistical variables, such as micro structures, surface roughness, flash temperatures, local contamination, adhesive transfers, free wear particles and tribochemical reactions on the contact surfaces on the microscale are all related to the constants through the local values of the friction coefficient and the wear resistance of tested material. If the fluctuations, which are about 0.2, were ignored, there was a smooth line changing fom 0,1775 to 0.2000 at the first 100 laps, corresponding to a 12.6% increase, however this increase becomes about 5% if the first five laps were ignored. This increase is an expected result as discussed earlier and is due to the change in the surface roughness.

As seen in Figure 4.3.(b), the friction coefficient changed from 0.1993 to 0.3250, between the 3000th and the 5000th laps. The curve of the variation of friction coefficient with increasing number of laps were very smooth until the 4875th lap, but then it increased abruptly. This behavior is seen also in Figure 4.2.(c), where the sliding speed is lower and applied load is higher. In addition, this behavior was observed at a sliding speed of 0.025 m/s with an applied load of 2N after the 7500th lap. It may be concluded that applied load is more dominant factor affecting the friction coefficient and therefore wear mechanisms than sliding speed. The tribological behavior is characterized by a very small flow of worn particles, when friction values remain stable during the experiments[71], This behavior is seen in Figure 4.3.(b) between the 3000th and the 4950th laps.

A comparison between Figures 4.3.(a) and 4.3.(b) made it obvious that the friction coefficient increased with increasing number of laps especially after about the 4900th lap. However if the comparison was made among the data obtained at loads of 2N and 4N at a sliding speed of 0.0025m/s, an unexpected result is seen. An increase in the mean friction coefficient with increasing applied load was expected according to Amonton’s Law of Friction, which states that the relationship between the friction force (F) and normal load (N) is linear, i.e., $F/N = \mu$. [72]. However the mean friction coefficients obtained were not increased by helding the other factors the same and even decreased when the applied load was increased from 2N to 4N. Our fundamental understanding to explain the behavior observed as yet is limited. However, this result could be mainly due to the experimental error. The data, in general, depends upon the amount of the surface irregularities that is the surface roughness. The decrease may be due to either the decrease in surface roughness or the microstructural arrangements that occurs during the test in the mica glass-ceramic. In addition the experimental errors may be due to the calibration of the tribometer and the arrangement between the pin and the disc. Calibration of the tribometer gives a maximum 2% uncertainity and deviations from the parallellism between the pin and the disc gives much more uncertainity. Moreover it can also be the result of the decrease in the true area of contact. The true area of contact was explained by most of the friction theories [73], and they assume that force per unit area that resists sliding (the shear strength) is constant, from which it follows that frictional force is proportional to the true area of contact. It is quite appropriate with the Amontons's second law[73], for the sum of all contact points, which is established by microscopic surface irregularities, determines the true area of contact and, hence, the observed frictional force.

The friction behavior observed is not sufficient to conclude that friction coefficient decreases with increasing applied load. Therefore, checking the experimental data obtained at 8N load and comparing them by the data obtained from earlier studies is a more logical way to evaluate the variation of friction coefficients of the mica glass-ceramic studied with increasing applied load.

The variation in the friction coefficient with increasing number of laps at a faster sliding speed of 0.025 m/s at a load of 4N was depicted in Figure 4.4. The variation at the first 100 laps were given in Figure 4.4.(a). The variation between the 3000th and between the 5000th and the 10000th laps were given in Figures 4.4.(b) and 4.4.(c), respectively.

In Figure 4.4.(a), at the beginning of the experiment (at 1st lap), friction coefficient was measured as 0.2030 and increased as the number of laps increased. The increase was not much before the 58th lap, but became immediately obvious afterwards. It reached the value of 0.5028 at the end of the 100th lap.

The appearance of the Figures 4.4.(b) and 4.4.(c) was more or less the same. There were some small fluctuations. The graphs were quite smooth. Friction coefficient had small change. It was 0.9037 at the 3000th lap, but increased to 0.9153 at the 5000th lap, and after the 10000th lap decreased to 0.9011.

Therefore these graphs depict that at a load of 4N and at the sliding speed of 0.0025 m/s, the overall friction coefficient value increased as the number of laps increased. The increase from the beginning till the end of the experiment was noticeable but not significant. That is it can be ignored. However, since the speed during mastication in the oral environment is 10 times slower than the applied sliding speed of 0.025 m/s, the results obtained at a load of 4N, and at a sliding speed of 0.0025 m/s is more realistic.

When a comparison is made between the data obtained at the applied loads of 2N and 4N at a sliding speed of 0.025m/s it can easily be concluded that as the load increased the friction coefficient increased. The increase was quite obvious after the 100th lap.

The values obtained for the friction coefficient of the mica glass-ceramic investigated in this study were comparable to those for the mica glass-ceramic of similar composition reported in the literature. Jahanmir and Dong[11] studied short term wear mechanisms of the glass-ceramics, DICOR, and they found that average friction coefficients for three tests ranged from 0.70 to 0.77 at a load of 4.9 N at a sliding speed of 0.0014 m/s by using alumina pin. Their results were equal to the results in long term friction data obtained in this study which is conducted at a load of 4N and at a sliding speed of 0.0025 m/s by using zirconia pin. Jahanmir and Dong conducted their experiment at a lower speed of 0.0014 m/s, and a higher applied load of 4.9N, therefore the obtained results were expected to differ. However the friction coefficient were more or less the same, which was attributed to the change in the dominant wear mechanism. By comparing two of the study, it can be said that, the dominant factor which yields to more increase in friction coefficient was sliding speed. However this was not the case in this study; the dominant factor was the applied load rather than the sliding speed. Therefore these results showed the dependency of the dominant wear mechanism to the increasing sliding speed and the applied loads. Dominant wear mechanism may also change during the experiment depending on the surface properties, and to find this change it is needed to investigate the velocity accommodations in microscopic level during the experiment. Results indicated that the friction coefficient of the mica glass-ceramic produced in this study was comparable to that of a commercially produced glass ceramic, DICOR.

In order to see the effect of applied loads higher than 4N on the friction coefficient of the mica glass ceramic, the tests were run also at the load of 8N. The sliding speeds were also changed to see the effect of sliding speed. The results were presented in Figures 4.5.(a) and 4.5.(b), and Figures 4.6.(a) - 4.6.(c) for the sliding speeds of 0.0025 m/s, and 0,025 m/s, respectively. The variation of the friction coefficient within the first 100 laps and between the 1000th and the 3000th laps were given in Figure 4.5.(a), and in Figure 4.5.(b), respectively. Friction coefficient was 0.1846 at the first lap and increased to 0.7068 at the end of the 100th lap. However after performing the surface profile analysis, a drastic decrease occurred in the friction coefficient. This sharp decrease may be due to the change in the contact surface during the mechanical arrangement after surface profile analysis. The arrangement between the pin and the surface of the mica glass-ceramic may be the cause of the decrease. In addition, clearing the worn particles away may have some decreasing effect. The friction coefficient changed from 0.1888 at the 1000th lap to 0.1892 at the end of the 3000th lap. The fluctuations in very short intervals reached to 0.34 approximately as seen in Figure 4.5.(a). In addition during experiment at a load of 8N the tribometer stopped in short intervals with a warning so-called “Absolute Tangential Force is too high”. Therefore it is believed that the results obtained at a load of 8N are not precise and are not reflecting the long-term friction behavior especially at the sliding speed of 0.025 m/s.

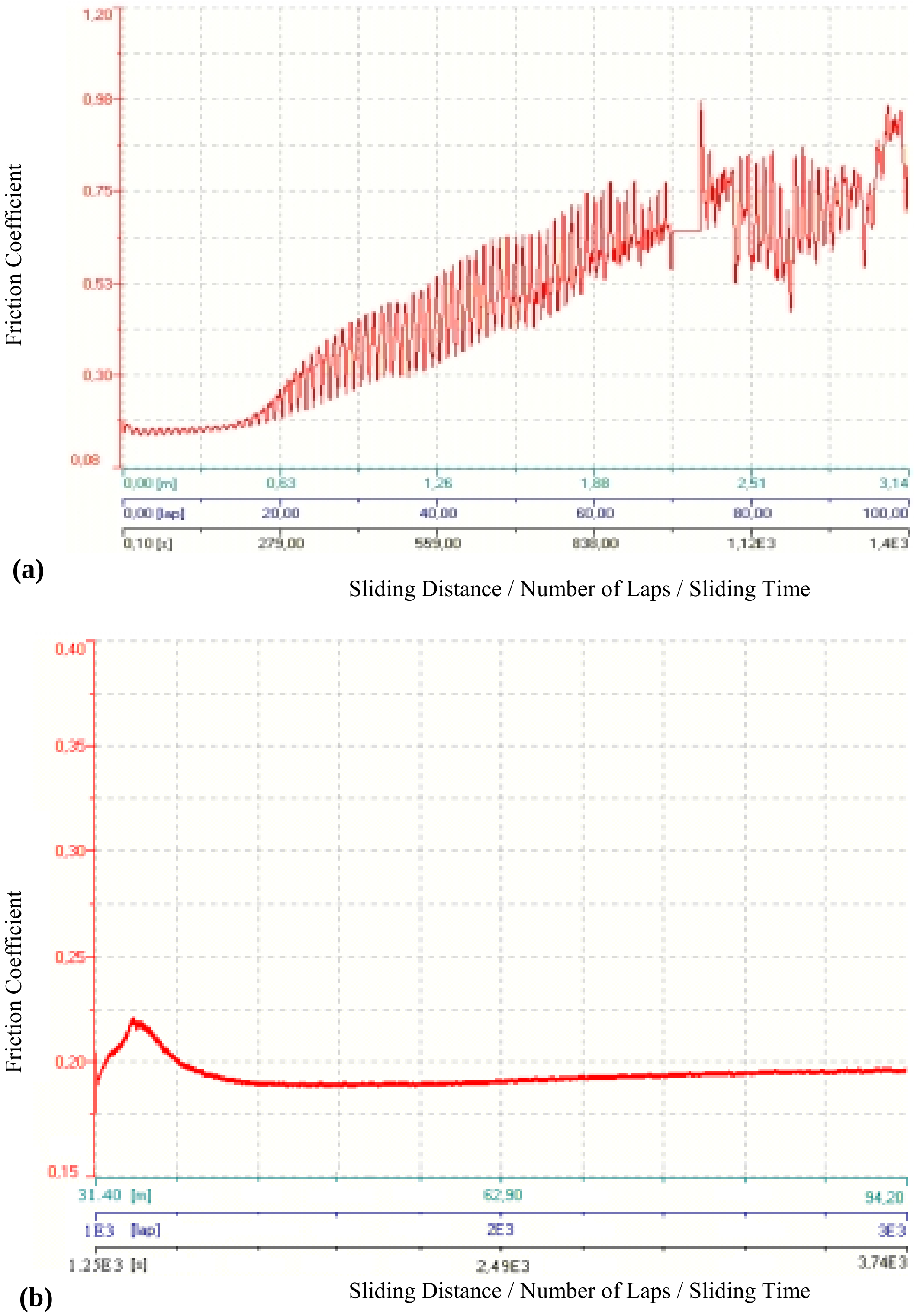

Figure 4.5 Variation of friction coefficient of the mica glass-ceramic studied as functions of number of laps, sliding distance, and sliding time. The applied load was 8N the sliding speed was 0.0025 m/s and the environment was ambient**.** Data was obtained between;

(a) 1-100 laps.

(b) 1000-3000 laps.

The strong fluctuations observed at the friction coefficient as seen in Figure 4.5.(a) suggest that several velocity accommodation mechanisms act simultaneously or in relay. The amplitude of these fluctuations decreases when the sliding speed and the normal load increase. They are associated with stick-slip phenomena, but can also be the consequence of a deviation from surface parallelism of samples[74].

In order to see the effect of a faster sliding speed on the friction coefficient of the mica glass-ceramic, the test were conducted also at 0.025 m/s at the same load. Since the tribometer gave an error sign during the experiment, the whole experiment could not be conducted continuously. Instead it was conducted in short intervals. Therefore no graphical representations was obtained for the variation of friction coefficient in long term. However the test was carried out till the 10000th lap. The friction coefficient results were given for the first 100 laps in Figure 4.6.(a), for the laps between the 4500th and the 5000th lap in Figure 4.6.(b), and for betweeen the 9000th and the 9744th laps in Figure 4.6.(c). There was a gradual and continuous increase in friction coefficient within the first 100 laps as seen in Figure 4.6.(a). The values corresponding to the 1st and 100th laps were 0.0650 and 0.2451, respectively. In Figures 4.6.(b) and 4.6.(c) appeared more or less the same as graphical representations although the number of laps differ. The friction coefficient changed in the range of 0.5201 to 0.9532. The maximum value of 0.9640 was seen during the experiment. If the friction coefficient value at the 10000th lap were considered, the diminishing effect of the counterface roughness as Kalin et al. pointed out in their study could be seen [75]. There is good correlation in the data after the 500th lap at applied loads of 2N, 4N, and 8N, at a sliding speed of 0.025 m/s, but the same correlation was not observed at a lower sliding speed of 0.0025 m/s. From the experiments conducted at an ambient atmosphere, it may be concluded that as the sliding speed increased, load is a dominant factor in increasing the friction coefficient. However at lower sliding speeds, it was not possible to determine the dominant factor by just loking to and comparing the data obtained. The experiments should be repeated and the scanning electron microscope(SEM) examination could be done to determine the actual behavior and the velocity accommodations.

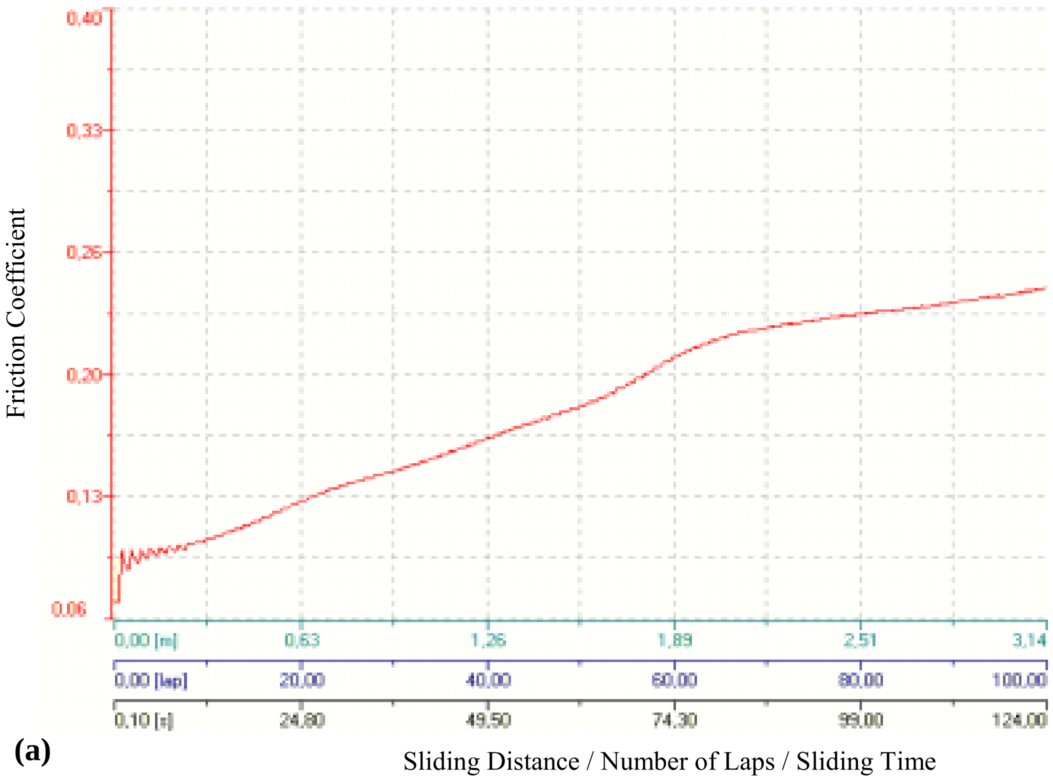
Friction Coefficient
0,40
0,33
0,26
0,20
0,13
0,06
0,00 [m]
0,63
1,26
1,89
2,51
3,14
0,00 [lap]
20,00
40,00
60,00
80,00
100,00
0,10 [s]
24,80
49,50
74,30
99,00
124,00
Sliding Distance / Number of Laps / Sliding Time

(a)


Friction Coefficient
1,00
0,90
0,80
0,70
0,60
0,50
1.42 [m]
1.49
1.57
4.5E3 [lap]
4.75E3
5E3
5.61E3 [s]
5.92E3
6.23E3
Sliding Distance / Number of Laps / Sliding Time

(b)

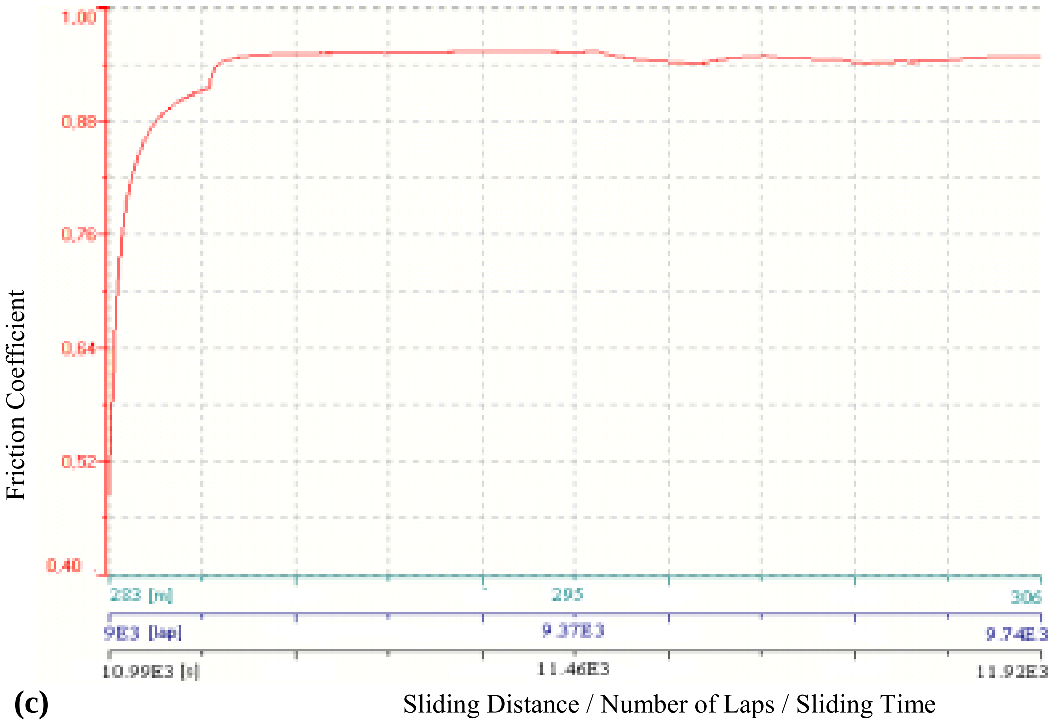

(c)

Figure 4.6 Variation of friction coefficient of the mica glass-ceramic studied as functions of number of laps, sliding distance, and sliding time. The applied load was 8N the sliding speed was 0.025 m/s and the environment was ambient. Data was obtained between;
(a) 1-100 laps.
(b) 4500-5000 laps.
(c) 9000-9744 laps.

In order to determine the environmental effect on the friction coefficient of the mica glass-ceramic, the tests were conducted at a constant load of 4N and at a constant sliding speed of 0.0025 m/s both in acidic solution of pH=5, and in basic solution of pH =9. The results of the friction coefficients were given in Figure 4.7 for acidic solution and in Figure 4.8 for basic solution. First 100 laps were depicted in Figure 4.7.(a), the laps between the 1000th and the 3000th and between the 3000th and the 5000th were given in Figures 4.7.(b) and 4.7.(c), respectively.

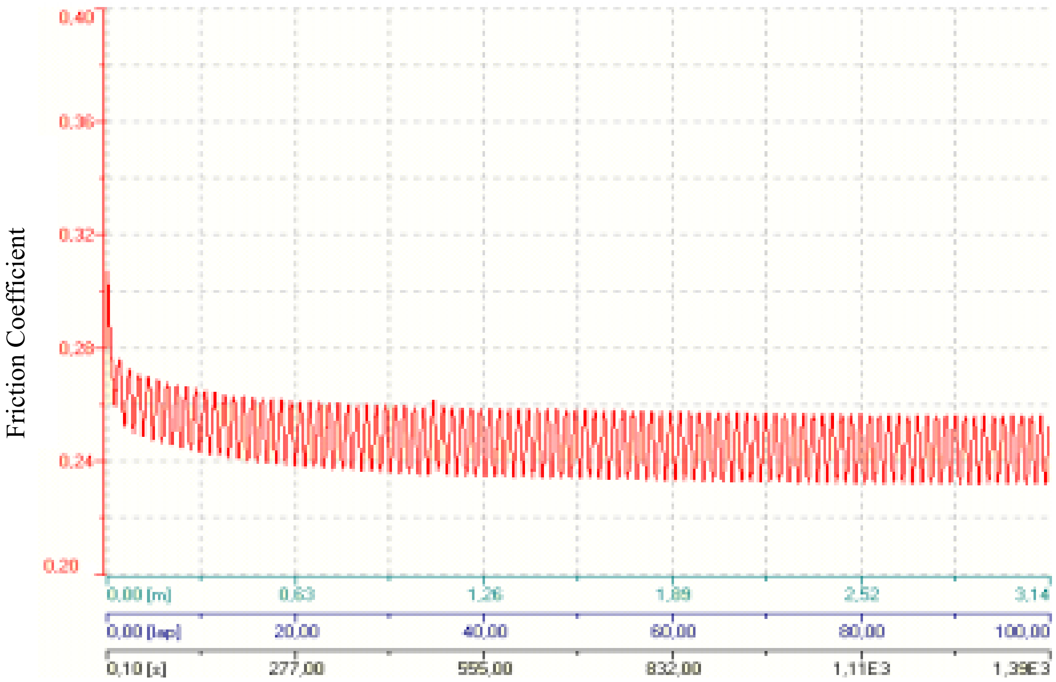
Friction Coefficient
0,40
0,36
0,32
0,28
0,24
0,20
0,00 [m]
0,63
1,26
1,89
2,52
3,14
0,00 [lap]
20,00
40,00
60,00
80,00
100,00
0,10 [s]
277,00
555,00
832,00
1,11E3
1,39E3
Sliding Distance / Number of Laps / Sliding Time

(a)

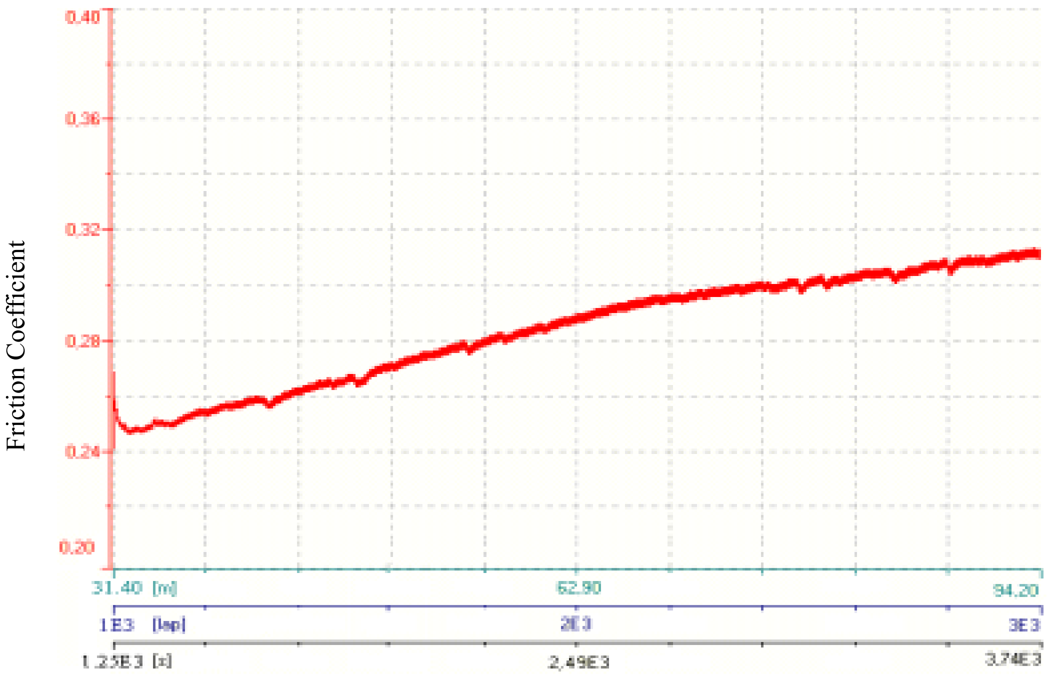
Friction Coefficient
0,40
0,36
0,32
0,28
0,24
0,20
31.40 [m]
62.80
94.20
1E3 [lap]
2E3
3E3
1.25E3 [s]
2,49E3
3.74E3
Sliding Distance / Number of Laps / Sliding Time

(b)

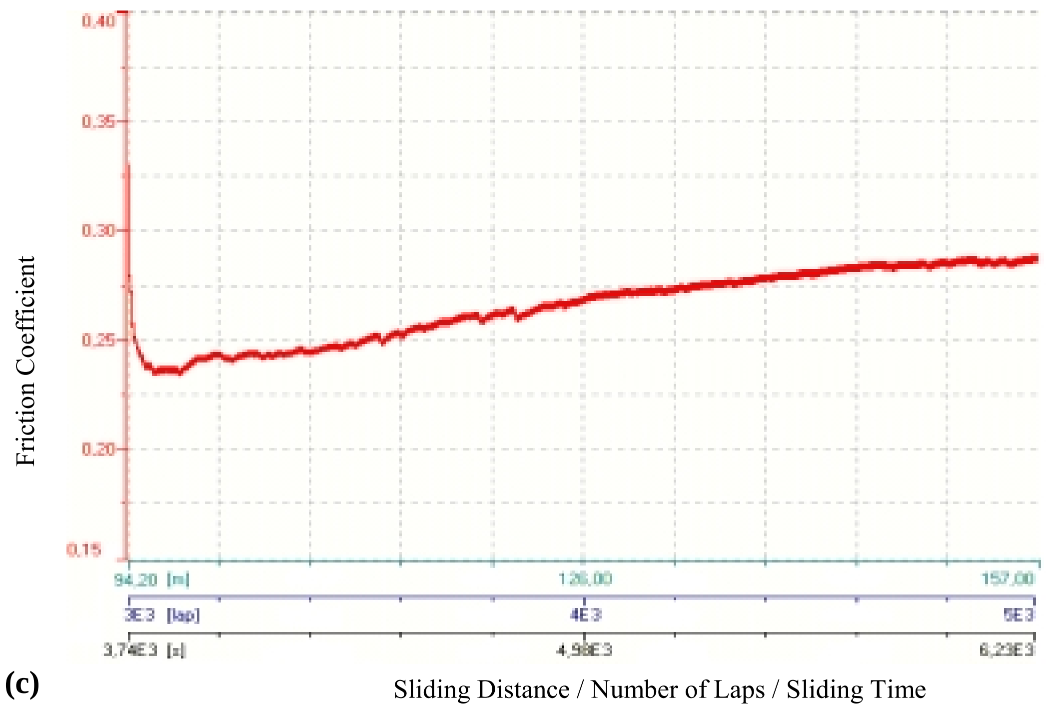

Figure 4.7 Variation of friction coefficient of the mica glass-ceramic studied as functions of number of laps, sliding distance, and sliding time. The applied load was 4N the sliding speed was 0.0025 m/s and in the acidic solution. Data was obtained between;
(a) 1-100 laps.
(b) 1000-3000 laps.
(c) 3000-5000 laps.

There was very smooth friction coefficient at about 0.24 in Figure 4.7.(a), however in Figure 4.7.(b) and 4.7.(c) there was a smooth and a continuous increase in the friction coefficient in the range of about 0.2300 to 0.2850. The friction coefficient in the acidic solution is lower than the experiment conducted at ambient atmosphere. Since acidic environment had an influence on the surface properties as an etching media which decreases the roughness of the tested material.

In order to determine the effect of basic environment, the tests were conducted at a load of 4N and a sliding speed of 0.0025 m/s in the basic solution. The results of the friction coefficient for first 100 lap, between the 1000th and the 3000th laps, and between the 3000th and the 5000th laps were given in Figures 4.8.(a) - 4.8.(c), respectively. The friction coefficient in the basic solution is higher than that at acidic and ambient atmosphere.

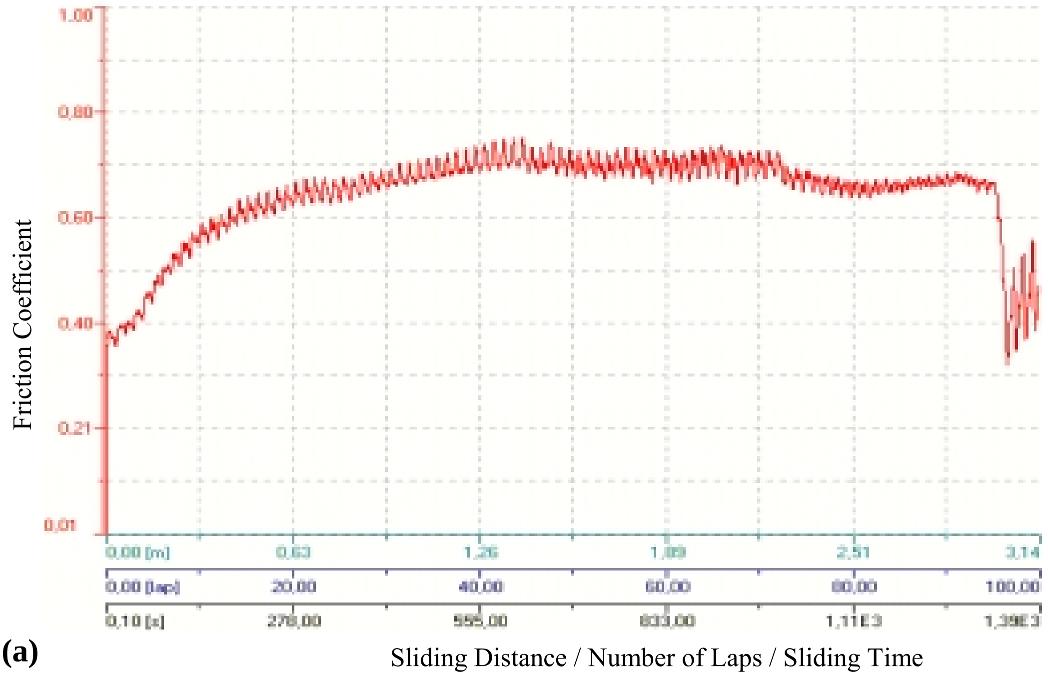
Friction Coefficient
1,00
0,80
0,60
0,40
0,21
0,01
0,00 [m]
0,63
1,26
1,89
2,51
3,14
0,00 [lap]
20,00
40,00
60,00
80,00
100,00
0,10 [s]
278,00
555,00
833,00
1,11E3
1,39E3
Sliding Distance / Number of Laps / Sliding Time

(a)

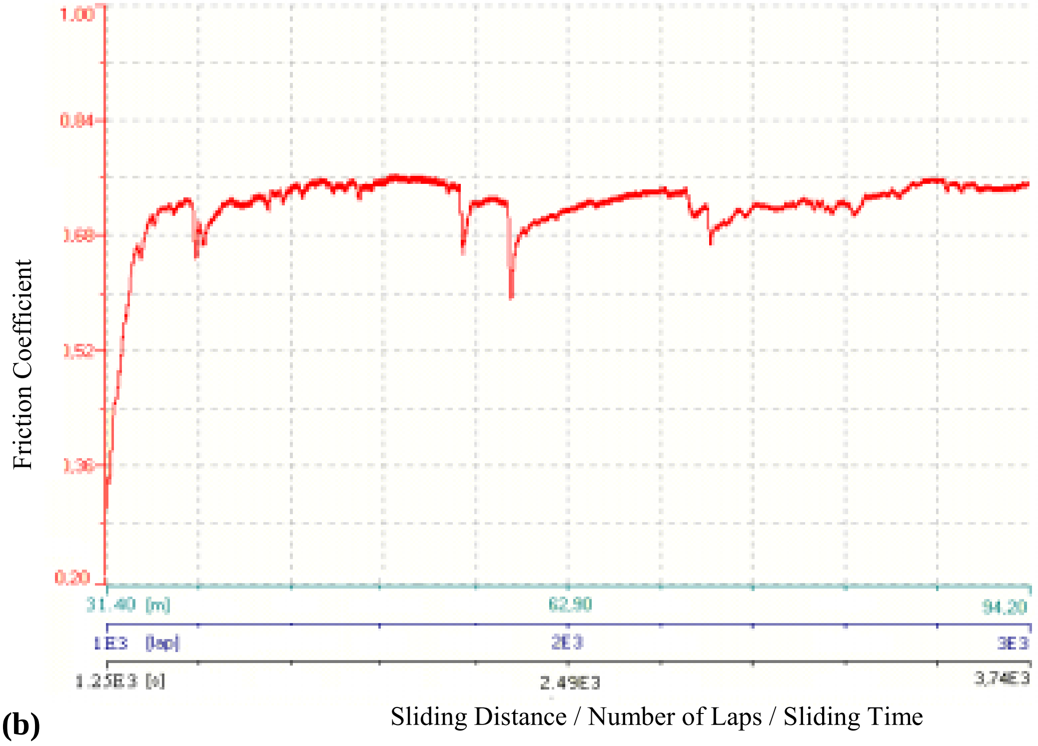
Friction Coefficient
1,00
0,84
0,68
0,52
0,36
0,20
31,40 [m]
62,80
94,20
1E3 [lap]
2E3
3E3
1,25E3 [s]
2,49E3
3,74E3
Sliding Distance / Number of Laps / Sliding Time

(b)

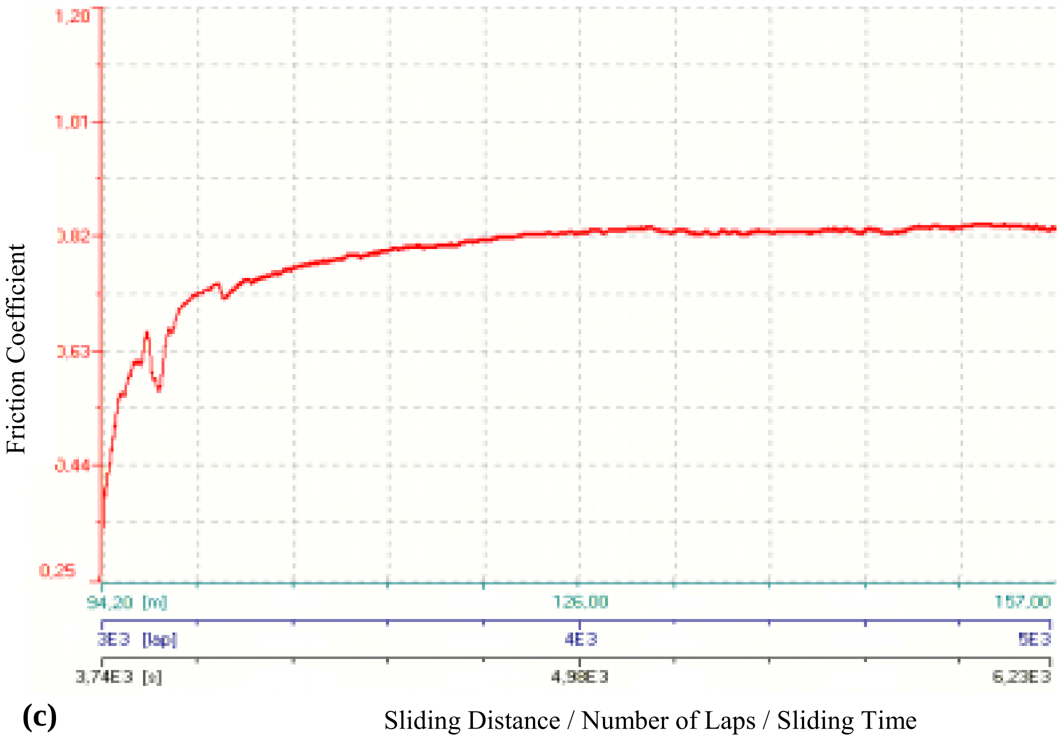

Figure 4.8 Variation of friction coefficient of the mica glass-ceramic studied as functions of number of laps, sliding distance, and sliding time. The applied load was 4N the sliding speed was 0.0025 m/s and in the basic solution. Data was obtained between;
(a) 1-100 laps.
(b) 1000-3000 laps.
(c) 3000-5000 laps.

Part of the decreases in Figures 4.8.(a) - 4.8.(c) reflects the chemical effects of basic solution and the mica glass-ceramic in modifying the forces between the contracting surfaces. By presenting the formation of bonds across the surfaces, the water molecules decrease both the adhesion and the friction coefficient[29].

Ravikiran and Jahanmir conducted a study by using high purity alumina balls and mica containing platelets in a glass matrix. In their study, two sets of experiments were conducted by using the sliding speed of 2.5 mm center dots $^{-1}$ and applied load of 20 N for a total constant sliding distance of 3 m. In the first one, which is referred as "nonflushing" experiment, the water initially added to the cup and it was retained until the end of experiment. In the second set, the submerged sliding interface was continuouly flushed with fresh distilled water by directing a referred pressurized water flow at the sliding interface with a flow rate of 1.5 ml/s and as flushing experiment.

In the nonflushing condition, after some decrease in the friction coefficient there was an increase and then it reached a relatively steady value at about 0.550. In the case of flushing condition, the friction coefficient continuously decreased until a steady value of 0.400 was reached.

Although the conditions were a little bit different in the study conducted by Ravikiran et. al., the material tested is the same. Therefore one can easily compare these two experiments. This study was conducted for the 5000th lap; i.e., 156.60m. Therefore the friction coefficients obtained in this study were, in general, higher than that of the study conducted by Ravikiran et. al. There was no flushing action which had an decreasing effect by taking the worn particles away from the wear track area in this study. In the flushing conditions water was flushing the worn particle, but in nonflushing conditions this was not completely flushed away. However they did not compare the effects of the different environments and therefore it is not logical to compare the tribo-chemical effect that was seen in this study with theirs[76].

As the oral environment means a constant flushing action by means of saliva, and by means of the sliding motion between teeth and the food during chewing, probably, there will not be a stable third body layer. Therefore the wear data from the tribometers that employ a continuous flushing action during testing could provide a better simulation, compared with an experiment conducted in a stagnant fluid.

4.3. WORN VOLUMES

4.3.1. Worn Volume of the Parent Glass

The geometry of contact surface changed as a result of wear. Wear particles agglomerated with time and covered the contact surfaces. After the end of each test, the agglomarated surfaces were cleaned and mean worn areas were determined by using surface profile. Some of the schematic representations of the surface profiles and the data obtained through the surface profile measurements were given in the figures and tables in Appendix B. Worn volumes were calculated by inserting the obtained data from the surface profiles to the Equation 1 as described in Section 3.4. The worn volumes were calculated under different loads, and at different sliding speeds for the parent glass were presented in Table 4.7. Also the effect of different environments on the worn volume of the parent glass was determined. The worn volume calculated for the parent glass for different environmental conditions were given in Table 4.8. The determinations indicated in the tables were obtained after surface profile analysis upon completion of the 100th, the 500th, the 1000th, the 3000th, the 5000th, and the 10000th laps and were tabulated in Tables 4.7 and 4.8. The data determined by averaging the values obtained from two of the reference points was presented.

There is an excellent agreement among the data obtained for different experimental conditions. As seen from tables, worn volumes of the parent glass varied between 0,0084mm^3 and 1.2949mm^3 at the ambient environment, and varied between 0.0035mm^3 and 0.3123mm^3 in the acidic and basic solutions. The worn volume of the parent glass increased as the sliding speed and applied load were increased. The worn volume was lower in the acidic solution than in the basic solution for a given test condition i.e., at the same load and at the same sliding speed.

Table 4.7 Worn volume of the parent glass measured at loads of 2N, 4N, and 8N and at sliding speeds of 0.025 m/s and 0.0025 m/s for different number of laps.

Number of Laps	Worn Volume (mm^3)					
	2N		4N		8N	
	0.0025 m/s	0.025m/s	0.0025 m/s	0.025m/s	0.0025 m/s	0.025m/s
100	0.0084	0.0137	0.0113	0.0351	0.0294	0.0683
500	0.0127	0.0200	0.0162	0.0457	0.0370	0.2076
1000	0.0247	0.0319	0.0300	0.0824	0.0501	0.4386
3000	0.0270	0.0359	0.0434	0.2561	0.1702	0.5305
5000	0.1360	0.0724	0.1492	0.4561	0.5739	0.5414
10000	-	0.1185	-	0.9482	-	1.2949

Table 4.8 Worn volume of the parent glass measured at a load of 4N and at a sliding speed of 0.0025 m/s in acidic and basic solutions for different number of laps.

Number of Laps	Worn Volume (mm^3)	
	pH=5	pH=9
100	0.0036	0.0035
500	0.0058	0.0244
1000	0.0071	0.0688
3000	0.0097	0.2426
5000	0.0244	0.3123

Representative figures showing the variation of the worn volume of the parent glass studied as a function of number of laps for the sliding speeds of 0.0025 m/s and 0.025 m/s were illustrated in Figure 4.9.(a) and 4.9.(b), respectively. As expected and seen from the figures that worn volume increased continuously with increasing number of laps for a given applied load and sliding speed condition.

The change in the worn volume with increasing sliding distance (number of laps) was linear in the initial number of laps; that is within the 1000 laps, but, a deviation from linearity was observed when the number of laps increased further. The deviations was distinct at higher loads. Deviations from the linearity for the worn volume vs. number of lap graphs may be interpreted as the counterface roughness changed during the experiment. Kalin et. al.[75] has also investigated the effect of the counterface roughness on abrasive wear of hydroxyapatite and concluded that the worn volume amount of hydroxypatite pins increased with increasing the surface roughness of the discs. This change may also be arised from the arrangement of the experimental system.

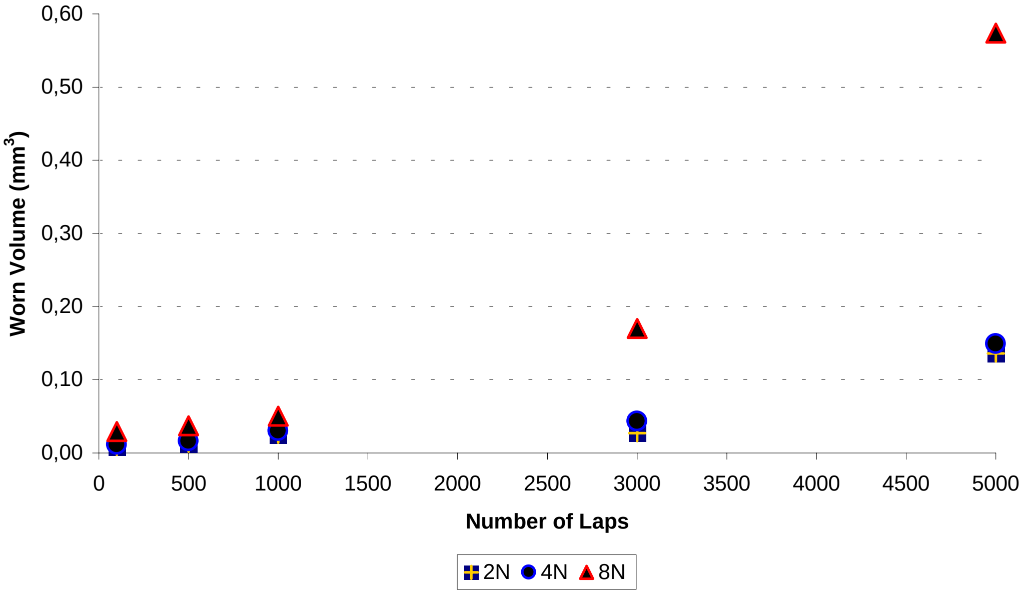

(a)

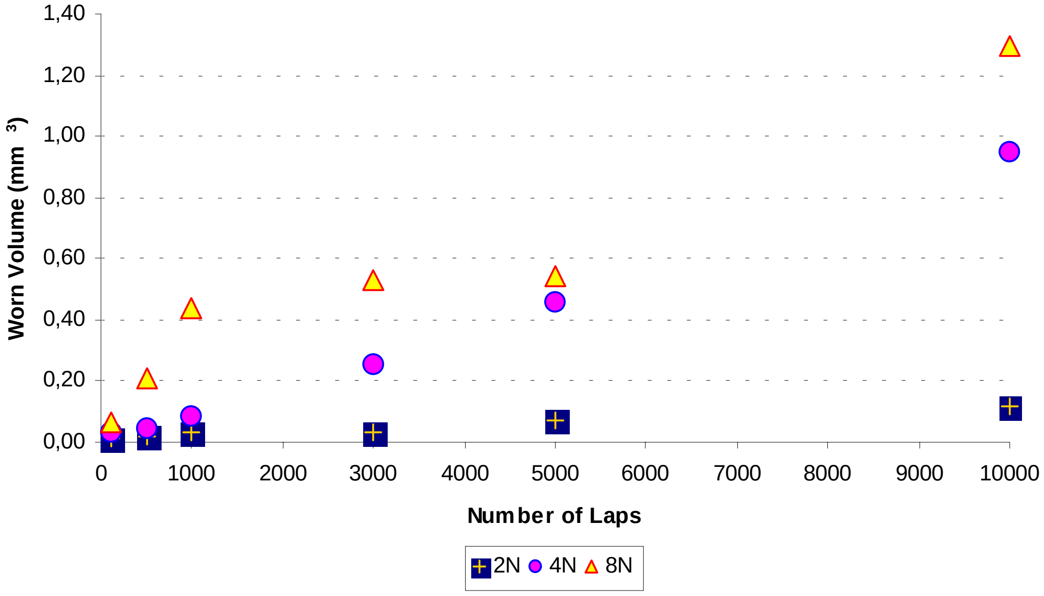

(b)

Figure 4.9 Variation of worn volume of the parent glass studied as a function of number of laps for the applied loads of 2N, 4N, and 8N. Environment was ambient. Data was obtained at the sliding speeds of;

(a) 0.0025 m/s between 1-5000 laps.

(b) 0.025 m/s between 1-10000 laps.

It can be easily seen from the figures that, in general, worn volume increased also with increasing applied load and sliding speed. The increase in the worn volume with increasing applied load was an expected behavior according to the Amounton's Law. The data fit almost the best line. Therefore the wear mechanism occurring in the parent glass suits Type 1 behavior as discussed in Section 2.4.

For a faster sliding speed of 0.025m/s the increase in worn volume with increasing number of laps was linear till the completion of the experiment to 10000th laps at loads of 2N and 4N as seen Figure 4.9.(b). However the linearity was interrupted at a load of 8N after the 1000th lap. The deviation from the linearity is attributed to the change in the dominant wear mechanism from abrasive to adhesive.

The state of any surface exposed to the laboratory environment (ambient atmosphere) is always uncertain since not only water but also some organic molecules are inevitably absorbed. Such contamination makes the interpretation of experimental data difficult. Therefore in an attempt to control the environmental effects better, and to check the environmental effects on the experimental data, tests were carried out in an acidic and a basic solution. The data were illustrated graphically in Figure 4.10 which is a typical worn volume vs number of laps graph for the parent glass at a load of 4N, and a sliding speed of 0.0025 m/s. The figure clearly shows that the worn volume increased as a function of number of laps for a given environment. In the basic solution, the increase in worn volume is the greatest among that at ambient environment and in acidic solution.

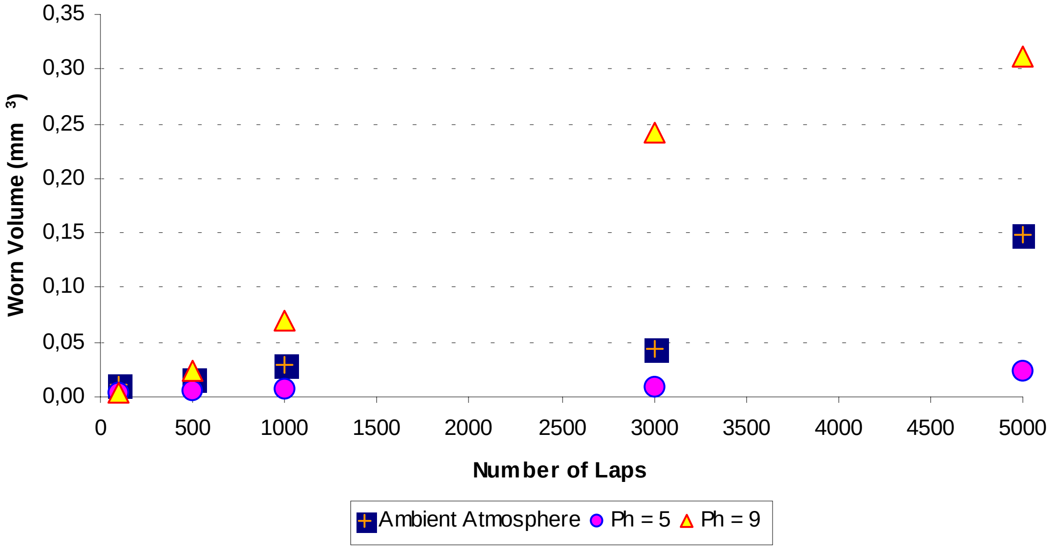

Figure 4.10 Variation of worn volume of the parent glass studied as functions of number of laps, sliding distance, and sliding time. The applied load was 4N and, the sliding speed was 0.0025 m/s, environments were ambient, acidic, and basic. Data was obtained between 0-5000 laps.

In order to determine the effect of sliding speed on the worn volume of the parent glass, tests were conducted at different speeds. Data obtained was illustrated graphically for different applied loads of 2N, 4N, and 8N in Figures 4.11.(a) - 4.11.(c). It is seen that as the worn volume increased as the sliding speed increased. The wear mechanism was different in the experiments conducted with the loads of 2N and 8N after the 3000th lap.

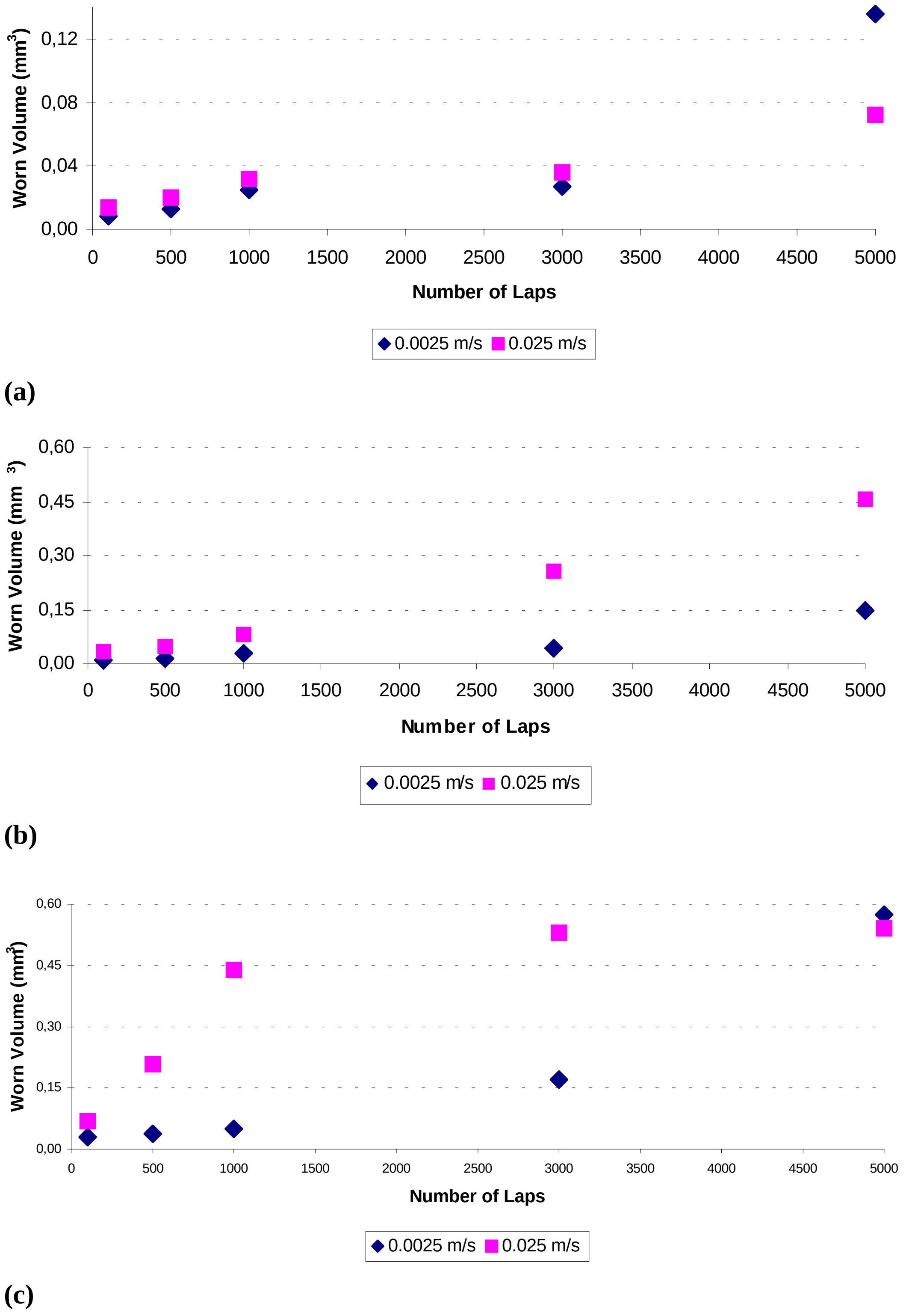

Figure 4.11 Variation of worn volume of the parent glass studied as a function of number of laps for the sliding speeds of 0.0025 m/s and 0.025 m/s. Environment was ambient and the data was obtained between 0-5000 laps at applied loads of;
(a) 2N.
(b) 4N.
(c) 8N.

4.3.2 Worn Volume of the Mica Glass-Ceramic

The worn volumes calculated under different loads, and sliding speeds for the mica glass-ceramic were presented in Table 4.9. The effect of the different environment on the worn volume of the mica glass-ceramic was also determined. The worn volume calculated for the mica glass-ceramic for different environmental conditions were given in Table 4.10.

Table 4.9 Worn volume of the mica glass-ceramic measured at loads of 2N, 4N, and 8N and sliding speeds of 0.025 m/s and 0.0025 m/s for different number of laps.

Number of Laps	Worn Volume (mm^3)					
	2N		4N		8N	
	0.0025 m/s	0.025m/s	0.0025 m/s	0.025m/s	0.0025 m/s	0,025m/s
100	0.0056	0.0076	0.0094	0.0206	0.0190	0.0594
500	0.0071	0.0169	0.0136	0.0361	0.0479	0.1734
1000	0.0184	0.0255	0.0255	0.0647	0.0894	0.1780
3000	0.0247	0.0523	0.0602	0.1858	0.1130	0.2084
5000	0.0377	0.0736	0.1119	0.2436	0.2529	0.2175
10000	-	0.113	-	0.3072	-	0.3528

Table 4.10. Worn volume of the mica glass-ceramic measured at a load of 4N and sliding speed of 0.0025 m/s in acidic and basic solutions for different number of laps.

Number of Laps	Worn Volume (mm^3)	
	pH=5	pH=9
100	0.0096	0.0036
500	0.0147	0.0124
1000	0.0193	0.0146
3000	0.0335	0.0325
5000	0.0381	0.0445

As seen from the tables, worn volumes of the mica glass-ceramic varied between 0.0056mm^3 and 0.3528mm^3 in ambient atmosphere and varied between 0.0036mm^3 and 0.0445 mm^3 in the solutions. If the data obtained were compared with the data for the parent glass, wear resistance of parent glass is better at ambient atmosphere. The maximum worn volume obtained for the mica glass-ceramic was approximately 3 times higher than that of the parent glass. However if in solution conditions are taken into consideration the results are controversary. In the acidic solution, worn volume is higher for the mica glass ceramic, however in the basic solution it is higher for the parent glass. In the acidic solution it is observed that white and shiny particles showed the tribo-chemical effect. The data obtained from this study supports the concept that smooth and shiny facets on contacting tooth surfaces have an erosive component in their development. The decrease of the worn volume in acidic solution is caused by the erosive effect of the acidic solution. Therefore the amount of worn volume is decreased in acidic solution. However the main result revealed from this comparison is that, worn volume decreased for the mica glass-ceramic in solution condition. At the beginning of this study, the main question was whether or not this material could be used in dental applications safely and in long term. The answer is that; in oral environment, the worn volume of this alternative material is lower than in the ambient atmosphere. Therefore, it can be used safely in dental applications since the oral environment contains some spits to wet the food like in solution condition. However it should be noticed that, in oral condition teeth are always within more acidic and basic drinks. Specifically in respect to tooth wear, this study can only indicate associations of variables with a condition and can never prove an aetiological role. In the literature the effect of long-term wear was not considered. However the aim of this research is to clarify the effect of long-term wear. Since tooth wear has a multi-factorial aetiology and in the future experiments, it should not be ignored the effect of interplay attrision, erosion, and wear in long-term[76].

The cycling experiments provided supportive evidence for a smoothing effect of acid with a pattern for greater wear. However the difference of the experiment in acidic solution than in other environments is the smoothing or polishing effect of the acid, which is the dominant factor [77].

Typical plots showing variation of worn volume for different applied loads as a function of number of laps or sliding distance were given in Figures 4.12.(a) and 4.12.(b). The increase in the worn volume except the experimental results obtained at a load of 8N is close to linearity. However at the 3000th lap at 8N load, there is deviation from the linearity. The discontinuity at this load is mainly due to the changes in the shape of the pin by increasing lap numbers. Therefore wear of pin should be taken under control, even though it had more wear resistance than the mica glass-ceramic.

The data presented in Figure 4.12.(b), for worn volumes at applied loads of 2N, 4N, 8N and at the sliding speed of 0.025 m/s show the correlation of the experimentally obtained worn volume data. The figure clearly shows that under any given load, the worn volume increased. There is linear behavior at 2N and 4N loads however the behavior is different at 8N load. The main problem changing the worn volume is the accumulation problem, which in turn results in causing a change the dominant wear mechanisms from abrasive to adhesive. Furthermore 'Archard Wear Law', which states that a linear relation between incremental wear volumes and local loads and sliding distances, emphasizes that even if every element at the loaded and wearing interface in the field application behaves locally, it is not immediately obvious how the overall or global volumetric wear loss from the component will be related to the total applied load or global sliding history[51]. This is because the interfacial pressure adjusts itself as wear proceeds so that the demands of equilibrium are satisfied and the overall geometry is consistent with the maintanance of geometric compatibility between both elements of the tribological pair. Therefore the increase in the worn volume at some laps may also be related to the 'Archard Wear Law'[78,79].

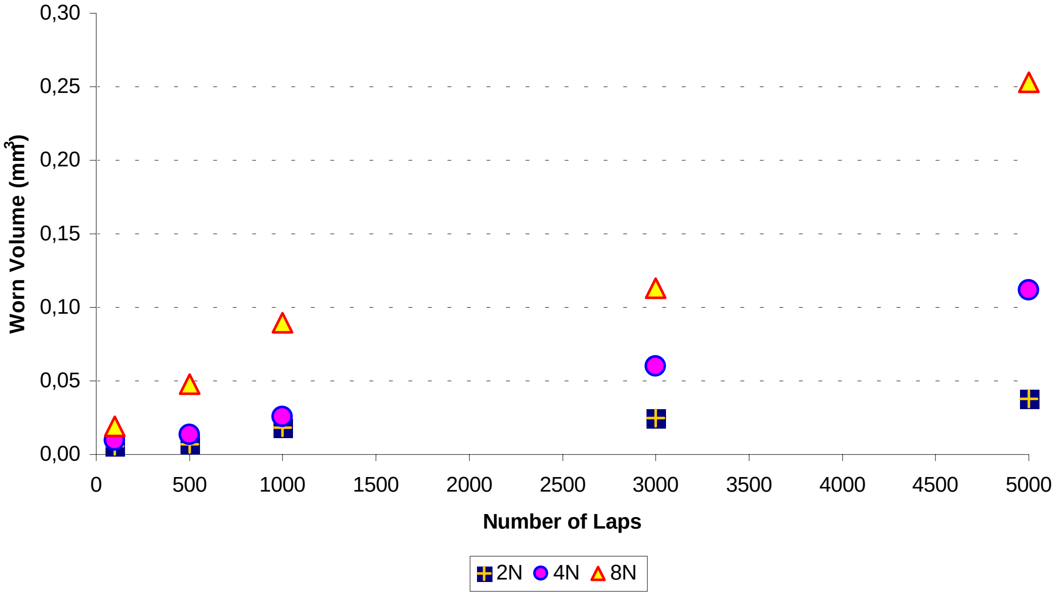

(a)

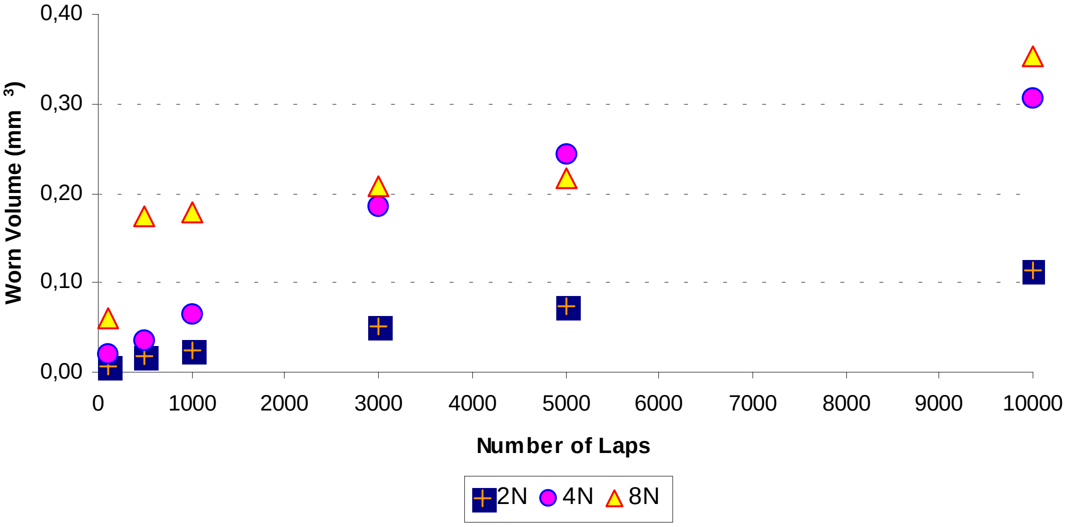

(b)

Figure 4.12 Variation of worn volume of the mica glass-ceramic studied as a function of number of laps for the applied loads of 2N, 4N, and 8N. Environment was ambient. Data was obtained at the sliding speeds of;
(a) 0.0025 m/s between 1-5000 laps.
(b) 0.025 m/s between 1-10000 laps.

However, there are many practical situations in which, as components wear, the area of apparent contact changes, so that, although the Archard relation may still be applicable on the microscale, the relation between either the macroscopic wear dimension, or the total wear volume, may be other than a linear function of sliding distance or load. Therefore to get rid of the accumulation problem by conducting experiments, it is necessary to use a lubricant, which cleans the surface while experiments are run.

In order to determine the effect of solutions to the worn volume of the mica glass-ceramic, tests were carried out in the acidic and basic solutions. The results were illustrated graphically in Figure 4.13, which is a typical worn volume vs. number of laps graph for the mica glass-ceramic sample at 4N load, and a sliding speed of 0.0025 m/s. The tests were conducted at ambient atmosphere, and in acidic and basic solutions.

It is clearly shown that, in acidic and basic solutions there is almost the same behavior, since the data overlapped. There is linearity for all cases. However at ambient atmosphere, the worn volume is the highest. The behavior for the mica glass-ceramic is different than that of the parent glass. The worn volume is the highest in the basic solution. However this value is lower than in the ambient atmosphere as seen in Figure 4.13.

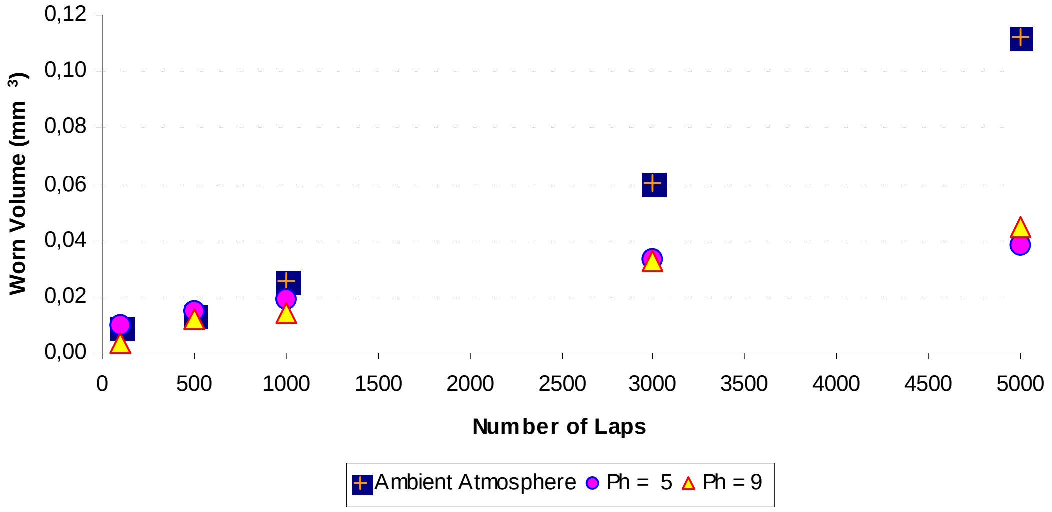

Figure 4.13 Variation of worn volume of the mica glass-ceramic studied as a function of number of laps for environments of ambient, acidic, and basic. The applied load was 4N and the sliding speed was 0.0025 m/s. Data was obtained between 0-5000 laps.

Typical worn volume vs number of laps graphs of the mica glass-ceramic were illustrated in Figures 4.14.(a) - 4.14.(c). In each figure the applied load was changed, and the effect of sliding speed to the worn volume of the mica glass-ceramic was investigated. The same behavior was not observed for the mica glass-ceramic as in case of the parent glass. Worn volume although directly depends on the sliding speed for the parent glass, the behavior was not observed under applied loads of 2N, and 4N. In general this result is sufficient to say that every mechanism composed of some small pieces and it becomes dominant in some point during the experiment. The problem is now to decide which mechanism becomes dominant or what is necessary to make a mechanism to dominate. To find a solution, a microcopic investigation is necessary.

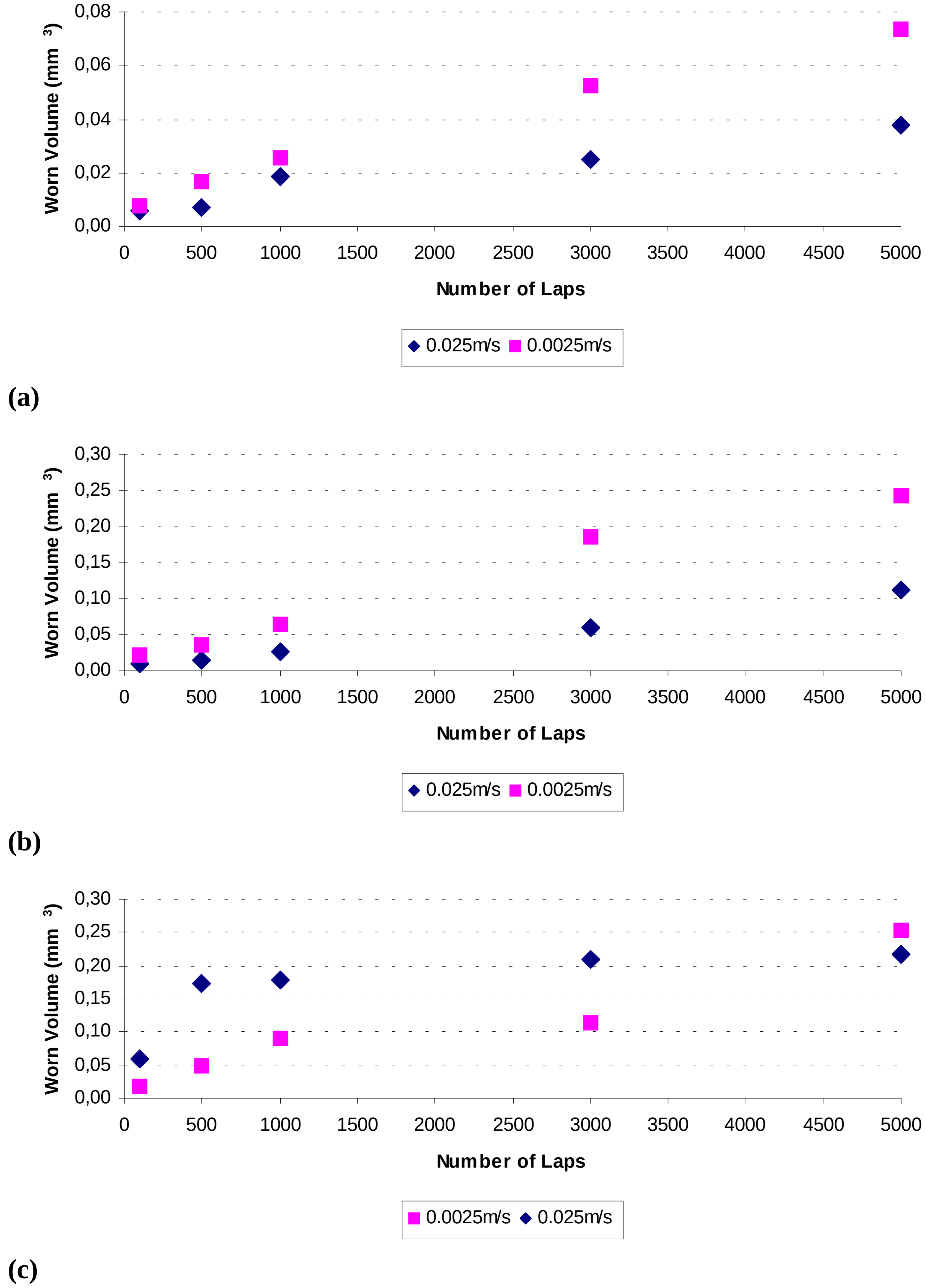

Figure 4.14 Variation of worn volume of the mica glass-ceramic studied as a function of number of laps for the sliding speeds of 0.0025 m/s and 0.025 m/s. Environment was ambient. Data was obtained between 0-5000 laps at the applied loads of;
(a) 2N.
(b) 4N.
(c) 8N.

4.4. SPECIFIC WEAR RATES

4.4.1. Specific Wear Rate of the Parent Glass

The specific wear rates for all of the experimental conditions were calculated as discussed in Section 3.3.3 employing Equation 2. The data tabulated in Tables 4.11 and 4.12 were given in 5 digits. As seen from the tables specific wear rate of the parent glass varied between 2.39 x 10^{-3} mm^3/N.m and 0.174 mm^3/N.m at the ambient environment, and varied between 5.6 x 10^{-5} mm^3/N.m and 7.96 x 10^{-3} mm^3/N.m in the solutions.

Table 4.11 Specific wear rate of the parent glass measured at loads of 2N, 4N, and 8N and sliding speeds of 0.0025m/s and 0.025 m/s for different numbers of laps.

Number of Laps	Specific Wear Rate (mm^3 / N.m)					
	2N		4N		8N	
	0.0025 m/s	0.025m/s	0.0025 m/s	0.025m/s	0.0025 m/s	0.025m/s
100	0.00535	0.00873	0.01433	0.04476	0.07503	0.17400
500	0.00162	0.00255	0.00412	0.01164	0.01887	0.10579
1000	0.00158	0.00203	0.00024	0.01050	0.01276	0.11175
3000	0.00057	0.00076	0.00012	0.01088	0.01445	0.04506
5000	0.00173	0.00092	0.00950	0.01162	0.02924	0.02759
10000	-	0.00076	-	0.01208	-	0.03299

Table 4.12 Specific wear rate of the parent glass measured at a load of 4N and sliding speed of 0.0025m/s in acidic and basic solutions for different number of laps.

Number of Laps	Specific Wear Rate (mm^3/N.m)	
	pH=5	pH=9
100	0.00464	0.00444
500	0.00147	0.00622
1000	0.00006	0.00055
3000	0.00003	0.00064
5000	0.00062	0.00796

Generally at the beginning of the experiment, the specific wear rate was higher. As shown in Figure 4.15.(a), at the first 100 laps, the specific wear rate was maximum, and it decreased for all the loading conditions up to the 1000th lap. However at a load of 8N, it increased after the 1000th lap, and data overlapped for loads of 2N, and 4N, since there is almost the same specific wear rate after the 1000th lap. In Figure 4.15.(b), at a load of 2N specific wear rate decreased except the value at the 5000th lap. At a load of 4N specific wear rate decreased upto the 3000th lap than it increased. At 8N load specific wear rate generally decreased, however there is increase between the 500th and the 1000th laps and between the 5000th and the 10000th laps.

As seen from the Figures 4.15.(a) and 4.15.(b), it can be stated that, as the sliding speed increased from 0.0025 m/s to 0.025 m/s specific wear rate increased with a few exceptions. As the sliding speed was increased the specific wear rate, at 2N load, decreased at the 5000th lap. The difference is not much, therefore, it may be due to an experimental error. It was an expected result that the specific wear rate changes through the repeated contact process under constant load and the sliding speed and it is generally high in an initial unsteady state and relatively low in the later steady one according to Kato[70].

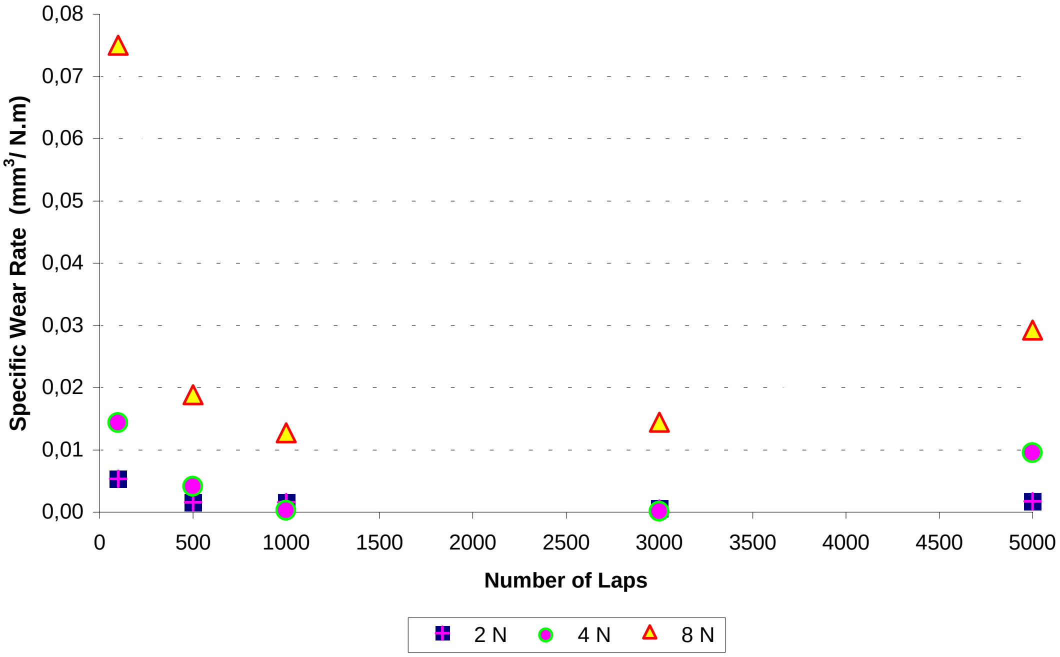

(a)

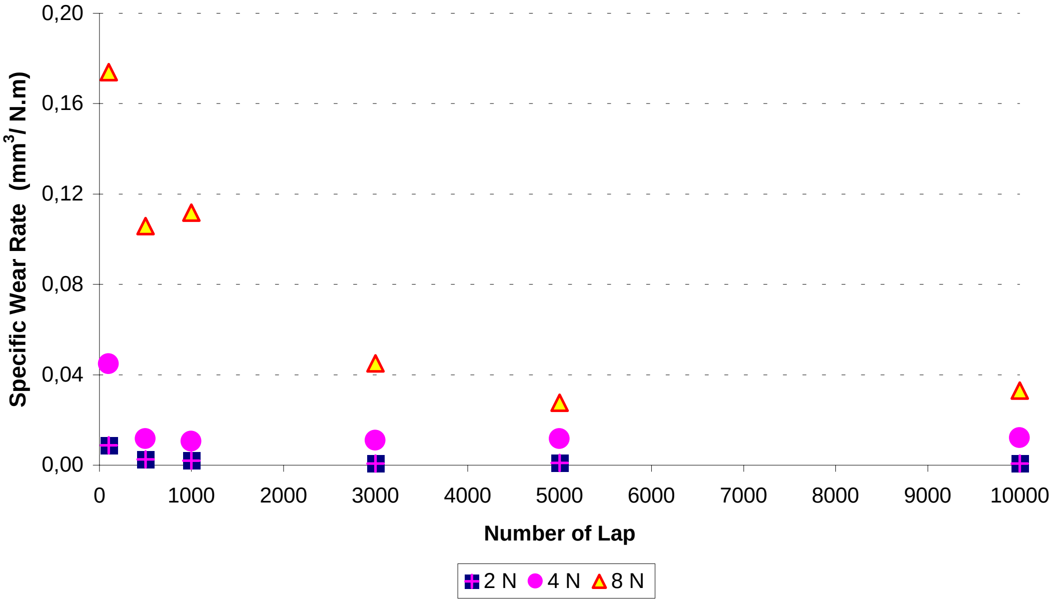

(b)

Figure 4.15 Variation of specific wear rate of the parent glass studied as a function of number of laps for the applied loads of 2N, 4N, and 8N. Environment was ambient. Data was obtained at the sliding speeds of;

(a) 0.0025 m/s between 1-5000 laps.

(b) 0.025 m/s between 1-10000 laps.

Initial wear and steady wear expressions were used to describe specific wear rate changes caused as a result of wear due to repeated contacts. The change in the specific wear rate are caused by the change of the wear mechanism from adhesive to oxidative wear in the contact situation of steel to steel contact. However the specific wear rate changes in the mica glass-ceramic are due firstly to the change of the dominant mechanism from abrasive to adhesive.

The variation in the specific wear rate as a function of number of laps for different environmental conditions were graphically illustrated in Figure 4.16. Observed specific wear rates changed depending on the environment, and in basic solution it was higher in general. In the basic solution, there is an unexpected behavior between the 100^{th} and the 500^{th} lap, compared to the behavior at other environments. There was an increase between these laps, however at ambient atmosphere and in acidic solution there was a decrease between these laps. The specific wear rates of the parent glass remarkably increased in the basic solution compared to those in the acidic solution, and in ambient atmosphere. As many researchers pointed out[76,80-82], the formation of transfer film was considerably prevented and the specific wear rate highly increased.

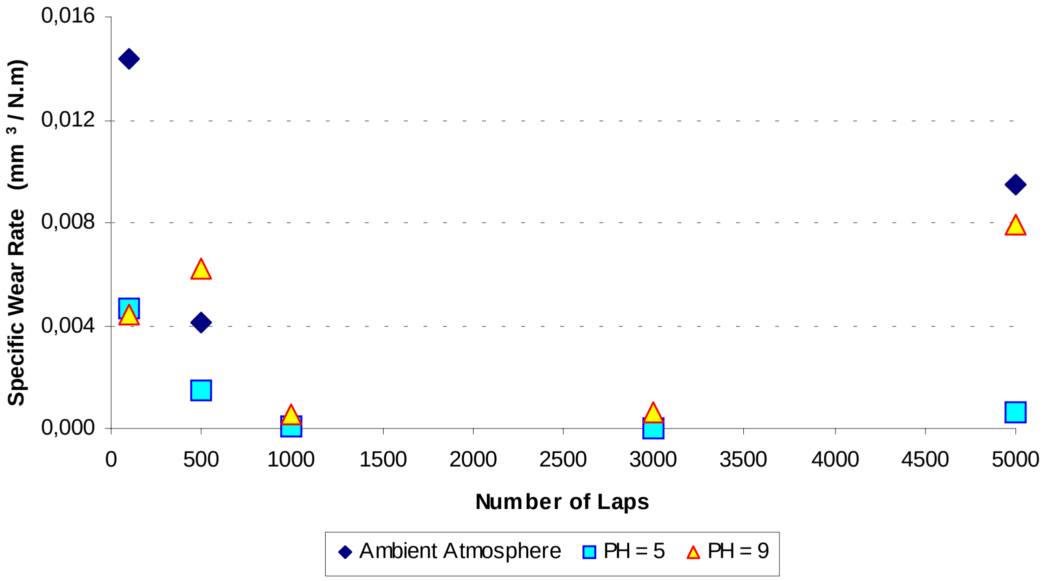

Figure 4.16 Variation of specific wear rate of the parent glass studied as a function of number of laps for the environments of ambient, acidic, and basic. The applied load was 4N and, the sliding speed was 0.0025 m/s. Data was obtained between 0-5000 laps.

Specific wear rate of glass as a function of load depending on the number of laps was evaluated and the results were graphically illustrated according to the specified sliding speed of 0.0025 m/s in Figure 4.17.(a), and for the sliding speed of 0.025 m/s in Figure 4.17.(b).

It is obvious in figures that, as the load was increased, specific wear rate increased. If the same number of laps under different loads were considered, minimum specific wear rate was obtained for 2N load. Specific wear rates overlapped at the 1000th lap and the 3000th lap at 0.0025 m/s. Specific wear rates except the 100th lap overlapped at 0.025 m/s for 2N and 4N load. The increase in specific wear rates depending on the applied load interprets the role of debris on wear. At higher loads consolidated batches of debris came into contact between the pin and the glass provide a powerful grinding media therefore the wear rate of the underlying substrate increases. High surface quality materials, especially ground or polished surface demonstrate higher wear resistance due to lower contacting area between material and acting abrasive media and lower turbulence at the surface [83].

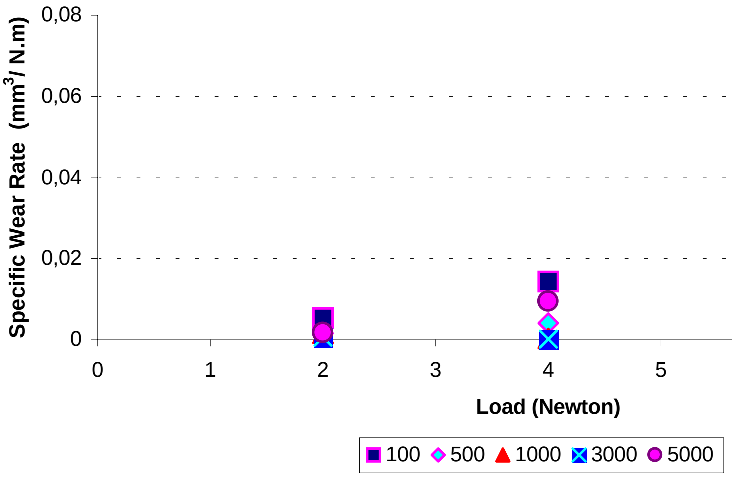

(a)

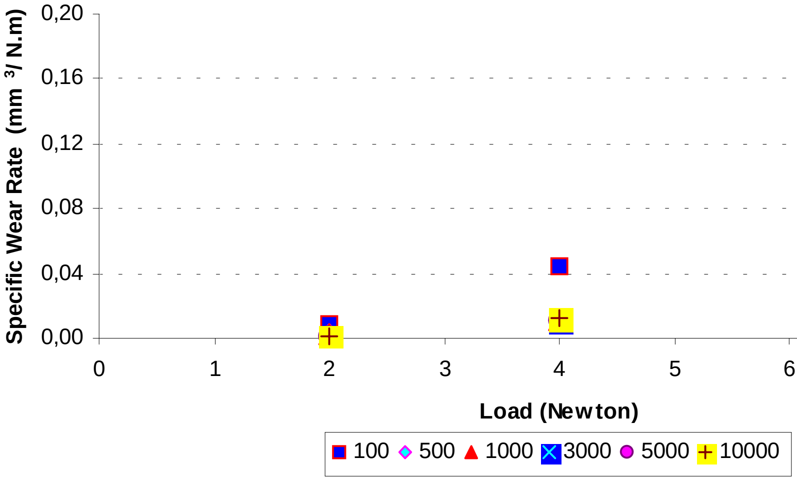

(b)

Figure 4.17 Variation of specific wear rate of the parent glass studied as a function of applied load for different number of laps. Data was obtained at the sliding speeds of;
(a) 0.0025 m/s.
(b) 0.025 m/s.

Specific wear rate of the parent glass as a function of number of laps depending on sliding speed was graphically depicted in Figures 4.18.(a) - 4.18.(c) for applied loads of 2N, 4N, and 8N. It can be stated that at higher sliding speed of 0.025m/s, specific wear rate is higher with small exceptions. In Figure 4.18.(a) after the 3500th lap, and in Figure 4.18.(c) at the end of the experiment, i.e., at the 5000th lap, this statement was not satisfied.

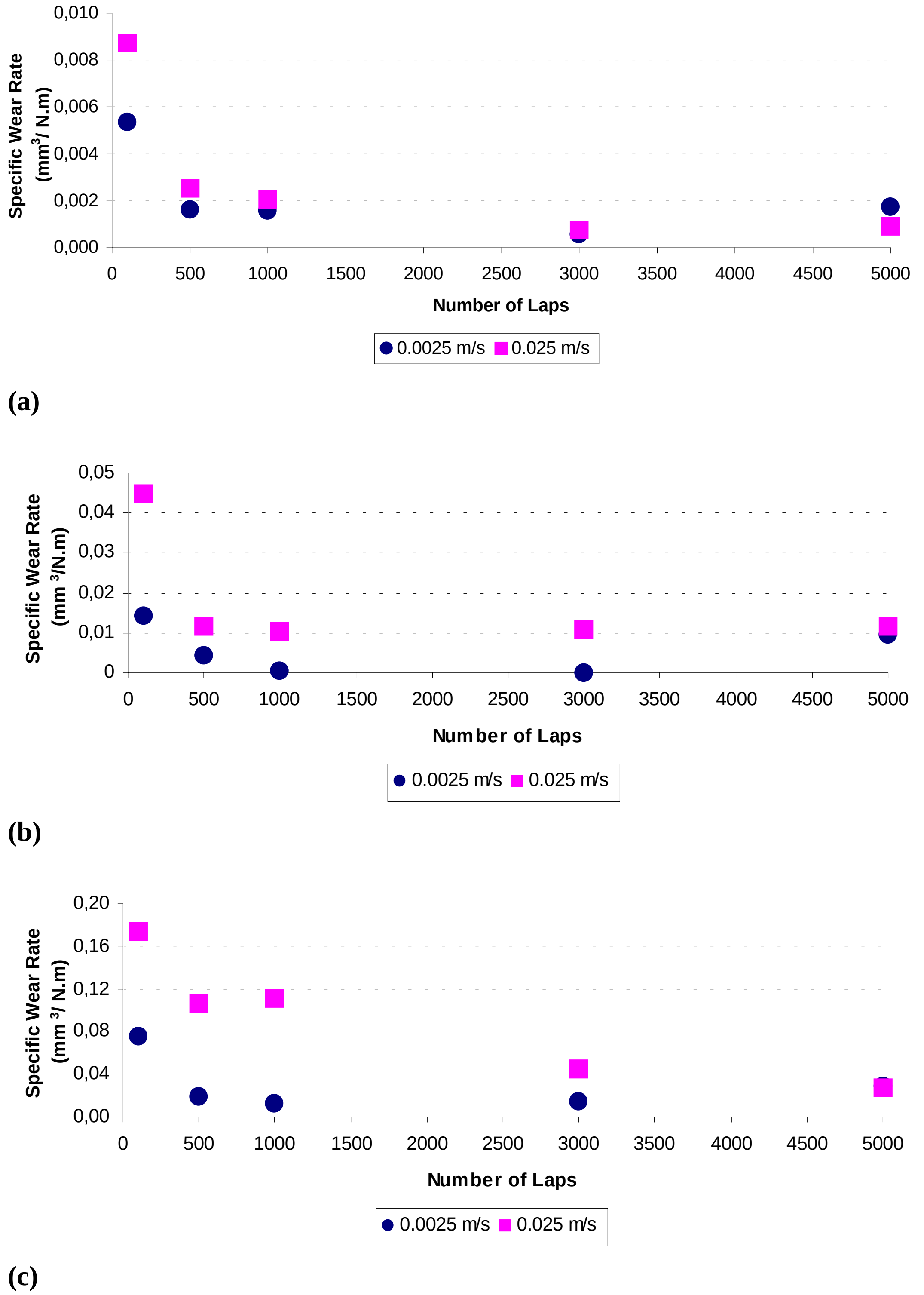

Figure 4.18 Variation of specific wear rate of the parent glass studied as a function of number of lap for the applied sliding speeds of 0.0025 m/s and 0.025 m/s. Environment was ambient. Data was obtained between 0-5000 laps at applied loads of;

(a) 2N.

(b) 4N.

(c) 8N.

4.4.2. Specific Wear Rate of the Mica Glass-Ceramic

The specific wear rate data for the mica glass-ceramic were tabulated in Tables 4.13 and 4.14, and the results varied between 4.80 x 10^{-4} mm^3/N.m and 0.15142 mm^3/N.m at the ambient environment, and varied between 9.7 x 10^{-4} mm^3/N.m and 1.225 x 10^{-2} mm^3/N.m in the acidic and basic solutions.

A comparison of the specific wear rate data for the mica glass ceramic with that of the parent glass reveals that specific wear rate of the mica glass ceramic is lower at a given environmental condition. However in basic solution at some laps there were exceptions that can be ignored if the results were completely taken into consideration.

Table 4.13 Specific wear rate of the mica glass-ceramic measured at loads of 2N, 4N, and 8N and sliding speeds of 0.0025m/s and 0.025 m/s for different number of laps.

Number of Laps	Specific Wear Rate (mm^3 / N.m)					
	2N		4N		8N	
	0.0025 m/s	0.025m/s	0.0025 m/s	0.025m/s	0.0025 m/s	0.025m/s
100	0.00358	0.00486	0.01193	0.02626	0.04852	0.15142
500	0.00091	0.00215	0.00346	0.00919	0.02439	0.08834
1000	0.00117	0.00162	0.00324	0.00825	0.02277	0.04535
3000	0.00053	0.00111	0.00256	0.00789	0.00960	0.01770
5000	0.00048	0.00094	0.00285	0.00621	0.01289	0.01109
10000		0.00072		0.00391		0.00899

Table 4.14 Specific wear rate of the mica glass-ceramic measured at a load of 4N and sliding speed of 0.0025m/s in acidic and basic solutions for different number of laps.

Number of Laps	Specific Wear Rate (mm^3/N.m)	
	pH=5	pH=9
100	0.01225	0.00452
500	0.00375	0.00316
1000	0.00246	0.00185
3000	0.00142	0.00138
5000	0.00097	0.00113

Specific wear rates of the mica glass-ceramic sample as a function of number of lap at measured loads of 2N, 4N, 8N were presented in Figures 4.19.(a), and 4.19.(b). As seen in the figures, the specific wear rate increased as the applied load increased. The decrease in the specific wear rate is mainly due to the abrasive particles. When abrasive particles sandwiched between two surfaces are loose, the specific wear rate is less than that when one material slides against hard protuberances of the counterface. This is due to that the loose abrasive particle spends most of its time to roll at the sliding interface[83]. Therefore at first laps, the specific wear rates were maximum, and they decreased as the experiment proceeded. In adition it is concluded that specific wear rates depend on the load, since specific wear rate was the highest at a load of 8N and the lowest at a load of 72N.

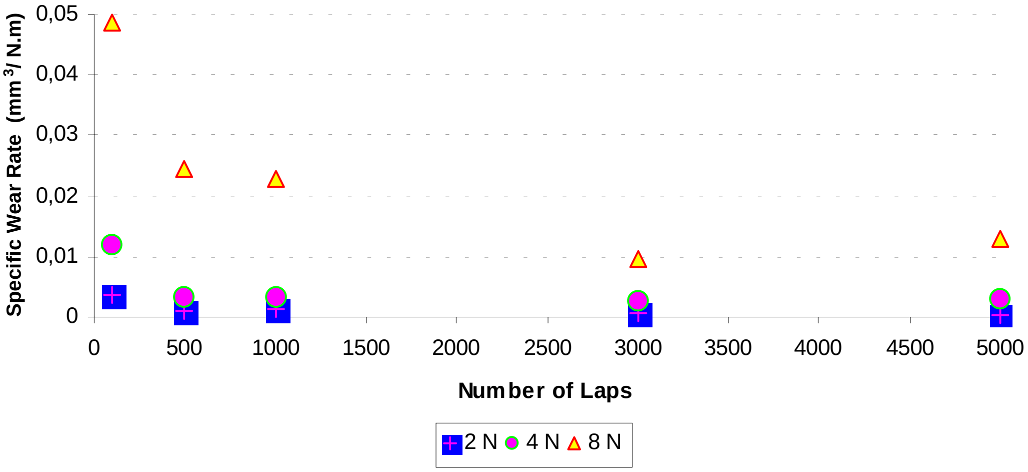

(a)

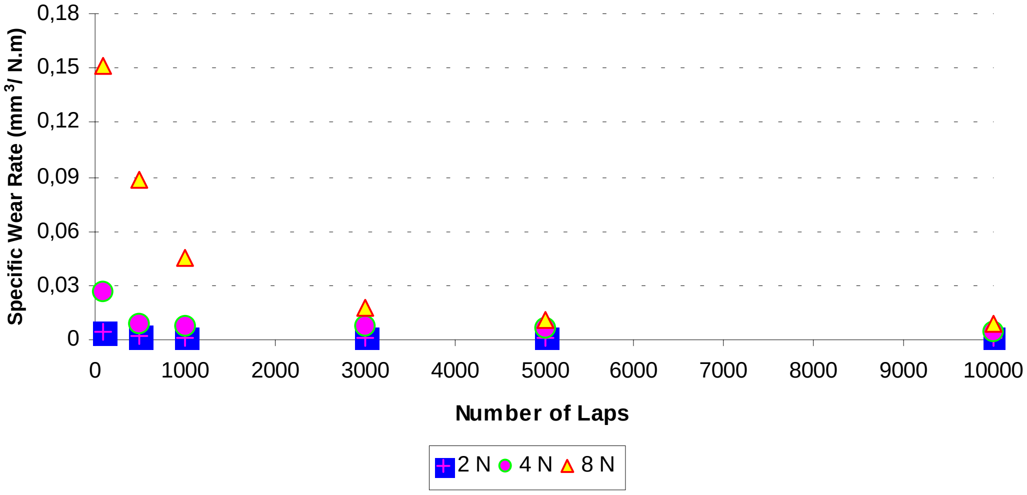

(b)

Figure 4.19 Variation of specific wear rate of the mica glass-ceramic studied as a function of number of laps for the applied loads of 2N, 4N, and 8N. Environment was ambient. Data was obtained at the sliding speeds of;
(a) 0.0025 m/s between 1-5000 laps.
(b) 0.025 m/s between 1-10000 laps.

At different environments, data on specific wear rates overlapped and were depicted graphically in Figure 20. This behavior was observed at ambient atmosphere and in acidic solution between the 1st and the 100th lap, and in acidic and basic solution between the 3000th and the 5000th laps. It is recognized that in the presence of chemically aggressive solution the erosion process is stronger, i.e, combined influence of abrasion and corrosion occurs[84].

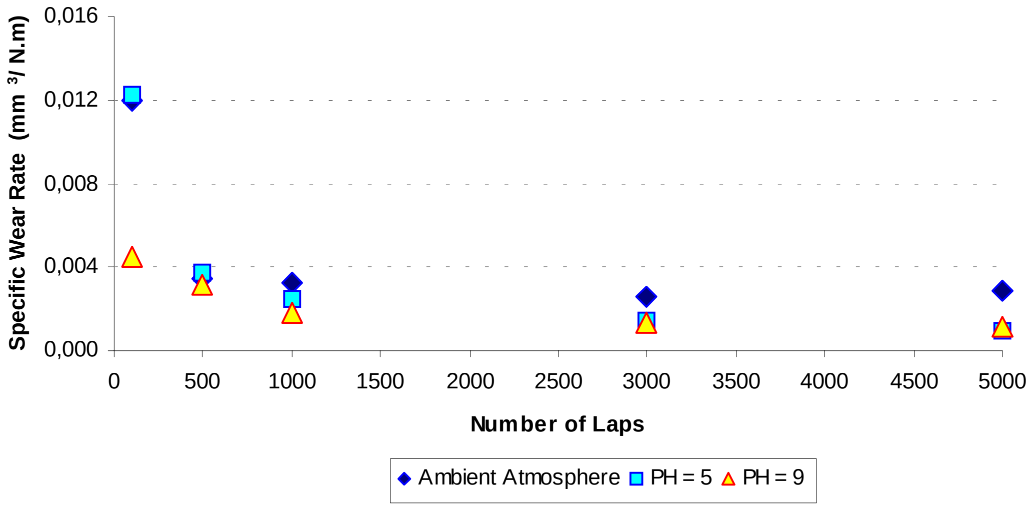

Figure 4.20 Variation of specific wear rate of the mica glass-ceramic studied as a function of number of laps for the environments of ambient, acidic, and basic. The applied load was 4N and the sliding speed was 0.0025 m/s. Data was obtained between 0-5000 laps.

Specific wear rate of the mica glass-ceramic as a function of load at different number of laps were also graphically presented for the sliding speed of 0.0025 m/s in Figure 4.21.(a), and for the sliding speed of 0.025 m/s in Figure 4.21.(b). In Figure 4.21.(a), and 4.21.(b) the specific wear rate increased as the load increased. Minimum specific wear rate was obtained at 2N load and maximumum specific wear rate was obtained at 8N load. Specific wear rate data at loads of 2N and 4N, except the 100th lap, overlapped. However there was not a good correlation in the specific wear rate data depending on the number of laps. That is, as the number of laps increased at the same applied load, there were not a constant increase or a constant decrease in the specific wear rates. The change independently occurred from the number of laps. These differences were due to the accumulation of worn particles as experiment proceeded. However, in Figure 4.21.(b), the increase in specific wear rate at 0.025m/s was obvious depending on the load, which is due to the increasing sliding distance. There is a negative correlation between the increase in specific wear rate and increase in number of laps. Therefore as the number of laps increased, specific specific wear rate decreased. This behavior can be easily seen by checking the data at 8N.

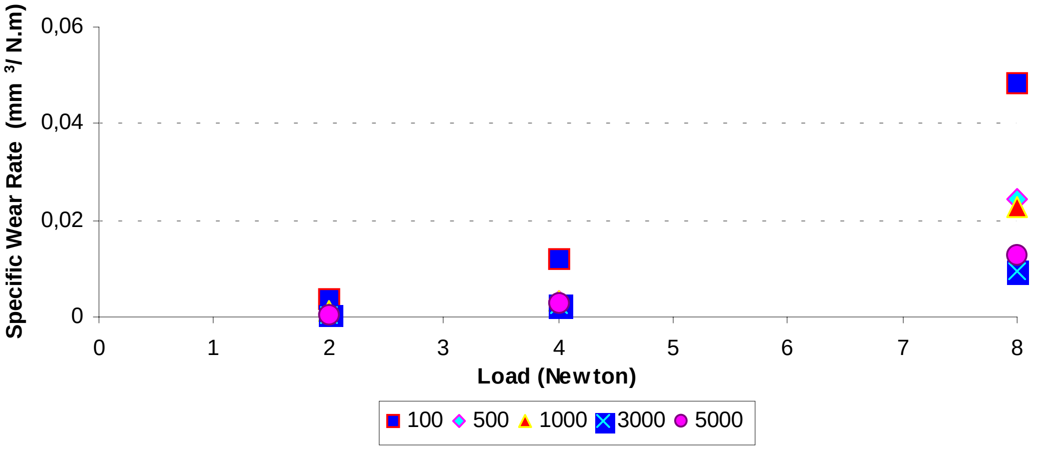

(a)

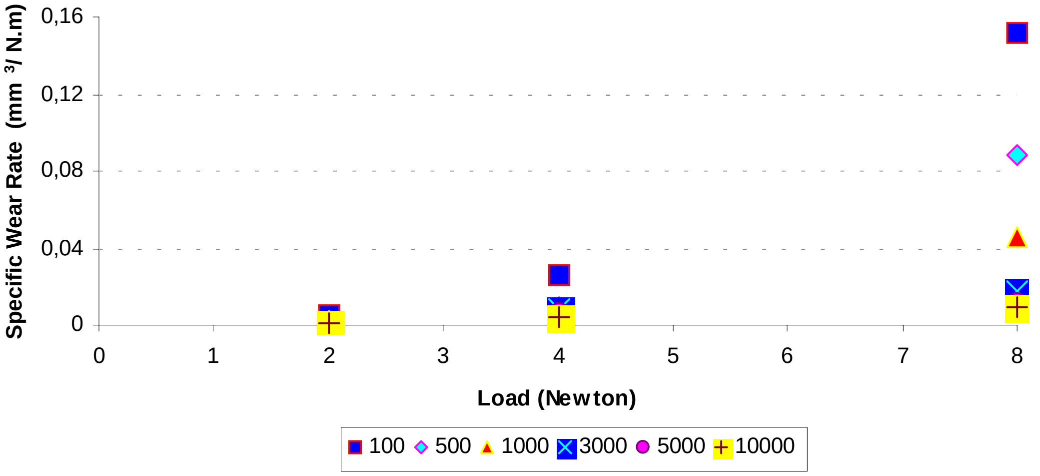

(b)

Figure 4.21 Variation of specific wear rate of the mica glass-ceramic studied as a function of applied load for different number of laps. Data was obtained at the sliding speeds of;
(a) 0.0025 m/s.
(b) 0.025 m/s.

Specific wear rate of the mica glass-ceramic as a function of number of laps depending on sliding speeds of 0.0025 m/s, and 0.025 m/s were graphically depicted in Figures 4.22.(a) - 4.22.(c), for applied loads of 2N, 4N, and 8N. In the following three figures, it is deduced that specific wear rate depends on the sliding speed, since, for all the cases, specific wear rates are rised as the sliding speed increased. In adition, for each figure, as the number of lap or sliding distance increased specific wear rate decreased.

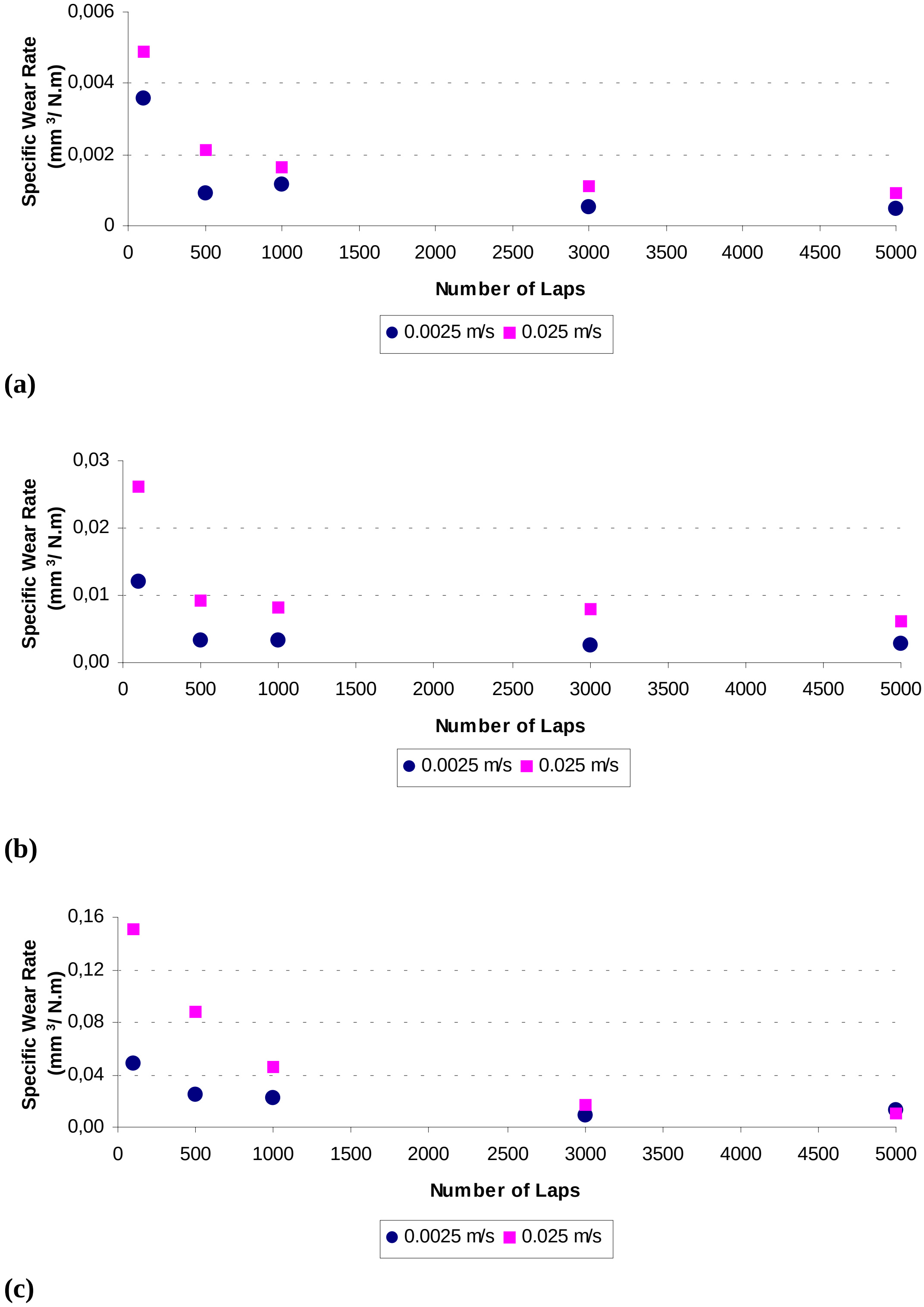

Figure 4.22 Variation of specific wear rate of the mica glass-ceramic studied as a function of number of laps for the sliding speeds of 0.0025 m/s and 0.025 m/s. Environment was ambient. Data was obtained between 0-5000 laps at the applied loads of;

(a) 2N.
(b) 4N.
(c) 8N.

4.4.3 Specific Wear Rates of the Parent Glass and the Mica Glass-Ceramic at Different Environments

In specific wear rate prediction it is important to consider the critical condition for the transition of the wear mode from one to another[70]. In the present study, to predict the specific wear rate and to compare whether different environments have the critical role for the use in dental applications, specific wear rates were calculated and depicted in Figures 4.23.(a) and 4.23.(b). The test conditions were the same as seen in Figures 4.13 and 4.16.

In Figure 4.23.(a), at the 100th lap, the specific wear rate is higher for the ambient atmosphere, however this was not observed as the number of laps increased. After this lap, specific wear rate decreased. However, in basic solution specific wear rate increased and reached a higher rate than those of others throughout the experiment.

In Figure 4.23.(b), the behavior is different than the behavior for the glass. The specific wear rate is higher at ambient atmosphere after the 1000th lap. The decrease in acidic and basic solution was attributed to the the tribo-chemical effect in the solutions. Since, the wear of mica glass ceramic occurred through a combination of processes that included the formation of aluminum hydroxide and silicon hydroxide by tribo-chemical reactions, formation of surface films containing a mixture of worn fragments and reaction products, and mechanical detachment of the surface films, as well as dissolution the reaction products, which decreased the specific wear rate.

The future studies would be conducted to determine whether or not such tribochemical reactions play a role in the wear process of mica glass-ceramic and to evaluate the possible influences of worn particle size and chemical composition on the wear behavior.

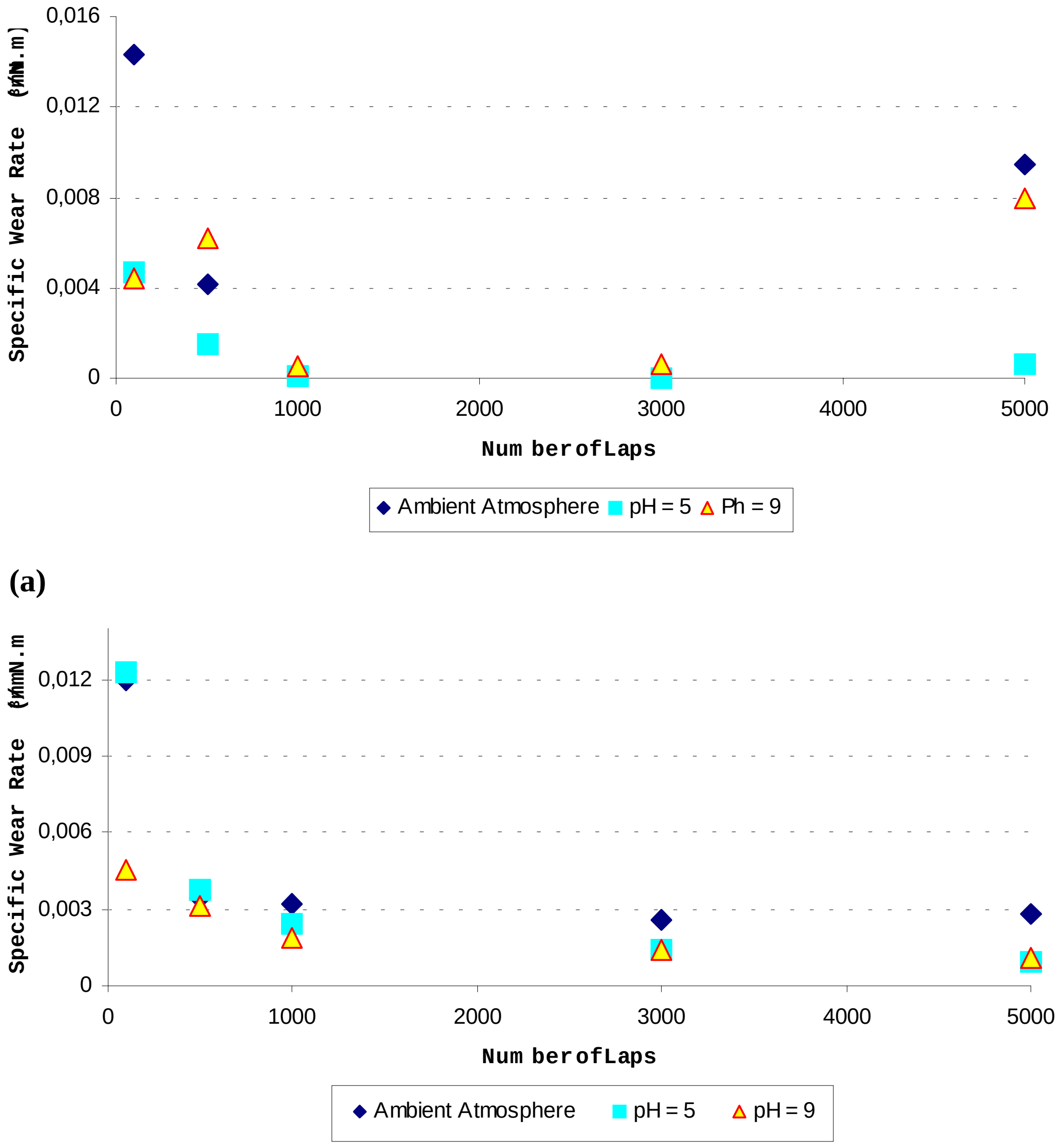

(a)

(b)

Figure 4.23 Variation of specific wear rate as a function of number of laps for the environments of ambient, acidic, and basic. The applied load was 4N. The sliding speed was 0.0025 m/s. Data was obtained between 0-5000 laps for the;
(a) parent glass.
(b) mica glass-ceramic.

Since the absolute value of specific wear rates depend also on the abrasive pin used, it can only express a value for that particular pair of interacting surfaces and can not be compared to the absolute values obtained by other researchers. It is reasonable however, to compare the relative behavior of similar materials tested under the same standard conditions.

Unfortunately, former reports and experimental results about mica glass-ceramics are rare, comparing the data obtained in this study with that of some similar materials used with the purpose of dental restorations, were preferred.

For instance, Wang et. al.[67] studied on the tribological properties of three commercial dental restorative products; Z-100(3M), Renamel (Cosmedent), and Clearfil AP-X (Kuraray). The study was aimed to obtain the friction coefficients and the specific wear rates of these dental materials. The experiment was conducted by using grinding wheel as the abrasive counterface at a sliding speed of 0.05m/s for the application time of 5 to 15 minute. They have obtained friction coefficients at loads of 40kPa and 80kPa, respectively. At first condition friction coefficient range was 0.27 to 0.32, for all three materials. The specific wear rates were 0.215 $mm^3/N.m$ for Z100, 0.194 $mm^3/N.m$ for Clearfil, and 0.113 $mm^3/N.m$ for Renamel. At the higher loading condition of 80 kPa friction coefficient range was 0.29 to 0.35, and the specific wear rates were 0.261 $mm^3/N.m$ for Z100, 0.241 $mm^3/N.m$ for Clearfil, 0.136 $mm^3/N.m$ for Renamel.

Although the experimental conditions were fully different in this study, the same behavior was observed, i.e., as the applied load increased the specific wear rate increased. By comparing the specific wear rate data obtained in this study with the above study conducted by Wang et. al., it may be concluded that specific wear rate for the mica glass-ceramic obtained in this study was better, since the maximum data obtained was 0.151420 $mm^3/N.m$ at a load of 8N and sliding speed of 0.025 m/s. Therefore mica glass-ceramic can be a candidate material for dental applications although it has higher friction coefficient.

As the specific wear rates stronly depend on the mechanism of the wear process, and which also depends on both the material properties and the conditions under which the material used, it can easily be concluded that at the beginning of the tests the wear mechanism is different from at the end.

There was a polished surface at the beginning and as the experiment proceed surface began to be damaged and caused to complicated wear mechanism. Since abrasive wear process was dominant in some interval, which depends on the loading condition and surface properties, as load increased the time of this dominant mechanism disrupts and another mechanism became dominant.

In the case of acidic solution tribo-chemical effect was observed as a white-thin layer on the tested surface at the end of the experiment. Therefore the obtained results were not precise for the experiment conducted in the acidic solution. Since profilometer could not detect whether the tribo-chemical effect in the wear track section is higher or not, i.e., the reaction between the rough and the polished surface can be different due to microstructural change.

Material subjected to the wear process has got two important parameters in predicting the specific wear rate; the hardness and fracture toughness; since the hardness defines the load concentration at the asperities and whether material removal can occur by fracture depends on toughness[75]. Therefore it would be better to make a study in the future which takes into account of this factors.

The observed load-independent wear behavior at high loads may be related to a combination of tribochemical and mechanical processes, since material removal by mechanical action alone should be load-dependent. The processes of tribochemical reactions, film formation, film fracture, and dissolution of reaction product can occur simultaneously. At high loads, the rate of film growth may be sufficiently large to compensate for dissolution or increase in mechanical wear; thus, resulted in a load-independent behavior, as explained by Nagarajan et. al.[84].

In experiments, the primary problem was the accumulation of the worn particles on the wear track section. Therefore it would have been better to use a continuous process during the experiment which will clear away the worn particles from the surface and simultaneously detect the worn volume and the friction coefficients. Another problem faced during the experimental studies was the electricity interruption in the process of long term experiments which was caused by the lack of a generator. Therefore in some lap numbers the data could not be fully gathered for friction coefficients, and experiments were conducted at small intervals instead of long term intervals.

It should be noted that the present investigation was carried out to assess the tribological behaviors of a mica glass-ceramic for dental use. Therefore, no attempt was made to assess the clinical relevance of the results. The effect of saliva to the friction coefficients and the specific wear rates should be conducted in real oral environment. And due to the differences in motion between the pin-on-disk tribometer and the occlusal motion in the oral cavity it is not clear whether the mechanisms causing the observed wear transition would occur in vivo.

CHAPTER 5

CONCLUSIONS

1. The mica glass ceramic exhibited a low friction coefficient within the range of 0.188 to 0.505 at a sliding speed of 0.0025 m/s and a high friction coefficient within the range of 0.325 to 0.913 at a sliding speed of 0.025m/s. Friction coefficient increased with increasing applied load in both sliding speed.

2. The mica glass ceramic had a low specific wear rate in the range of 10^{-1} $mm^3/N.m$ to 10^{-4} $mm^3/N.m$. Therefore it may be an alternative to many commercial materials commonly used for wear-protection for dental applications such as tooth restoration.

3. The applied load, sliding speed, sliding distance or sliding time and test environment had an influence on the friction coefficient and specific wear rate of the mica glass ceramic. Friction coefficient varied depending on these parameters within the range of 0.188 to 0.913 at ambient atmosphere, and within the range of 0.245 to 0.793 in solutions.

4. The surface quality of the samples had an influence on the friction coefficient, and specific wear rate. Friction coefficient varied between 0.0718 and 0.3013 at initial laps of the test, but these values increased to 0.2266 and 0.9425 at the end of the experiment. Specific wear rates were higher at initial laps. At the end of experiments, the diminishing effect was observed.

5. Mica glass ceramic had lower friction coefficient than the parent glass. The maximum value obtained for glass was higher (1.035) at ambient atmosphere, and at in solutions (0.964) than that for the glass ceramic.

6. The dominant wear mechanism was changed from abrasive to adhesive at higher loads and / or after a large number of sliding laps.

REFERENCES

[1]. C.K. Chyung, G.H. Beall, and D.G. Grossman, “Microstructures and Mechanical Properties of Mica Glass Ceramics”, pp: 1167-94 in Electron Microscopy and Structure of Materials, Proceeding of 5th International Materials Symposium. University of California Press, Berkeley, CA. (1971).

[2]. L. Rounan, and Z. Peinan, “Phologopite-Based Glass-Ceramics” Journal of Non-crystalline Solids Vol.80 (1986) pp:600-604

[3]. M.S. Bapna, and H.J. Mueller, “Study of Devitrification of Dicor Glass” Biomaterials, Vol.17 (1996) pp:2045-2052

[4]. P. F. James, “Glass Ceramics: New Compositions and Uses” Journal of Non-crystalline Solids, Vol. 181 (1995) pp:1-15

[5]. J.L. Xie, H. Feng, and S. Wenhua, “Crystallization Properties of Phologopite-Based Machinable Glass Ceramic”,Glass Technology, Vol.37 (1996) pp:175-178

[6]. A.R. Boccaccini, “Short Communication: Machinability and Brittleness of Glass Ceramics” Journal of Materials Processing Technology, Vol.65 (1997) pp:302-304

[7]. J. M. Tzeng, J. G. Duh, K. H. Chung, and C. C. Chan, “Al_2O_3 and ZrO_2 Modified Dental Glass Ceramics” Journal of Materials Science, Vol.28 (1993) pp:6127-6135

[8]. G. H. Beall, “Glass Ceramics: Current Problems and Prospects for 2004” Journal of Non-crystalline Solids, Vol. 73 (1985) pp:413-419

[9]. P.J. Adair, “Glass Ceramic Dental Products”, US Patent No: 4431420 (1984) pp:4

[10]. D.G.Grossman, and L.M. Johnson Janet, “Glass-Ceramic Compositions for Dental Constructs”, US Patent No:4652312 (1987), pp:3

[11]. S. Jahanmir, and X. Dong “Wear Mechanism of a Dental Glass Ceramic”, Wear, Vol.181-183 (1995), pp:821-825.

[12]. T. Uno, T. Kasuga, and K. Nakjima, “High Strength Mica Containing Glass-Ceramics” Journal of American Ceramic Society, Vol.74 (1991), pp:3139-3141

[13]. D. S. Baik, K. S. No, J. S. Chun, Y. J. Yoon, and H. Y. Cho, “A Comparative Evaluation Method of Machinability for Mica-Based Glass Ceramics”, Journal of Material Science, Vol.30 (1995) pp:1801-1806

[14]. W. Vogel, W. Höland, and K. Nauman, “Development of Machinable Bioactive Glass-Ceramics for Medical Uses”, Journal of Non-Crystalline Solids Vol.80(1986), pp:34-51

[15]. D.G. Grossman, in J.D. Preston (Ed.) “Perspectives in Dental Ceramics, Proceedings of the Fourth International Symposium on Ceramics”, Quintessence Publishing Co. Chicago, (1998), pp:177

[16]. D.G. Grossman, in W.J. O`Brien, and R.G. Craig (Ed.), “Proceedings of Conference on Recent Developments in Dental Ceramics” , The American Ceramic Society, Columbus, Ohio, (1985), pp:19

[17]. R. V. Mckinney, Jr. “Endosteal Dental Implants” Mosby Year Book, (1992), pp:3,28,29

[18]. K. Kodaira, H. Fukuda, S. Shimada, T. Matsushita, and A. Tsunashima, “Preparation and Characterisation of Fluorphlogopite and Fluormuskovite Mica Glass-Ceramics” Mat. Res. Bull., Vol.19 (1984) pp:1427-1432.

[19]. D.S. Baik, K.S. No, J.S-S. Chun and Y.J.Yoon “Mechanical Properties of Mica Glass Ceramics”, Journal of American Ceramic Society, Vol.78 (1995), pp:1217-1222.

[20]. D. S. Baik, K. S. No, J. S. Chun, and H. Y. Cho,” Effect of the Aspect Ratio of Mica Crystals and Crystallinity on the Microhardness and Machinability of Mica Glass Ceramic” Journal of Materials Processing Technology, Vol.67 (1997) pp: 50-54

[21]. T.Uno, T.Kasuga, S. Nakayama, and A. J. Ikushima, “Microstructure of Mica Based Nanocomposite Glass-Ceramics” Journal of American Ceram,c Society, Vol.76 (1993), pp:539-541

[22]. W. Bonfield. “New Trends in Implant Materials” In Pizoferrato L, Editor,”Biomaterials and Clinical Applications”, Amsterdam: Elsevier, (1987).

[23]. D. W. Jones, P. A. Jones, and H. J. Wilson,”A Simple Abrasion Test for Composites”, Journal of Dentistry, Vol.1 (1972) pp:28-34

[24]. G. E. Monasky, and D. F. Taylor , “Studies on the Wear of Porcelain, Enamel, and Gold”, Journal of Prostheses Dentistry., Vol.25 (1971), pp: 299-306

[25]. E. W. Tillitson, R. G. Craig, and F. A. Peyton, “Friction and Wear of Restorative Dental Materials”, Journal of Dentistry Research. Vol.50 (1971), pp:149-154

[26]. A. Harrison and T. T. Lewis, “The Development of an Abrasion Testing Machine for Dental Materials“, Journal of Biomedical Materials Research, Vol.9 (1975), pp:341-353

[27]. R. DeLong, C. Sasik, M. R. Pintado, and W. H. Douglas, “The Wear of Enamel When Opposed by Ceramic Systems” Dental Materials, Vol.5, (1989), pp:266-271

[28]. V.S. Nagarajan, and S. Jahanmir: Wear Vol.200 (1996), pp:176-185

[29]. J. Hu, X. D. Xiao, D. F. Ogletree, and M. Salmeron, “Atomic Scale Friction and Wear of Mica”, Surface Science, Vol:327 (1995), pp:358-370

[30]. LL. Hench “Bioactive Ceramics”, In: Ducheyene, Lemons J, editors. ”Bioceramics Material Characterisation versus in Vivo Behaviour”, Vol.523, New York:Annals of New York Academy of Sciences, (1986).

[31]. Z. Strnad “Role of Glass Phase in Bioactive Glass-Ceramics”, Biomaterials, (1992), 13 pp:13:317-21

[32]. B.M. Tracy, and R.H. Doremus “Direct Electron Microscopy Studies of the Bone-Hydroxyapatite Interface”, Journal of Biomedical Materials Research, (1984), 18:719-26

[33]. M. Yoshimari, Y. Ohtsuka, and T. Derand, “Thin Hydroxyapatite Coating Produced by the Ion Beam Dynamic Mixing Method” Biomaterials, (1994), 15:529-35.

[34]. D. Wood, and R. Hill "A Glass-Ceramic Approach to Controlling the Properties of a Glass-Ionomer Bone Cement",Biomaterials, Vol.12 (1991), pp:164-70

[35]. Dr. S H Kilcoyne in collaboration with Dr D Wood at Leeds Dental Institute The Development of Kinetic Neutron Techniques for Dental Applications http://www.stoner.leeds.ac.uk/vacancies/phd_neutronteeth.htm

[36]. T. Kokubo, S. Ito, S. Sakka, and T. Yamamuro, "Formation of a High Strength Bioactive Glass-Ceramic in the System MgO-CaO-SiO_2 –P_2O_5, Journal of Material Science,(1986), Vol.21, pp:529-35

[37]. W. Vogel, "Glass Chemistry", 2nd Edition, (1994.)

[38]. H. Hockin, K. Xu, Douglas T.Smith, and S. Jahanmir, "Influence of Microstructure on Indentation and Machining of Dental Glass-Ceramics", Journal of Materials Research, Vol.11, No.9 (1996), pp: 2325-2337.

[39]. W. Vogel, W.Höland, and Angewand. Chemistry. Vol.26 (1987) 527.

[40]. P. W. McMillan, "The Crystallization of Glasses", Journal of Non-Crystalline Solids, Vol.52 (1982), pp:67-76

[41]. J. Shyu, J. Wu, "Effect of TiO_2 Addition on the Nucleation of Apetite in an MgO- CaO- SiO_2 –P_2O_5 Glass" Journal of Materials Science Letters, Vol.10 (1991), pp:1056-1058

[42]. S. Jordery, W. E. Lee, P. F.James, "Crystallization Hierarchy of CaO –P_2O_5 – SiO_2 – Al_2O_3 – TiO_2 Glass Ceramics" Journal of American Ceramic Society, Vol.81 (1998), pp: 2237-2244

[43]. R.G. Bayer, "Design for Wear Resistance", ASM Handbook, Vol.20, Material Selection and Design, (1997), pp:603-614

[44]. R. G. Bayer, “Wear Testing” Metals Handbook 9th Edition Mechanical Testing Vol.8 (1985), pp: 601-608

[45]. J.A. Williams, “Engineering Tribology” Oxford Science Publication pp:1-3,27-37

[46]. W. Gwidon Stachowiak, and W. Andrew Batchelor, “Engineering Tribology” pp:1-9, (2000)

[47]. R. DeLong, and W. H. Douglas, “Development of an Artificial Oral Environment for the Testing of Dental Restoratives; Bi-Axial Force and Movement Control” J. Dent. Res., Vol.62 (1983), pp: 32-36

[48]. R. DeLong, W. H. Douglas, R. L. Sakaguchi, and M. R. Pintado, “The Wear of Dental Porcelain in an Artificial Mouth” Dent.Materials, Vol.2 (1986), pp: 214-219

[49]. D. S. Palmer, M. T. Barco, G. B. Pelleu Jr., and J.E.McKinney, ”Wear of Human Enamel Against a Commercial Castable Restorative Material” Journal of Prostheteses. Dentistry, Vol.65 (1991), pp: 192-195

[50]. J. W. McLean,”Current Status and Future of Ceramics in Dentistry” Ceramic Engineering Science Proceedings, Vol.6 (1985), pp: 1-9

[51]. J. F. Archard, “Contact and Rubbing of Flat Surfaces” , Journal of Applied Physics, (1953), pp:24,981-988

[52]. K. J. Bhansali, “Wear Coeffcient of Hard-Surfacing Materials” in Wear Control Handbook, Peterson, M.B. and Winer, W.O(Eds), ASME, (1980), pp:373-383

[53]. W. Hirst, in Proceedings of the Conference on Lubrication and Wear, Imech E., London, (1957), pp:674

[54]. K. Hokkirigawa, “Wear Maps of Ceramics”, Bulletin of the Ceramic Society of Japan, (1997), pp:1,19-24

[55]. S. C. Lim, and M. F. Ashby,”Wear Mechanism Maps”,Acta Metallurgica, Vol:35 (1987), pp:1-24

[56]. K.Hokkirigawa, and K. Kato, “An Experimental and Theoretical Investigation of Ploughing, Cutting and Wedge Formation During Abrasive Wear”, Tribology International, (1988), Vol:21, pp:1,51-57

[57]. K.Kato, and K. Adachi “Wear Mechanism” (Bharat Bhushan Ed.), Modern Tribology Handbook Vol.1, pp: 273-300

[58]. Y. C .Chiou, K. Kato, and T. Kabaya, ”Effect of Normal Stiffness in Loading System on Wear of Carbon Steel-Part1:Severe-Mild Wear Transition 1985, ASME, Journal of Tribology, Vol.107 (1985), pp:107, 491-495

[59]. S. J. Cho, B. J. Hockey, and B. R., “Grain Size and R-Curve Effects in the Abrasive Wear of Alumina”, Journal of American Society, Vol:72 (1989), pp:7,1949-1952.

[60]. C. S. Yust, and R. G. Bayer Eds., “Selection and Use of Wear Tests for Ceramics”, ASTM STP 1010, Philadelphia, (1998)

[61]. ASTM Standard G-132, “Test Method for Pin Abrasion Testing”, ASTM Annual Book of Standards, Vol.: 03.02 (1995), West Conshohocken, PA,

[62]. Peter Blau, and G. Kenneth Budinski, “Development and Use of ASTM Standards for Wear Testing” Wear 225-229 (1999), pp:1159-1170

[63]. W. Yan, P.Noel O'Dowd, and P. Esteban Busso, ”Numerical Study of Sliding Wear Caused by a Loaded Pin on a Rotating Disc", Journal of Mechanics and Physics of Solids, Vol.:50 (2002), pp:449-470

[64]. H.Der, "Production of Biocompatible Mica Glass Ceramics for Dental Applications" (1998)

[65]. "Materials Selector 1986", Materials Engineering, A Penton Publication, (1986), pp:20

[1]. A.Öztürk, M. Timuçin, N. Koç, and H. Der "Protez Diş Yapımında Kullanılabilecek Mika Cam Seramiklerin Üretilmesi" Ağustos 2000

[67]. W. Wang, A.T. DiBenedetto, and A. Jon Goldberg, "Abrasive Wear Testing of Dental Restorative Materials", Wear, Vol.:219 (1998), pp:213-219

[68]. R. Westergard,A. Ahlin, N.Axen, and S. Hogmark, "Sliding Wear and Friction of Si_3N_4-SiC Based Ceramic Composites Containing Hexagonal Boron Nitride", proc. Instn. Mech. Engrs Vol.: 212 (1998) part J.

[69]. E. M. Kopalinsky, and A. J. Black "Metallic Sliding Friction Under Boundary Lubricated Conditions; Investigation of the Influence of Lubricated at the Start of Sliding", Wear Vol.:190 (1995), pp:197-203

[70]. K. Kato, "Classification of Wear Mechanisms/Models", Proc. Instn. Mech. Engrs, Vol.:216, PartJ, Journal of Engineering Tribology.

[71]. P. Fournier, Ph. Reynaud, F. Platon, and J. Absi, "Tribological Behavior of Carbon-fibre-reinforced SiC Matrix Composites",2000, Proceedings of Instn. Mechanical Engineers, Vol.:214, Part J

[72]. S.S. Rankumar and Nichole A. Hester, “Study of the Frictional Properties of the Needlepunched Nonwoven Fabrics”, Texas Tech University, International Textile Center Lubbock, TX, in the Proceedings of the Beltwide Cotton Conference, Vol.:1, pp:696-696 (2001)

[73]. Hahner, Georg; Spencer, and Nicholas “Rubbing and Scrubbing”, TRIBOLOGY; TABOR, David, Physics Today, Sep98, Vol. 51 Issue 9, pp:22, 6p, 1 chart, 5 diagrams, 1 graph, 1bw,

[74]. V. Bianchi, P. Fournier, F. Platon, and P. Reynaud, “Carbon Fibre-Reinforced (YMAS) Glass-Ceramic Matrix Composites: Dry Friction Behaviour”, Journal of European Ceramic Society, Vol.19(1999), pp:581-589

[75]. M. Kalin, S. Jahanmir, and Lewis K. Ives “Effect of Counterface Roughness on Abrasive Wear of Hydroxypatite” Wear Vol.:252(2002), pp:679-685

[76]. A. Ravikiran, and S. Jahanmir, “Effect of Interfacial Layers on Wear Behavior of a Dental Glass Ceramic”, Journal of the American Ceramic Society, 0028720, July 2000 Vol.:83, Issue 7.

[77]. M. Eisenburger, and M. Addy, “Erosion and Attrition of Human Enamel in Vitro Part I: Interaction Effects”, Journal of Dentistry Vol.:30 (2002), pp:341-347

[78]. Archard J. F., and Hirst, W. “Wear of Metals Under Unlubricated Conditions” Pros. R. Soc. Land. A.,1956, Vol.:236, pp: 3-55

[79]. J. A. William, “Archard Wear and Component Geometry” Proceedings of Institiution of Mechanical Engineers Part J, Journal of Engineering Tribology, Vol 215(2001), Issue.4, pp:387, 17p

[80]. A Ravikiran, G.R. Subbanna, and B. N. Pramila Bal,”Effect of Interfacial Layers Formed During Dry Sliding of Zirconia Toughened Alumina (ZTA) and Monolithic Alumina Against Steel”, Wear, Vol:192(1996), pp:56-65

[81]. M. Godet, “The Third-Body Approach: A Mechanical View of Wear” Wear, Vol:100(1984), pp:437,52

[82]. E. Medvedovski “Wear Resistant Engineering Ceramics” ,Wear 249, 2001, pp:821-828

[83]. S. A. Chizhik, A. V. Goldade, S. V. Korotkevich, and A. M. Dubravin, “Friction of Smooth Surfaces with Ultrafine Particles in the Clearance”, Wear Vol.:238 (2000) pp:25-33

[84]. V.S. Nagarajan, B.J. Hockey, S. Jahanmir, and V.P. Thompson, “Wear Mechanisms of a Dental Composite with High Filler Content”, Journal of Material Science, Vol.: 35 (2000), pp: 487–496.

APPENDIX A

Table A.1 Mean friction coefficient of the parent glass measured at loads of 2N, 4N, and 8N and at sliding speeds of 0.0025m/s and 0.025 m/s for different number of laps.

Number of Laps	Mean Friction Coefficients (μ)					
	2N		4N		8N	
	0.0025 m/s	0.025m/s	0.0025 m/s	0.025m/s	0.0025 m/s	0.025m/s
0-100	0.285	0.311	0.192	0.767	0.164	0.174
100-500	0.284	0.313	0.189	0.898	0.256	0.202
500-1000	0.301	0.315	0.187	0.870	0.556	0.270
1000-3000	0.306	0.331	0.175	0.893	1.020	0.535
3000-5000	-	0.559	-	0.899	1.035	0.886
5000-10000		0.925		0.897		0.903

Table A.2 Mean friction coefficient of the parent glass measured at a load of 4N and at a sliding speed of 0.0025m/s in acidic and basic solutions for different number of laps.

Number of Laps	Mean Friction Coefficients (μ)	
	pH=5	pH=9
0-100	0.266	0.695
100-500	0.247	0.853
500-1000	0.296	0.871
1000-3000	0.333	0.964
3000-5000	0.169	0.823

Table A.3 Standard deviations of the mean friction coefficient of the parent glass measured at loads of 2N, 4N, and 8N and at sliding speeds of 0.0025m/s and 0.025 m/s for different number of laps.

Number of Laps	Mean Friction Coefficients (μ)					
	2N		4N		8N	
	0.0025 m/s	0,025m/s	0.0025 m/s	0.025m/s	0.0025 m/s	0.025m/s
0-100	0.006	0.017	0.012	0.140	0.015	0.010
100-500	0.007	0.014	0.012	0.063	0.011	0.020
500-1000	0.007	0.014	0.010	0.085	0.248	0.068
1000-3000	0.008	0.012	0.011	0.028	0.08	0.141
3000-5000	-	0.190	-	0.020	0.06	0.072
5000-10000		0.030		0.017		0.139

Table A.4 Standard deviations of the mean friction coefficient of the parent glass measured at a load of 4N and at a sliding speed of 0.0025m/s in acidic and basic solutions for different number of laps.

Number of Laps	Mean Friction Coefficients (μ)	
	pH=5	pH=9
0-100	0.018	0.171
100-500	0.007	0.135
500-1000	0.095	0.139
1000-3000	0.078	0.119
3000-5000	0.039	0.173

Table A.5 Friction coefficient of the parent glass measured at loads of 2N, 4N, and 8N and at sliding speeds of 0.0025m/s and 0.025 m/s at the end of different number of laps.

Number of Laps	Friction Coefficients (μ)					
	2N		4N		8N	
	0.0025 m/s	0.025m/s	0.0025 m/s	0.025m/s	0.0025 m/s	0.025m/s
100	0.2792	0.3003	0.1754	0.9212	0.1606	0.1821
500	0.2760	0.3337	0.1799	0.9249	0.4453	0.2455
1000	0.3050	0.3309	0.1803	0.7519	0.7060	0.4901
3000	0.3125	0.3517	0.1961	0.9025	1.0432	0.6406
5000	-	0.8921	-	0.9116	1.0577	0.9059
10000		0.9495		0.8972		0.9121

Table A.6 Friction coefficient of the parent glass measured at a load of 4N and at a sliding speed of 0.025 m/s in acidic and basic solutions at the end of different number of laps.

Number of Laps	Mean Friction Coefficients (μ)	
	pH=5	pH=9
100	0.2826	0.9336
500	0.2549	1.1890
1000	0.5541	1.1868
3000	0.4918	1.0339
5000	0.1599	0.9981

APPENDIX B

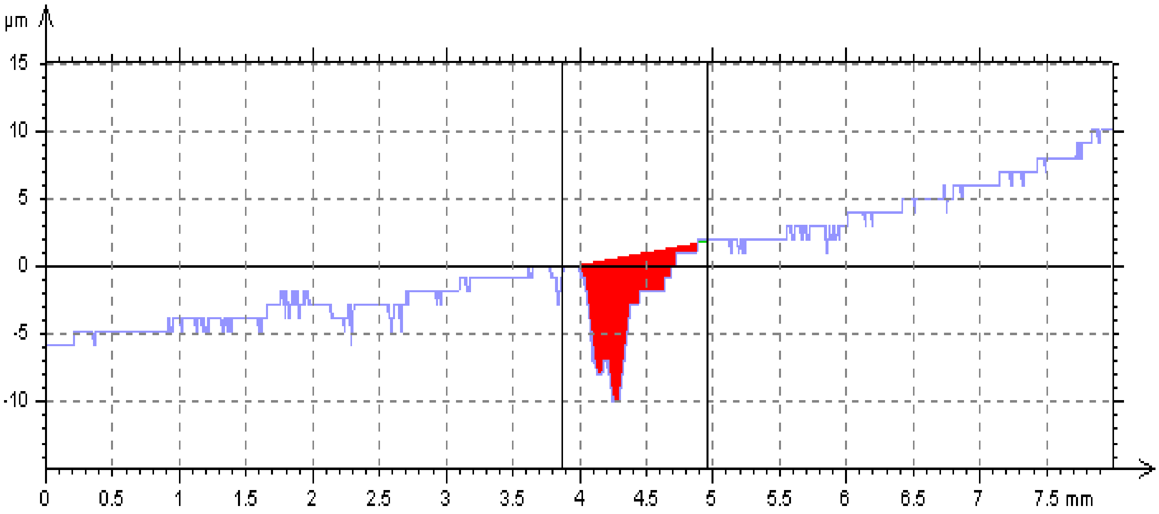

Figure B.1 Schematic representation of the wear track of the parent glass obtained at a load of 2N and sliding speed of 0.025 m/s at the end of 10000th lap

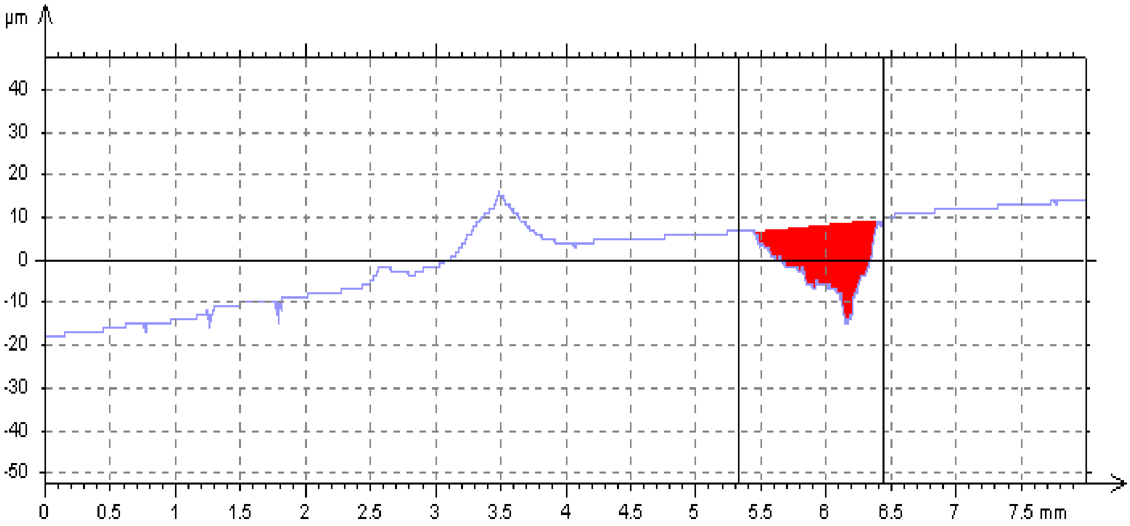

Figure B.2 Schematic representation of the wear track of the mica glass-ceramic obtained at a load of 8N and sliding speed of 0.025 m/s at the end of 10000th lap

Table B.1 Mean wear track area of the parent glass measured at loads of 2N, 4N, and 8N and at sliding speeds of 0.025 m/s and 0.0025 m/s for different number of laps.

Number of Laps	Mean Wear Track Area (mm^2)					
	2N		4N		8N	
	0.0025 m/s	0.025m/s	0.0025 m/s	0.025m/s	0.0025 m/s	0.025m/s
100	0.0027	0.0044	0.0036	0.0112	0.0094	0.0217
500	0.0040	0.0064	0.0051	0.0145	0.0118	0.0661
1000	0.0079	0.0102	0.0095	0.0262	0.0159	0.1396
3000	0.0086	0.0114	0.0138	0.0814	0.0542	0.1688
5000	0.0433	0.0230	0.0474	0.1451	0.1826	0.1723
10000	-	0.0377	-	0.3161	-	0.4120

Table B.2 Mean wear track area of the parent glass measured at a load of 4N and at a sliding speed of 0.0025 m/s in acidic and basic solutions for different number of laps.

Number of Laps	Mean Wear Track Area (mm^2)	
	pH=5	pH=9
100	0.0011	0.0011
500	0.0018	0.0078
1000	0.0023	0.0219
3000	0.0031	0.0772
5000	0.0078	0.0994

Table B.3 Mean wear track area of the mica glass-ceramic measured at loads of 2N, 4N, and 8N and sliding speeds of 0.025 m/s and 0.0025 m/s for different number of laps.

Number of Laps	Mean Wear Track Area (mm^2)					
	2N		4N		8N	
	0.0025 m/s	0.025m/s	0.0025 m/s	0.025m/s	0.0025 m/s	0,025m/s
100	0.0018	0.0024	0.0030	0.0066	0.0060	0.0189
500	0.0023	0.0054	0.0043	0.0115	0.0152	0.0552
1000	0.0059	0.0081	0.0081	0.0206	0.0284	0.0566
3000	0.0079	0.0166	0.0192	0.0591	0.0360	0.0663
5000	0.0120	0.0234	0.0356	0.0775	0.0805	0.0692
10000	-	0.0359	-	0.0977	-	0.1123

Table B.4 Mean wear track area of the mica glass-ceramic measured at a load of 4N and sliding speed of 0.0025 m/s in acidic and basic solutions for different number of laps.

Number of Laps	Mean Wear Track Area (mm^2)	
	pH=5	pH=9
100	0.0031	0.0011
500	0.0047	0.0039
1000	0.0061	0.0046
3000	0.0113	0.0103
5000	0.0121	0.0142